ABSTRACT

Title of Dissertation:	MOBILIZATION OF CHEMICAL COCKTAILS BY FRESHWATER SALINIZATION SYNDROME IN THE CHESAPEAKE BAY WATERSHED
	Joseph George Galella Doctor of Philosophy, 2023
Dissertation directed by:	Professor Sujay Kaushal Department of Geology

Increasing trends in base cations, pH, and salinity of urbanizing freshwaters have been documented in U.S. streams for over 50 years. These patterns, collectively known as Freshwater Salinization Syndrome (FSS), are driven by multiple processes, including applications of road salt and human-accelerated weathering of impervious surfaces, reductions in acid rain, and other anthropogenic legacies of change. FSS mobilizes chemical cocktails of distinct elemental mixtures *via* ion exchange, and other biogeochemical processes. Urban streams in temperate areas experience chronic salinization throughout the year punctuated by acute salinization during winter storms with associated road salting.

My research analyzed impacts of FSS on stream water chemistry in the field with routine bi-weekly and targeted high frequency sampling during road salting events. Field sites were proximal to USGS stream sensors using multiparameter datasondes, allowing for additional parameters to be monitored at 5-15 minute resolution. In the laboratory incubation analyses were

also conducted using sediment and water samples to assess the function of stormwater best management practices (BMPs) during road salting events.

Acute FSS associated with road salting was found to mobilize chemical cocktails of metals (Mn, Cu, Sr^{2+}), base cations (Na^+, Ca^{2+}, Mg^{2+}, K^+), nutrients (TDN), and organic matter (NPOC). Regression relationships were developed among specific conductance and major ion and trace metal concentrations. These linear relationships were statistically significant in most of the urban streams studied (*e.g.*, $R^2 = 0.62$ and 0.43 for Mn and Cu, respectively), and showed that specific conductance could be used as a proxy to predict concentrations of major ions and trace metals.

Principal component analysis (PCA) showed co-mobilization (*i.e.*, correlations among combinations of specific conductance, Mn, Cu, Sr^{2+}, and all base cations during certain times of year and hydrologic conditions). Co-mobilization of metals and base cations was strongest during peak snow events but could continue over 24 hours after specific conductance peaked, suggesting ongoing cation exchange in soils and stream sediments.

Increased salt concentrations of all three major road salts (NaCl, $CaCl_2$, and $MgCl_2$) had profound effects on major and trace element mobilization, with all three salts showing significant positive relationships across nearly all elements analyzed. Salt type showed preferential mobilization of certain elements. NaCl mobilized Cu, a potent toxicant to aquatic biota, at rates over an order of magnitude greater than both $CaCl_2$ and $MgCl_2$.

Hourly mass fluxes of TDN in streams were also found to be elevated during winter months with peaks coinciding with road salting events. Targeted winter snow event sampling and high-frequency sensor data suggested plateaus in NO_3^- / NO_2^- and TDN concentrations at the highest peak levels of SC during road salt events between 1,000 and 2,000 µS/cm, which possibly indicated source limitation of TDN after extraction and mobilization of watershed nitrogen reservoirs by road salt ions.

My results may help guide future regulations on road salt usage as there are currently no federally enforceable limits. NaCl is the most commonly used deicer in the United States, largely because it is often the least expensive option. Other technologies such as brines and other more efficient deicers ($CaCl_2$ and $MgCl_2$) should be considered in order to lessen the deleterious effects of FSS.

MOBILIZATION OF CHEMICAL COCKTAILS BY FRESHWATER SALINIZATION SYNBDROME IN THE CHESAPEAKE BAY WATERSHED

by

Joseph George Galella

Dissertation submitted to the Faculty of the Graduate School of the
University of Maryland, College Park, in partial fulfillment
of the requirements for the degree of
Doctor of Philosophy
2023

Advisory Committee:
  Professor Sujay S. Kaushal, Advisor/Chair
  Paul M. Mayer Ph.D
  Associate Professor Karen L. Prestegaard
  Associate Professor Vedran Lekić
  Associate Professor Mitchell A. Pavao-Zuckerman, Dean's Representative

Dedication

To my friends and family, both at UMD and around the country who provided love and positivity over the past five years. To my parents Elaine and Joe who have always nurtured my love of science even from a young age. And to my Fiancé Kristie who has supported me both physically and emotionally beyond measure.

I love you all,

Joe

Acknowledgements

I’d like to thank Sujay Kaushal and Paul Mayer for meeting with me every week for the past five years rain or shine. You gave me the knowledge, guidance, skills, and support necessary for me to thrive at UMD. I consider myself fortunate for having you both as my advisor and spiritual co-advisor. I’d like to thank Karen and Ved for their open doors whenever I needed to meet and talk about science, math, or just life in general.

To my previous science teachers, mentors, and advisors (Mr. Blueglass, Dr. Robert Walter, Dr. Dorothy Merritts, and Dr. Michael Applegarth), thank you for always believing in me and giving me the skills and guidance to complete my degree. I’m sure you will all continue to inspire young minds and make learning fun for many generations to come.

Table of Contents

List of Tables

List of Figures

Chapter 1: Introduction

Freshwater salinization is an emerging environmental problem around the world, universally degrading the quality of ground and surface waters. Due to freshwater salinization, streams, rivers, reservoirs, and lakes in major regions of North America have exhibited increasing trends in total dissolved solids, and major ions such as chloride, sodium, calcium, magnesium, and potassium for over half a century (*e.g.,* Anning and Flynn, 2014; Corsi *et al.*, 2010; Dugan, Bartlett, *et al.*, 2017; Dugan, Summers, *et al.*, 2017; Kaushal *et al.*, 2005, 2013, 2017, 2018, 2019). In addition, over the past century there have been similar increasing trends in concentrations of base cations in streams, rivers, reservoirs, and lakes (Na^+, Ca^{2+}, Mg^{2+}, and K^+) across not only North America but also in Europe, China, Russia and Iran (Kaushal *et al.*, 2019). Coinciding increases in major ions, changes in specific conductance and pH, and the increased direct and indirect impacts of salt ions on water quality, ecosystems, and infrastructure has been termed the "Freshwater Salinization Syndrome" (FSS) (Kaushal *et al.*, 2018, 2019). FSS is caused by various salt ions originating from diverse sources such as road deicers, irrigation, agricultural liming and potash, sewage, mining, and weathering of concrete in the built environment and surficial geology due to erosion and acidic precipitation (Dugan, Bartlett, *et al.*, 2017; Haq *et al.*, 2018; Kaushal *et al.*, 2018; Kunz *et al.*, 2013; Schulz and Cañedo-Argüelles, 2019). FSS has been shown to mobilize elemental mixtures known as chemical cocktails (Kaushal *et al.*, 2018, 2019, 2020), but relatively little is known about which elements are mobilized and when; in fact, the chemical causes and consequences of FSS are not yet fully understood in watersheds across varying land use, hydrologic conditions, and stormwater management.

1.1 Scope and Sources of Freshwater Salinization Syndrome

Salinity, specific conductance, and base cation concentrations of freshwater streams and rivers in North American and Europe have shown an increasing trend over the past century (Anning and Flynn, 2014; Corsi *et al.*, 2010; Dugan, Summers, *et al.*, 2017; Kaushal *et al.*, 2005, 2018, 2019). More locally, increased salinization has been observed in 37% of the area of the contiguous United States (Kaushal *et al.*, 2018). Increasing trends in base cations are often observed in the Eastern and Midwestern US, thought to be driven by anthropogenic land use, increased impervious surface cover and increased population density and road salting. (Kaushal *et al.*, 2018). However, these trends are not uniform across the nation, with declining trends of major ions and total dissolved solids observed in the southwest of the U.S. This is thought to be related to increased prevalence of large dams, crop irrigation and water diversions (Kaushal *et al.*, 2019).

Sources of freshwater salinization include weathering of bedrock, built infrastructure, agriculture and, in temperate regions, predominantly road salting (Demars and Benoit, 2019; Dugan, Summers, *et al.*, 2017; Kaushal *et al.*, 2018, 2019; Moore *et al.*, 2020). These sources can be broken down into three main drivers: agricultural land use, urban and suburban land use, and the quantity of snowfall deposited in a region. Agricultural land use usually presents itself as a more gradual baseline shift in specific conductance due to slow build up in groundwater through irrigation (NaCl) and the addition of lime and potash to fields during growing season K^+ and HCO_3^- (Kaushal *et al.*, 2018). Urbanized land use also contributes base cations into waterways through dissolution of concrete, cement and other calcium carbonate-rich materials (sometimes referred to as “urban karst”). Most impervious surfaces are slowly altered and weathered over time as concrete reacts with the atmosphere $Ca(OH)_2 + CO_2 \rightarrow CaCO_3 + H_2O$. Slightly acidic precipitation, even that which is just in equilibrium with CO_2 in the atmosphere can chemically weather this further into aqueous $Ca(HCO_3)_2$ (Zhang, 2011). Chemical dissolution happens particularly readily in concrete based drainage infrastructure which is constantly exposed to urban runoff (Davies *et al.*, 2010; Wright *et al.*, 2011). Areas which accumulate large volumes of snowfall are also at heightened risk for episodic salinization during the winters, with potential for baseline fluctuations as NaCl and other deicers build up in groundwater and soils. Annual U.S. highway road salt sales have increased from 0.28 megatons to 16 megatons from the 1940s to the 2000s, following increasing roadway cover within temperate regions (Jackson and Jobbagy, 2005; Kaushal *et al.*, 2018; “MRLC”). Data from the local Baltimore Long-Term Ecological Research site show a positive relationship between road salt application and mobilization of base cations (Bird *et al.*, 2018; Kaushal *et al.*, 2017; Moore *et al.*, 2017). Cations likely originate from storage reservoirs in ground water and soils, which can be flushed to streams and rivers (Kaushal *et al.*, 2017; Shanley, 1994). Base cation levels in urban streams were found in concentrations 60 times greater than found in agricultural and forested catchments (Kaushal *et al.*, 2017).

Land use has a large effect on the salinity monitored streams. Studies in Chicago, Maryland and New Hampshire have identified a positive relationship between urban land use and Na^+ and Cl^- concentrations in streams (Jackson and Jobbagy, 2005; Daley *et al.*, 2009; Kelly *et al.*, 2012; Cooper *et al.*, 2014; Kaushal *et al.*, 2005; Baker *et al.*, 2019; Moore *et al.*, 2017, 2020; Stets *et al.*, 2020). Percent impervious surface coverage and percent road pavement are also used as proxies for urbanization in many of these studies as road surface coverage is a major factor for the quantity of road salt applied (Baker *et al.*, 2019; Daley *et al.*, 2009). Some studies have noted as much as a 27 fold change in ion concentrations along a rural to urban gradient (Moore *et al.*, 2017). Increased urbanization and road surface cover act to not only increase the quantity of salt applied to a watershed but also decrease infiltration and transport time. Channelization and the use of storm drains increase the hydrological connection between roadways and the aquatic environment, decreasing transport times and increasing the flashiness of storm hydrograph responses (Kaushal *et al.*, 2005).

Base cation exchange rates, metal bioavailability, pH, and, ionic strength are often altered by the addition of road salt (Kaushal *et al.*, 2019). Changes in Cation Exchange Capacity (CEC) can disrupt the number of cations attached to negatively charged soil particle surfaces. This can increase aqueous loading of metals including cadmium, zinc, and copper (Cooper *et al.*, 2014; Kaushal *et al.*, 2019; Löfgren, 2001). The addition of sodium cations have been shown to displace copper, lead and zinc from soils adjacent to streams after road salting (Kaushal, 2016; Nelson *et al.*, 2009; Norrström and Jacks, 1998). This has the potential to increase mobile metal concentrations throughout riparian and aquatic environments. The solubility of metals can also be influenced by elevated soil salinity adjacent to roadways (Zehetner *et al.*, 2009). In particular, heightened dissolved chloride (Cl^-) ligand concentrations can increase the solubility of metals including cadmium. This is a concern for both drinking water and crops irrigated with heavy metal contaminated water (Romic *et al.*, 2012). The risk of road salts mobilizing metals is particularly significant for cities and other areas with aging infrastructure. Lead piping and solder is still pervasive in aged drinking water supply networks, along with associated metal enriched sediments (Amrhein *et al.*, 1992; Kaushal, 2016). Salt displacement and corrosion often mobilizes these metals, often going unnoticed as water quality is often monitored at its treatment facility or source and not at the end user (Amrhein *et al.*, 1992; Kaushal, 2016). Trace elements including metals are often transported as aqueous complexes. These complexes are made up of associated cations and anions or as neutral molecules known as ligands (Gaillardet *et al.*, 2003). Colloids, miniscule particles between 0.2µm and 1 nm (often small enough to pass through conventional filters), are also a carrier of trace elements (Gaillardet *et al.*, 2003). Increased Na^+ has been shown to displace metals from their exchange sites and into solution in both waters and soils (Kaushal *et al.*, 2019). Higher valence base cations including Mg^{2+}, and Ca^{2+}, sometimes found in deicers or mobilized through cation exchange, are even more efficient at displacing metals in soils (Kaushal *et al.*, 2019). Ca^{2+} outcompetes Zn, Pb, and Cd in soil cation exchange sites (Acosta *et al.*, 2011; Kaushal *et al.*, 2019). Similarly Mg^{2+} outcompetes Cu, with Cu concentrations often being the highest at the soil surface (Acosta *et al.*, 2011; Kaushal *et al.*, 2019). NaCl is known to increase the solubility of Pb and Cd, which increases solubility through chloro-complexation (Kaushal *et al.*, 2019; Lopez-Chuken and Young, 2010). It should be noted that there is constant competition between ions and cations at exchange sites in complexes, ligands, and organic matter. Because of this complex nature, unique ratios of major ions and organic matter can yield different metal solubility, increasing the difficulty of predicting toxicity (Duan and Kaushal, 2015; Haq *et al.*, 2018; Kaushal *et al.*, 2019).

1.2 Applications of Stream Sensors as Proxies for FSS Chemical Cocktail Transport

Using high frequency specific conductance sensors as proxies for chloride has been explored in resent research, highlighting their usefulness in detecting water quality exceedances (Moore *et al.*, 2020). This is particularly useful in the case of studying road salting events as sample collection and lab resources are not able to provide 5 to 15-minute resolution data for prolonged periods of time as readily or efficiently as data sondes are. However, Site specific calibration is necessary as some sites seem to be best explained via a linear fit model and other sites seem to be best explained via a piecewise model (Moore *et al.*, 2020).

As road salting is an episodic event in response to local precipitation, it is manifested as “pulses” in concentrations of ions, often lasting days after the storm itself (Haq *et al.*, 2018). These acute events are often associated with increased base cation mobility, nitrogen and phosphorus loading, elevated metals, and altered pH (Haq *et al.*, 2018; Mangani *et al.*, 2005). The “first flush phenomenon” is exemplified in episodic salinization with accumulated contaminants and anthropogenic salts becoming mobilized along with precipitation (Cooper *et al.*, 2014).

Chronic NaCl pollution has been shown to persist in the environment long after road salting has ended. Elevated salinity is found in both groundwater and surface water well into the summer months, accumulating in the ecosystem over years or decades (Cooper *et al.*, 2014). The flashier hydrograph responses associated with urbanization and densely packed roadways often limit infiltration into groundwater, potentially slowing the effect of salinization locally. Unfortunately, certain environmentally conscious stormwater management practices such as stormwater retention ponds and wetlands may have detrimental effects to groundwater salinity. Similar to episodic salinization, chronic salinization has been shown to elevate sodium, calcium, magnesium, and potassium levels while decreasing pH. Recent studies indicate that infiltration due to stormwater retention may induce exceedances in both chronic and acute chloride concentrations (Cooper *et al.*, 2014). This may be tempered by stormwater management features retaining metals (Cu, Zn, and Pb), but the joint effect of high salinity have yet to be studied (Davis *et al.*, 2009).

1.3 Examples of Environmental Implications of FSS

Increased freshwater salinization is not only harmful to aquatic organisms, but human health as well. The Environmental Protection Agency (EPA) has placed an acceptable drinking water advisory at 20 mg/l of Na. This primary advisory is mainly put in place for those on salt restricted diets but there is a secondary limit of 30-60 ml for taste (Cooper *et al.*, 2014). The EPA also has regulations for ambient chloride concentrations. Aesthetic and cosmetic concerns limit chloride to 250 mg/l for drinking water. Recommended maximums are also in place for acute levels greater than 860 mg/L and chronic concentrations greater than 230 mg/L (Cooper *et al.*, 2014; Corsi *et al.*, 2010; Moore *et al.*, 2020). Despite these regulations, 13 cities in the northern US and 4 in southern metro areas were found to be in violation of the set chronic maximum 55 % of the time while exceeding the acute maximum 15 % of the time during cold weather (November to April) (Corsi *et al.*, 2010). Exceedances dropped to 16% for chronic pollution and 1% for acute during warm weather (May to October), indicating a likely link to road salting (Corsi *et al.*, 2010). Aquatic organisms are also affected by salt exceedances with changes in food webs, fish species assemblages, and species die offs found to be associated with increased salinity (Cañedo-Argüelles *et al.*, 2013; Hintz and Relyea, 2017; James *et al.*, 2003; Morgan *et al.*, 2012). Metals mobilized by FSS can also be toxic to various aquatic species. Injury or death to some species, such as salmon, may also represent potential economic losses (Berntssen *et al.*, 1999; Mahrosh *et al.*, 2014). Key questions regarding drinking water quality are related to what types of chemical cocktails are mobilized by FSS, and how often there may be exceedances in thresholds.

Chapter 2: Sensors track mobilization of ‘chemical cocktails’ in streams impacted by road salts in the Chesapeake Bay watershed

2.1 Abstract

Increasing trends in base cations, pH, and salinity of freshwaters have been documented in U.S. streams for over 50 years. These patterns, collectively known as Freshwater Salinization Syndrome (FSS), are driven by multiple processes, including applications of road salt and human-accelerated weathering of impervious surfaces, reductions in acid rain, and other anthropogenic legacies of change. FSS mobilizes chemical cocktails of distinct elemental mixtures *via* ion exchange, and other biogeochemical processes. We analyzed impacts of FSS on stream water chemistry across five urban watersheds in the Baltimore-Washington, USA metropolitan region. Through combined grab-sampling and high-frequency monitoring by USGS sensors, regression relationships were developed among specific conductance and major ion and trace metal concentrations. These linear relationships were statistically significant in most of the urban streams (*e.g.*, $R^2 = 0.62$ and 0.43 for Mn and Cu, respectively), and showed that specific conductance could be used as a proxy to predict concentrations of major ions and trace metals. Major ions and trace metals analyzed *via* linear regression and principal component analysis (PCA) showed co-mobilization (*i.e.*, correlations among combinations of specific conductance, Mn, Cu, Sr^{2+}, and all base cations during certain times of year and hydrologic conditions). Co-mobilization of metals and base cations was strongest during peak snow events but

could continue over 24 hours after specific conductance peaked, suggesting ongoing cation exchange in soils and stream sediments. Mn and Cu concentrations predicted from specific conductance as a proxy indicated acceptable goodness of fit for predicted *vs.* observed values (Nash-Sutcliffe Efficiency > 0.28). Metals concentrations remained elevated for days after specific conductance decreased following snowstorms, suggesting lag times and continued mobilization after road salt use. High-frequency sensor monitoring and proxies associated with FSS may help better predict contaminant pulses and contaminant exceedances in response to salinization and impacts on aquatic life, infrastructure, and drinking water.

2.2 Introduction

Freshwater salinization is an emerging environmental problem around the world, degrading the quality of ground and surface waters (Cañedo-Argüelles *et al.*, 2016; Kaushal *et al.*, 2005; Kaushal, Likens, *et al.*, 2018a; Kaushal, Likens Gene E., *et al.*, 2019). For example, freshwater salinization has impacted streams, rivers, reservoirs, and lakes in North America, with concurrent positive trends in major ions such as Cl-, Na+, Ca2+, Mg2+ over half a century (Anning and Flynn, 2014; Corsi *et al.*, 2010; Dugan, Summers, *et al.*, 2017; Kaushal *et al.*, 2005; Kaushal, Likens, *et al.*, 2018a; Stets *et al.*, 2020). Similar increasing trends in concentrations of base cations (Na+, Ca2+, Mg2+, and K+) have been observed in Europe, China, Russia and Iran over the past century (Kaushal, Likens Gene E., *et al.*, 2019). Coinciding increases in major ions, changes in specific conductance and pH, and the increased direct and indirect impacts of salt ions on water quality, ecosystems, and infrastructure have been called the Freshwater Salinization Syndrome (FSS) (Davies *et al.*, 2010; Kaushal *et al.*, 2013; Kaushal, Gold, *et al.*, 2018; Kaushal, Likens Gene E., *et al.*, 2019). FSS is an emerging environmental issue caused by multiple salt ions originating from diverse sources such as road deicers, irrigation, agricultural liming and potash, sewage, mining, and weathering of concrete in the built environment and surficial geology due to erosion and acidic precipitation (Davies *et al.*, 2010; Dugan, Bartlett, *et al.*, 2017; Haq *et al.*, 2018; Kaushal, Gold, *et al.*, 2018; Kaushal *et al.*, 2020; Kunz *et al.*, 2013; Schulz and Cañedo-Argüelles, 2019). FSS is expected to increase due to increased use of roadway deicers, construction materials, fertilizers, and other anthropogenic substances. For example due to the legacy of human construction, annual road salt sales in the United States have increased nearly an order of magnitude in ~60 years (Corsi *et al.*, 2010) coinciding with an accumulation of road salt ions in soils and groundwater (Kaushal *et al.*, 2005; Kaushal, Likens, *et al.*, 2018a; Moore *et al.*, 2017), a phenomenon that may be exacerbated by long (over 50 year) residence times of road salts in watersheds (Shaw *et al.*, 2012). FSS mobilizes chemical cocktails of metals, nutrients, organics, and other ions through shifts in ion exchange, solubility, and microbial activity (Amrhein *et al.*, 1992; Duan and Kaushal, 2015; Green and Cresser, 2008; Haq *et al.*, 2018; Kaushal, Likens Gene E., *et al.*, 2019; Miller *et al.*, 2008).The indirect and direct effects of major ion pollution on water quality, ecosystems, and urban infrastructure are not well known, a concerning gap in knowledge.

Increased urbanization and impervious surface cover in the Mid-Atlantic have increased the quantity of salt ions applied to a watershed but also amplify “pulses” of salinization due to decreased infiltration and transport time (Daley *et al.*, 2009; Kaushal, Mayer, *et al.*, 2014). Stream and river channelization and the use of storm drains increase the “hydrological connectivity” between roadways and aquatic ecosystems (Elmore and Kaushal 2008, Kaushal and Belt 2012), increasing the ‘hydrologic flashiness’ of storm hydrograph responses, and the magnitude and frequency of road salt pulses (Kaushal *et al.*, 2015; Moore *et al.*, 2020; Trowbridge *et al.*, 2010). Increased specific conductance from episodic road salt pulses can last for days, weeks, and months, with associated chemical cocktails of metals and cations sometimes remaining elevated for longer (Haq *et al.*, 2018; Kaushal, Likens Gene E., *et al.*, 2019).

Increased major ion loading from road salts enhances base cation exchange and mobilization of trace metals in both stream sediments and soils to surface waters (Amrhein *et al.*, 1992; Kaushal, Likens Gene E., *et al.*, 2019; Löfgren, 2001; Shanley, 1994). For example, monovalent and divalent cations can displace and mobilize trace metals from exchange sites on negatively charged colloids, such as Mn, Sr2+, Cu, Hg and Zn, (throughout this paper we don’t include charges on some trace metals due to their complex multiple oxidation states) into the dissolved load (D’Itri, 1992; Fay and Shi, 2012; Kaushal, 2016; Kaushal, Likens Gene E., *et al.*, 2019; Nelson *et al.*, 2009). Though research on this topic is only just beginning, increased Na+, for example, can displace metals from their exchange sites on stream sediments and soil particles and into solution (Kaushal, Likens Gene E., *et al.*, 2019; Lazur *et al.*, 2020). Higher valence base cations including Mg2+, and Ca2+, sometimes found in deicers or mobilized through cation exchange, are even more efficient than Na+ at displacing metals in soils (Kaushal, Likens Gene E., *et al.*, 2019). Ca2+ outcompetes Zn, Pb, and Cd in soil cation exchange sites (Kaushal, Likens Gene E., *et al.*, 2019). Similarly Mg2+ outcompetes Cu, with Cu concentrations often being the highest at the soil surface (Kaushal, Likens Gene E., *et al.*, 2019). Following these ion exchange reactions, trace metals are often transported as aqueous complexes. These complexes are made up of a central metal ion bound to an ion or molecule, forming a metal-ligand bond order (Gaillardet *et al.*, 2003). Cl- is known to increase the solubility of Cd and Pb, which increases solubility through chloro-complexation (Kaushal, Likens Gene E., *et al.*, 2019; Norrström and Bergstedt, 2001). Because most research has been conducted on mobilization of individual element mobilization knowledge gaps still exist regarding the full suite of metals released by FSS.

One of the key challenges in understanding the magnitude and scope of FSS is characterizing peaks and lag times in specific conductance and elemental concentrations as a result of road salting events and associated geochemical processes. Here we use high-frequency sensor data, coupled with bi-weekly grab sampling of stream water chemistry to test the hypothesis that FSS has substantial, negative impacts on urban freshwater systems and to characterize the chemical cocktails formed due to FSS in urban streams across seasons. Changes in the composition of these chemical cocktails are thought to be most significant during and after instances of winter precipitation events. Knowledge of seasonal changes in the magnitudes and mixtures of chemical cocktails mobilized by FSS has implications for protection of aquatic life, safe drinking water, and how the public and government can best mitigate this emerging environmental issue (Corsi *et al.*, 2010; Herbert *et al.*, 2015; Hintz and Relyea, 2017b; James *et al.*, 2003; Kaushal, 2016). Most research has focused on documenting increasing long-term annual trends in specific conductance, Cl-, and Na+ in streams, rivers, lakes, and reservoirs (Corsi *et al.*, 2010; Dugan, Bartlett, *et al.*, 2017; Dugan, Summers, *et al.*, 2017; Kaushal *et al.*, 2005; Kaushal, Likens, *et al.*, 2018a; Stets *et al.*, 2020). However, with increased availability of high- frequency sensor data in streams, episodic salt pulses can be detected in real time and quantified in urban and suburban watersheds (Haq *et al.*, 2018; Kaushal, Likens Gene E., *et al.*, 2019; Moore *et al.*, 2020; Morel *et al.*, 2020; Trowbridge *et al.*, 2010).

Monitoring elemental flux in highly dynamic urban streams is very time and resource intensive; therefore proxies can be developed using high frequency specific conductance data to estimate other elemental concentrations.(Haq *et al.*, 2018; Kaushal, Gold, *et al.*, 2018; Kaushal *et al.*, 2020; Moore *et al.*, 2020; Morel *et al.*, 2020). Previous work using specific conductance as a proxy for Cl- has shown that Cl- pulses during road deicing events are difficult to capture using traditional grab sampling methods (Trowbridge et al. 2010, Moore et al. 2019). Less work has focused on characterizing the dynamics of metals that are also mobilized by deicing events (Haq *et al.*, 2018; Kaushal, Likens Gene E., *et al.*, 2019; Morel *et al.*, 2020). Due to these knowledge gaps, the main research goals answered in this study are to: (1) identify what metals are mobilized during snow events, and (2) develop proxies to predict the mobilization of these metals.

2.3 Methods

2.3.1 Study Sites

All 5 study watersheds, totaling 381 km2 were located throughout the Baltimore and Washington D.C. metropolitan areas and within the greater Chesapeake Bay Watershed (Figure 1). Sampling locations were chosen at USGS gauge stations, providing higher temporal resolution data (5-15 minutes) than could be obtained via grab-sampling (USGS NWIS, 2020).

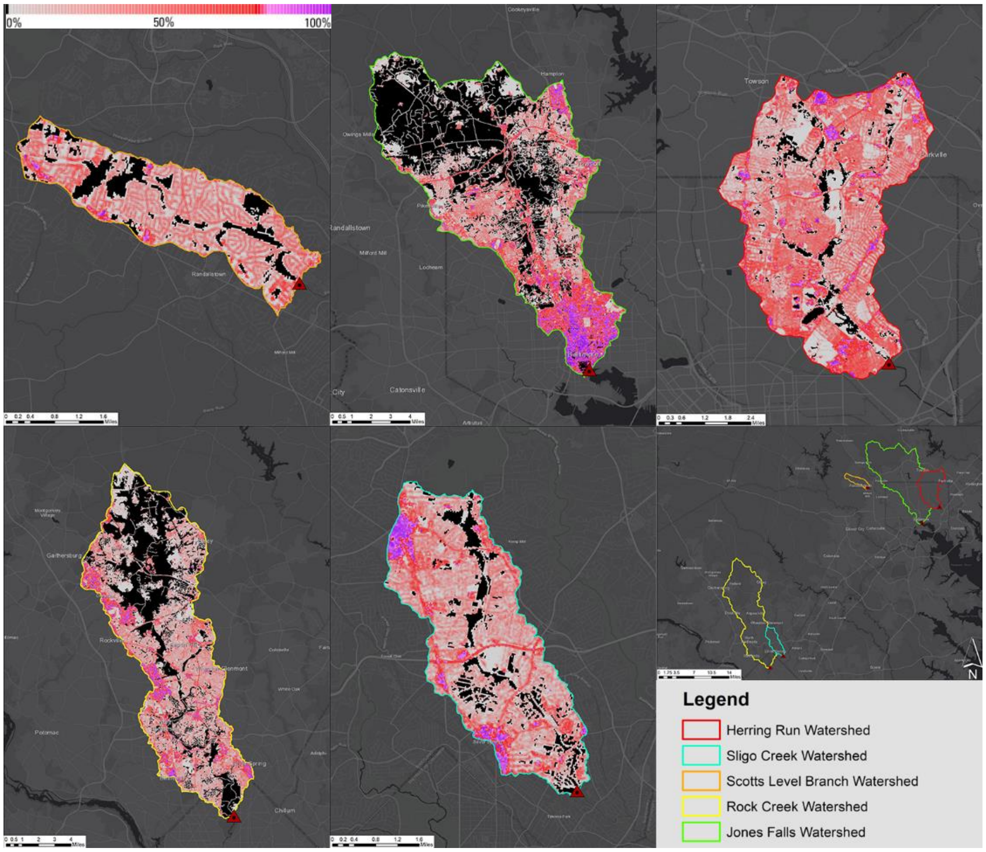

Figure 1. Map of Sampling Sites

Impervious surface cover within the watersheds of sample collection sites in the Baltimore and D.C. metropolitan areas (Esri *et al.*; MRLC, 2020; StreamStats, 2020). Red triangles indicate sampling sites.

USGS monitoring stations utilize multiparameter datasondes which take instantaneous measurements of specific conductance, dissolved O2, turbidity and NO3- / NO2- (USGS NWIS, 2020). Watersheds were delineated via the StreamStats USGS web application and remotely sensed watershed characteristics, including land use and impervious surface cover, were obtained from a 30-m resolution datasets provided by the 2016 National Land Cover Database (NLCD) (MRLC, 2020; StreamStats, 2020). Site characteristics were analyzed via ArcMap 10.4 and Microsoft Excel.

Five urban streams were sampled for this study (Figure 1 and Table 1): Rock Creek, a stream with large riparian buffer and the lowest proportion of impervious surface cover; Sligo Creek, an urbanized stream with a walking trail and road that follows much of its length; Scotts Level Branch, a stream influenced by suburbanization and a small riparian buffer abutted by houses; Herring Run, a heavily urbanized stream which has a small water treatment plant about two miles upstream (Jones, 1996; Parks, 2016); and Jones Falls, a mainly buried, heavily polluted tidal stream flowing directly into the inner harbor of the Chesapeake Bay (Table 1).

Table 1. Site Characteristics

Site characteristics for all sampling sites and their accompanying USGS stations (“USGS NWIS”; “MRLC”).

Study Site	Metro Area	Latitude	Longitude	USGS Site #	Drainage Area mi^2	NLCD 2016 % Impervious Surface Cover
Rock Creek	D.C.	38°57'36.6"	77°02'31.4"	1648010	63.7	18.35
Sligo Creek	D.C.	38°59'10.4"	77°00'17.5"	1650800	6.45	27.19
Scotts Level Branch	Baltimore	39°21'41.7"	76°45'42.3"	1589290	3.23	22.24
Herring Run	Baltimore	39°19'04.7"	76°33'18.5"	1585219	16.3	32.76
Jones Falls	Baltimore	39°17'02.8"	76°36'13.1"	1589485	57.5	21.28

2.3.2 USGS Continuous Monitoring Data

High frequency (5-15 minute resolution) data for specific conductance (SC), in micro-siemens per centimeter at 25°C, discharge (Q) in cubic feet per second, and temperature (T) in degrees Celsius, turbidity (TB) and pH were obtained from the USGS National Water Information System (NWIS) for the duration of the study (October 2017 – October 2019). SC is measured using contact sensors with electrodes, which are temperature compensating and have an accuracy greater than 0.5±0.5 percent of readings, or ±2 µS/cm (Gibs *et al.*, 2012; Wagner *et al.*, 2006). T is measured with a thermistor with an accuracy of ± 0.1oC and Q is accurate to the nearest 0.01 ft or 0.2 % stage height, or whichever is larger (USGS, 2020; Wagner *et al.*, 2006). Instrumental error, calibrations, and accuracy of USGS multiparameter datasondes are further described in Gibs et al. (2012) and Wagner et al. (2006).

2.3.3 Bi-Weekly Grab Sampling and Targeted Snow Event Sampling

Water samples were collected approximately bi-weekly from all five sites across the Washington D.C. and Baltimore metropolitan areas (red triangles in Figure 1). Two 125-ml acid-washed HDPE Nalgene bottles of stream water were collected from each site after being triple rinsed with stream water before sample collection. Samples were kept on ice until being transported back to the University of Maryland College Park for analysis. Grab samples were filtered through pre-combusted 0.7 µm glass fiber filters to separate dissolved and suspended load. A 60-ml aliquot of the filtered sample was stored in acid-washed HDPE Nalgene bottles with 0.5% high-purity nitric acid. Acidified samples were analyzed within 6 months via inductively coupled plasma optical emission spectrometry (ICP-OES) on a Shimadzu Elemental Spectrometer (ICPE-9800; Shimadzu, Columbia, Maryland, USA) (Haq *et al.*, 2018). ICP-OES analysis determined elemental concentrations of Na+, Ca2+, Mg2+, K+, Cu, Sr2+, and Mn. The remaining unacidified samples were kept at 4 oC for up to two weeks before being analyzed on a Shimadzu Total Organic Carbon Analyzer (TOC-V CPH/CPN; Shimadzu, Columbia, Maryland, USA) (Haq *et al.*, 2018). The TOC-V analyzer uses a combustion-catalytic-oxidation-NDIR method to dissolved inorganic carbon (DIC)content. The Jones Falls site often exhibited brackish water due to its tidal nature, due to this all samples were diluted with four parts high purity Milli-Q water (conductivity below detection limit) to one-part sample before analysis as to not damage the instrument. In addition to bi-weekly sampling, hourly sampling was also conducted in response to 2 road deicing events (during the peak and directly following snow events) at Sligo Creek in the winter of 2019.

2.3.4 Synoptic Sampling

Longitudinal, synoptic surveys of Sligo Creek and Rock Creek were conducted during July of 2018. Samples were collected via the bi-weekly methodology described above along the length of both streams at approximately 1-1.6 km intervals. Samples were intentionally collected above or at least 100 m below any large tributaries to increase the likelihood obtaining a homogenized sample (Kaushal, Delaney-Newcomb, *et al.*, 2014). Impervious surface cover was calculated upstream of the sampling point to determine how anthropogenic ground cover might affect analytes (MRLC, 2020; StreamStats, 2020). Patterns in stream water chemistry measurements were then evaluated and related to the drainage area above each point.

2.3.5 Statistical Analysis

Regression relationships were developed among elemental concentrations and ancillary variables. All ICP-OES data were analyzed in triplicate to improve data quality. The relative standard deviation (RSD) of these three samples was divided by a calculated RSD derived from sample concentration to determine the error acceptability (Burgess, 2000; Horwitz *et al.*, 1980; Horwitz and Albert, 2006). The acceptable error threshold is based upon the assumption that RSD increases as analyte concentration decreases (Burgess, 2000; Horwitz *et al.*, 1980). Equation 1 below was used to determine the calculated RSD.

Eq. 1

$$RSD\ calculated = 2^{(1-0.5\log C)}$$

Where

C is relative concentration

Equation 2 determines the Horwitz ratio or HORRAT. If the HORRAT is < 2 it is generally an acceptable value. If it the HORRAT is > 2, the corresponding measurement is excluded from the results (Burgess, 2000).

Eq. 2

$$\text{HORRAT} = \frac{RSD\ observed}{RSD\ calculated}$$

The Nash-Sutcliffe model efficiency coefficient (NSE) (equation 3) was utilized to determine the predictive power of the model relating concentrations of metals to specific conductance (Moriasi *et al.*, 2007; Nash and Sutcliffe, 1970). Samples were arranged by date and alternating data points (odd) were used to develop the linear relationships. The NSE test was then performed on the half of the dataset (even data points) not used for model calibration.

Eq.3

$$NSE = 1 - \frac{\sum_{i=1}^{n}(Y_i^{obs} - Y_i^{sim})^2}{\sum_{i=1}^{n}(Y_i^{obs} - Y^{mean})^2}$$

Where

Y_i^{obs} is the *i*th observation of the data being tested

Y_i^{sim} is the *i*th simulated value of the data being tested

Y^{mean} is the mean of the observed data n is the number of observations in the dataset

Principal component analysis (PCA) was used to quantify more complex multivariate patterns in metals mobilization. PCA analysis was performed in MATLAB with normalized datasets in order to correct for the different scales and units of the data used (e.g., µS/cm and mg/L) in the analysis. PCA was able to illustrate the changing correlations between major and trace elements as a result of FSS across seasons and in response to road salt events.

2.4 Results

2.4.1 Linear Relationships between Specific Conductance and Metals across Sites

There were seasonal trends, with greater concentrations of base cations and metals during winter than the rest of the year (Figure 2 and Table 2).

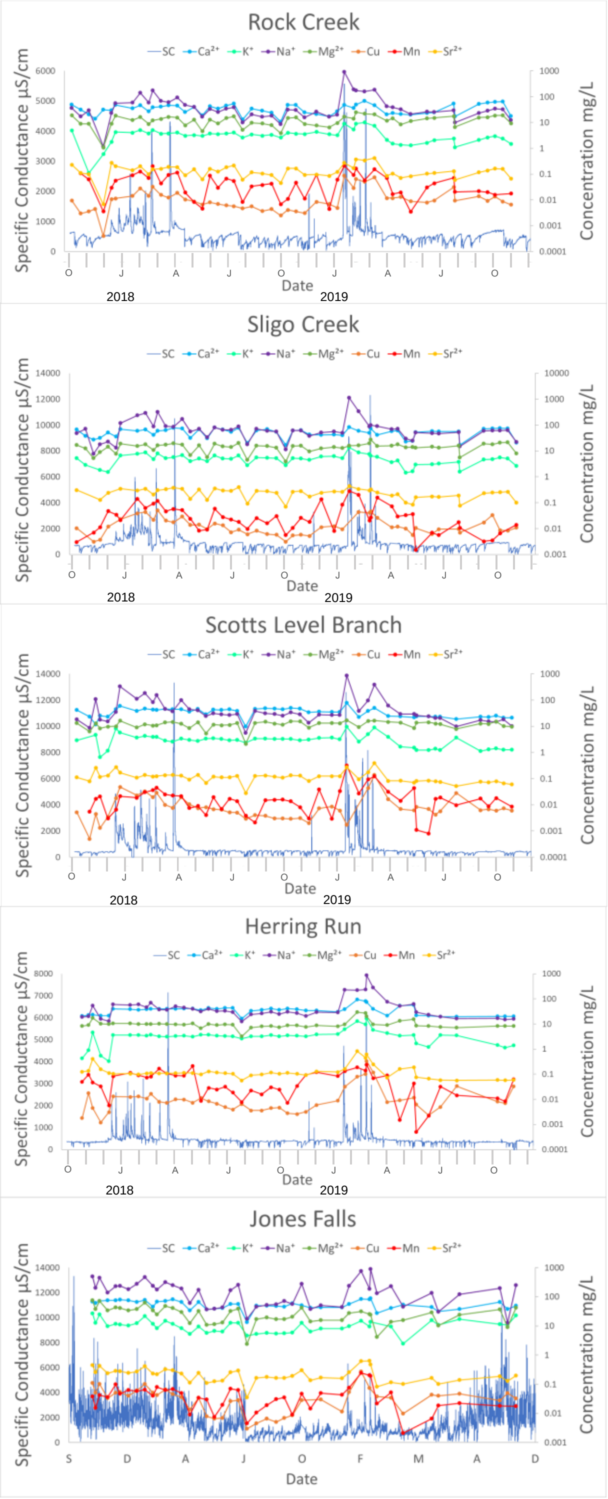
Rock Creek

Sligo Creek

Scotts Level Branch

Herring Run

Jones Falls

Figure 2. Elemental Mobilization Over Time
Time series of major and trace elements (mg/l) plotted against specific conductance (µS/cm). Discharge is also included for each site (cfs) (USGS NWIS, 2020)

Table 2. Elemental Statistics

Elemental concentrations for all sampling sites and their accompanying USGS stations (USGS NWIS, 2020).

Attribute	Ca^{2+}	Cu	Fe	K^+	Mg^{2+}	Na^+	Sr^{2+}	Mn
Average Winter mg/l	52.7	0.0479	0.122	7.28	18.5	224	0.203	0.146
Winter Std Dev	18.2	0.0578	0.0973	4.1	10.6	251	0.151	0.137
Average Summer mg/l	40.3	0.0104	0.0914	4.19	13	42.3	0.122	0.0565
Summer Std Dev	17.9	0.0104	0.131	3.01	7.1	44.3	0.0834	0.0729
% Difference	131	468	134	174	142	529	166	258

Winter 2019 had the most significant snowfall and summer 2018 received the most rain across all sites (Supplemental Figure 2.1). The estuarine nature of Jones Falls diminished the site’s relationship to winter storms, as brackish water would frequently interact with the sensor. This saltwater intrusion likely does not affect the entire Jones Falls watershed however, with more upstream areas mainly being affected by road salt application. We typically observed significant positive linear relationships between specific conductance, base cations and select trace metals across all sites (Figure 3 and Supplemental Figure 2.2).

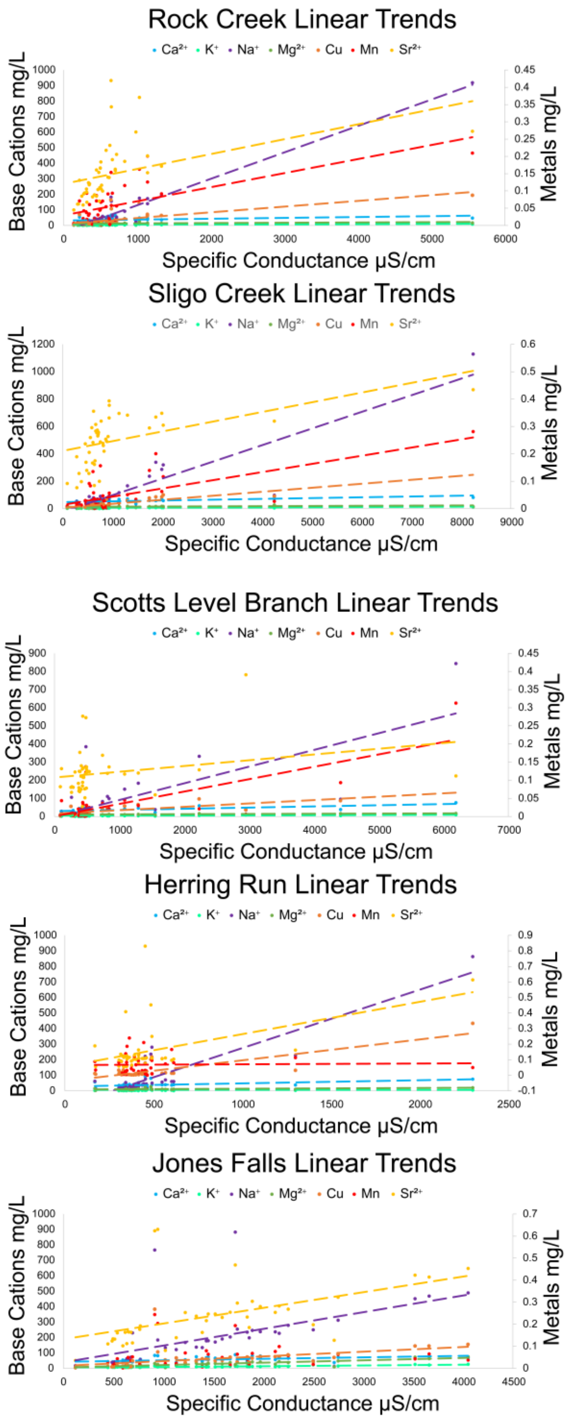

Figure 3. Linear Relationships

Positive linear relationships between base cations, metals and specific conductance in D.C. and Baltimore (USGS NWIS, 2020). (Linear trends with a p value <.05 shown on the right)

R^2 values differed among sites and elements, but relationships remained positive and significant across all sites (except for Fe at most sites and Mn at Jones Falls) ($p<0.05$) (Table 3).

Table 3. Linear Statistics

Linear trend statistics for all sampling sites and their accompanying USGS stations (USGS NWIS, 2020).

Rock Creek

Element	Slope of relationship	p value (Element / SC)	R^2 (Element / SC)	Slope
Ca^{2+}	Positive	0.05	0.08	0.006
Cu	Positive	4.55E-08	0.49	1.65E-05
Fe	Negative	0.54	0.01	-1.59E-05
K^{+}	Positive	1.68E-04	0.28	0.001
Mg^{2+}	Positive	0.04	0.09	0.002
Mn	Positive	7.16E-06	0.38	4.07E-05
Na^{+}	Positive	8E-30	0.94	0.170
Sr^{2+}	Positive	0.01	0.16	4.31E-05

Sligo Creek

Element	Slope of relationship	p value (Element / SC)	R^2 (Element / SC)	Slope
Ca^{2+}	Positive	4.70E-03	0.16	0.006
Cu	Positive	1.08E-10	0.62	1.46E-05
Fe	Positive	0.81	0.04	1.59E-06
K^{+}	Positive	5.61E-09	0.54	0.001
Mg^{2+}	Positive	0.02	0.12	0.001
Mn	Positive	6.32E-07	0.43	2.98E-05
Na^{+}	Positive	3.18E-18	0.81	0.122
Sr^{2+}	Positive	3.57E-04	0.26	3.55E-05

Jones Falls

Element	Slope of relationship	p value (Element / SC)	R^2 (Element / SC)	Slope
Ca^{2+}	Positive	5.00E-04	0.26	0.010
Cu	Positive	4.46E-03	0.19	2.12E-05
Fe	Negative	0.15	0.05	-1.36E-05
K^{+}	Positive	7.94E-12	0.70	0.005
Mg^{2+}	Positive	1.24E-13	0.75	0.015
Mn	Positive	0.40	0.02	7.65E-06
Na^{+}	Positive	2.20E-04	0.29	0.108
Sr^{2+}	Positive	7.67E-04	0.25	7.1E-05

Herring Run

Element	Slope of relationship	p value (Element / SC)	R^2 (Element / SC)	Slope
Ca^{2+}	Positive	7.31E-03	0.16	0.020
Cu	Positive	1.94E-10	0.67	0.000134
Fe	Positive	4.08E-03	0.18	5E-05
K^{+}	Positive	5.24E-07	0.48	0.006
Mg^{2+}	Positive	0.03	0.11	0.005
Mn	Positive	3.7E-05	0.34	0.000104
Na^{+}	Positive	5.62E-16	0.80	0.375
Sr^{2+}	Positive	2.84E-03	0.21	0.000208

Scotts Level Branch

Element	Slope of relationship	p value (Element / SC)	R^2 (Element / SC)	Slope
Ca^{2+}	Positive	9.75E-05	0.28	0.006
Cu	Positive	0.04	0.11	9.3E-06
Fe	Positive	0.67	0.00	4.39E-06
K^{+}	Positive	7.78E-07	0.43	0.001
Mg^{2+}	Positive	0.02	0.11	0.001
Mn	Positive	7.18E-10	0.61	3.42E-05
Na^{+}	Positive	2.87E-09	0.55	0.092
Sr^{2+}	Positive	7.96E-05	0.30	3.05E-05

Though the data appears to be skewed towards low concentrations at some of the sites represented in Figure 3, additional data collected at Sligo Creek further supports the trends observed (Supplemental Figure 2.3). Discharge integrated daily loads were explored as an alternative but provided less favorable results (Supplemental Figure 2.4). Alternate trends were also explored including power and logarithmic but models which had the best fit varied across sites and analytes (Supplemental Figure 2.5). As expected, Na^+ exhibited the strongest relationships with specific conductance, with R^2 values up to 0.94. Mn and Cu also exhibited strong positive linear relationships with specific conductance (R^2 values up to 0.61 and 0.67 respectively) (Table 3). Across all sites, Fe was not significantly related to specific conductance, potentially due to higher sensitivity to redox conditions than stream salinity. Mn can also be sensitive to changes in redox but its mobilization does not follow that of Fe. Concentrations of base cations also exhibited significant positive relationships with watershed impervious surface cover at Sligo Creek; with K^+ and DIC showing similar trends at Rock Creek (Figure 4 and Supplemental Table 2.1). There was some variability in the goodness of fit in the regressions due to tributary inputs influencing concentrations, but there were statistically significant relationships for base cations ($p<0.05$).

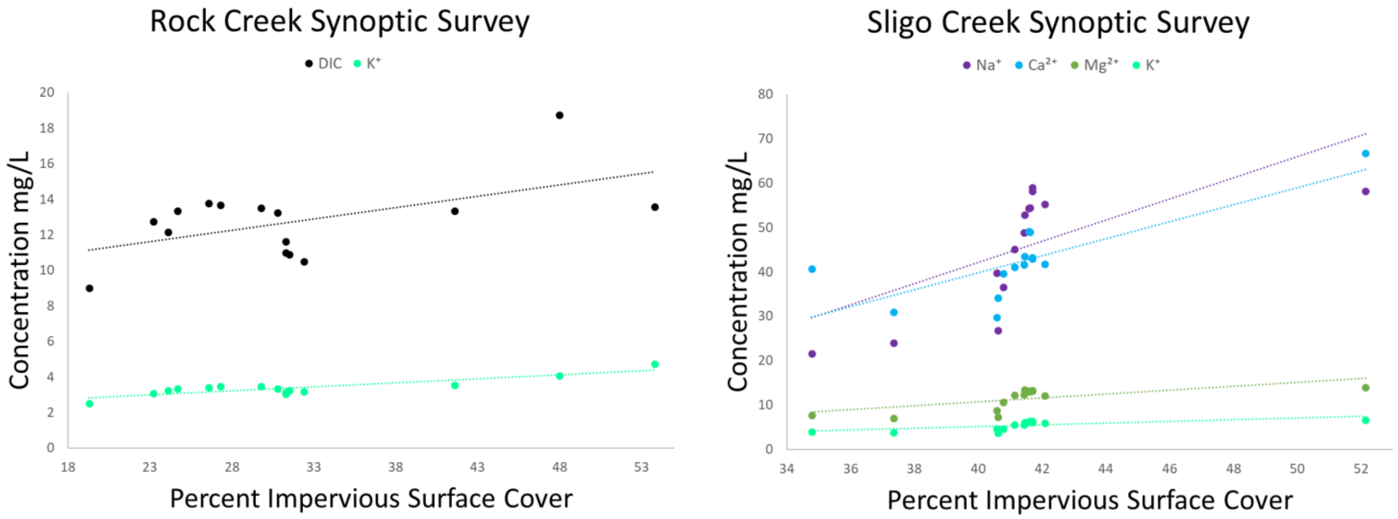

Figure 4. Increasing Trends with Impervious Surface Cover

Synoptic survey results illustrating increasing dissolved inorganic carbon (DIC) and base cations with increasing impervious surface cover. Dotted lines represent linear trends (MRLC, 2020).

Using the linear relationships from Figure 3 and Table 3, specific conductance values were used to predict Mn and Cu concentrations. Data from Sligo Creek were selected, as it was the only site where (high frequency) hourly metals data was collected during snowstorms, giving it the most robust dataset for this analysis. NSE and Root Mean Square Error (RMSE) results for the dataset containing regular bi-weekly measurements were mixed with an NSE of 0.5 for Cu and 0.06 for Mn (Table 4). By incorporating high frequency (hourly data) collected during a snowfall event into the regression, overall predictability improved, with an NSE of 0.4 for Cu and 0.3 for Mn (Table 4). However, observed data after peak snowfall were harder to predict using the relationships developed from regular sampling combined with hourly snowfall data, resulting in negative NSE values, and suggesting a deviation between predicted and observed values after snow events (Figure 5 and Table 4).

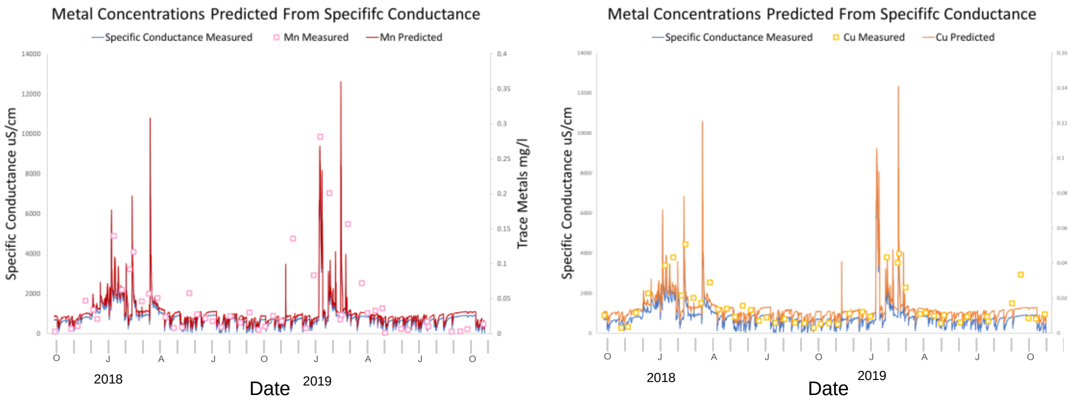

Figure 5. Estimated Metal Concentrations Using Proxies

Estimated metals concentrations using linear relationships developed at Sligo Creek (USGS NWIS, 2020).

Table 4. Root Mean Square Error and Nash Sutcliffe Efficiency

Root Mean Square Error and Nash Sutcliffe Efficiency for predicted values at Sligo Creek (USGS NWIS, 2020). SC = Specific Conductance µS/cm at each time interval. Samples were arranged by date; odd samples were used to generate the regression and even samples were used as a test of model validity.

Dataset generated	Dataset Applied	Equation	Element	RMSE	NSE
Regular sampling odd	Regular sampling even	1.1*10-5*SC+0.0045	Cu	0.0093	0.502
Regular sampling odd	Regular sampling even	2.89*10-5*SC+0.005	Mn	0.0523	0.059
Regular sampling + high frequency peak odd	Regular sampling + high frequency peak even	1.9*10-5*SC+0.0016	Cu	0.0255	0.366
Regular sampling + high frequency peak odd	Regular sampling + high frequency peak even	3.2*10-5*SC+0.0112	Mn	0.0477	0.282
Regular sampling + high frequency peak odd	Sampling after peak of storm	1.9*10-5*SC+0.0016	Cu	0.1154	-5.006
Regular sampling + high frequency peak odd	Sampling after peak of storm	3.2*10-5*SC+0.0112	Mn	0.0878	-0.326

This lag time in metals concentrations returning to baseline levels with specific conductance is most noticeable for Mn during March and April of 2019 (Figure 5). There also may be Mn lag times evident in November 2018 and January 2019 associated with a snowstorm on November 15th. However, due to the limited size of the dataset, it is unclear if these are outliers or caused by another mechanism.

2.4.2 Changes in Composition of Chemical Cocktails across Seasons and Snow Events

Across seasons at Sligo Creek, there was a general pattern where distinct chemical cocktails were more correlated with specific conductance during winter deicer use. During the spring and summer (Figure 6A) a weak clustering of Cu and Sr2+ and some base cations (Na+, K+, Mg2+) is present. During the peak of an episodic salinization event however (Figure 6B) Mn, Sr2+, and all base cations (Na+, Ca2+, Mg2+ and K+) were correlated with specific conductance. As specific conductance begins to slowly return to baseline levels (Figure 6C and 6D) base cations and trace metals remain correlated but Na+ and specific conductance are anti-correlated.

All PCA biplots illustrate correlations between base cations and trace metals throughout the year with the strongest groupings (highest correlation between co-mobilized elements) occurring at the peak of episodic salinization events. Less distinct groupings of elements were observed in spring and summer of 2019, and less variability was explained on the primary axis (55%), meaning co-mobilization was less distinct (Figure 6A). All metals, except Cu and Fe, were tightly clustered during a snowstorm salinity spike along with base cations and specific conductance (Figure 6B). A large proportion of the data was explained by principal component 1 (~72%)

in this plot, suggesting that co-mobilization was strong. Figure 6C illustrates a similar biplot to Figure 6B, but is taken from a dataset collected during the descending specific conductance limb of a snow event following deicer use. There was a looser cluster of major and trace elements, with two smaller subgroups therein. Specific conductance was not correlated to mobilized base cations and trace metals in this plot. As specific conductance reached a temporary elevated baseline a day after the peak of the storm, (Figure 6D) clustering of base cations and trace metals remained strong though Na+ was also found to be anti-correlated with specific conductance.

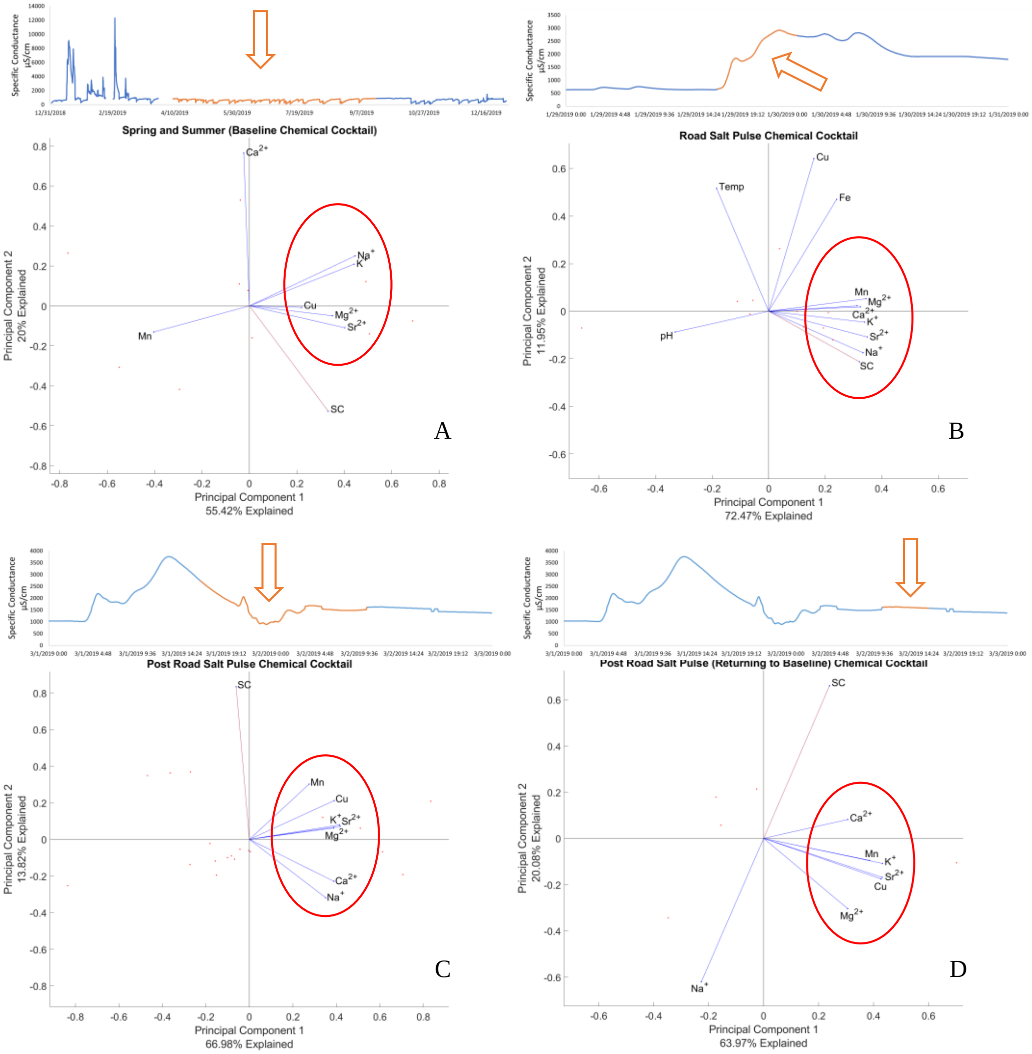

Figure 6. Principal Component Analysis

Principal Component Analysis of data collected from Sligo Creek. The X axis describes the most variance and Y axis describes the second most variance. In the PCA biplots, a small angle between analytes indicates positive correlation. At 90° of each other, analytes are considered uncorrelated, while diametrically opposed analytes are considered anti-correlated. Figure 6A illustrates a PCA for data collected during spring and summer 2019 representing a "baseline" chemical cocktail absent from road salting. The PCA in Figure 6B shows the peak of a winter storm captured between 1/29/19 and 1/30/19 illustrating a very tight grouping of major and trace elements mobilized through base cation exchange. Figure 6C illustrates a dataset collected during the descending limb of specific conductance during a storm between 3/1/19 and 3/2/19. A grouping of elements similar to #B can be seen in #C as well but with specific conductance and Na$^+$ becoming a less significant portion of the cocktail. Figure 6D shows data collected later in the day on 3/2/19, metal mobilization in this plot appears to be driven primarily by Ca^{2+}, Mg^{2+} and K$^+$ instead of Na$^+$ or specific conductance. This process is likely cyclic year to year, illustrating the complex and ever-changing nature of chemical cocktails in urban streams (USGS NWIS, 2020).

2.5 Discussion

Although there are multiple causes and sources of FSS in urban environments (Kaushal et al. 2017, 2019, 2020), episodic road salting events can be a driver of “winter” chemical cocktails in temperate regions (Kaushal, Likens Gene E., *et al.*, 2019; Löfgren, 2001). Our results show that chemical cocktail mobilization of base cations and trace metals begins within an hour of the start of snowstorms (Supplemental Figure 2.6), which correlates with the addition of large quantities of road salt (Haq *et al.*, 2018; Kaushal, Gold, *et al.*, 2018; Moore *et al.*, 2020; Snodgrass *et al.*, 2017). These chemical cocktails evolve in concentration and composition quickly over time, mobilizing Mn, Cu, Sr2+, and potentially other metals into solution (Figure 3 and 6); this mobilization may occur on exchange sites on colloids present in stream and bank sediment (Kaushal, Likens Gene E., *et al.*, 2019). Some of the mechanisms behind metal and base cation mobilization are thought to be a combination of base cation exchange and chloro-complexation among other mechanisms of chemical cocktail formation in urban environments (Kaushal *et al.*, 2017; Kaushal, Likens Gene E., *et al.*, 2019; Kaushal *et al.*, 2020).

2.5.1 FSS Increases with Impervious Surface Cover: Anthropogenic Inputs and Urban Karst

We observed increasing trends in concentrations of base cations with impervious surface cover at Sligo Creek and inorganic carbon and K+ with impervious surface cover at Rock Creek (Figure 4). Our results are similar to those reported elsewhere when increased chemical weathering of concrete urban infrastructure in the form of buildings, sidewalks, and drainage infrastructure (urban karst), leads to elevated base cations and inorganic carbon (Bonneau *et al.*, 2017; Kaushal *et al.*, 2015, 2020). Concrete weathering releases carbonates and base cations ($CaCO3$ and $Ca(OH)_2$) into downstream urban waterways (Demars and Benoit, 2019). Human-accelerated weathering in urban environments increases the potential for river alkalinization as carbonates are released during the chemical weathering process (Kaushal *et al.*, 2013, 2017). In Baltimore, MD, USA, drinking water alkalinity has increased by over 50% over almost 50 years due to release of carbonates from weathering of concrete infrastructure (buildings, pavements and pipes) as in other areas (Baker *et al.*, 2008; Davies *et al.*, 2010; Demars and Benoit, 2019; Kaushal *et al.*, 2017). The increase in dissolved inorganic carbon that we observed in our study may also be a function of concrete weathering. The increase in weathering products such as Ca2+, Mg2+, K+, and other ions has also been observed across space and time in other urban watersheds in Maryland (Kaushal *et al.*, 2017) and elsewhere (Barnes and Raymond, 2009; Demars and Benoit, 2019; Moore *et al.*, 2017). Increasing pH and alkalinity may also be due to reduced nitrogen and sulfur oxide emissions due to the implementation of the Clean Air Act and its amendments.

2.5.2 Episodic Salinization: Acute Mobilization of Chemical Cocktails due to FSS

We observed increased mobilization of chemical cocktails of base cations and trace metals in response to episodic road salting events (Figure 2 and 6). Na+, Ca2+, Mg2+, K+, Mn, Cu, Sr2+, and Fe were all more elevated during winters than summers, potentially due to ion exchange or chloro-complexation and other geochemical processes (Kaushal *et al.*, 2017; Kaushal, Likens Gene E., *et al.*, 2019;

Löfgren, 2001; Norrström and Bergstedt, 2001). We observed strong seasonal effects in metals (Table 2) with Mn and Cu being more than 2.5 and 4.6 times higher respectively in the winter than they were in the summer. Copper is toxic to aquatic organisms at these concentrations and can cause injury or death (Berntssen *et al.*, 1999; Mahrosh *et al.*, 2014). Mn pulses during winter storms reached 0.631 mg/L, over 12 times the EPA drinking water standard (US EPA, 2015a). Base cation and metal peaks were found at all sites during both winters immediately after winter storms and road salting. Similar effects may be causing elevated Mn in drinking water (Shaver, 2015). Previous work has shown that pure laboratory grade salt ions mobilize the exact same metals and base cations mobilized in this study (Haq *et al.*, 2018; Kaushal, Likens Gene E., *et al.*, 2019).

2.5.3 Episodic Salinization Shifts Mixtures in Chemical Cocktails

Mixtures of base cations and metals continuously evolve throughout seasons in regions effected by FSS. During the summer (Figure 6A), specific conductance was weakly associated with metals and cations (Cu, Mg2+, and Sr2+). Specific conductance peaks during the summer were often associated with periods of drought whereas precipitation events had a dilution effect (Figure 2). Specific conductance peaks associated with road salting (Figure 6B) were strongly correlated with almost every element (Na+, Sr2+, K+, Ca2+, Mg2+, and Mn); these strong correlations suggest that beyond a salinity threshold, co-mobilization increases dramatically. As specific conductance begins to decrease (Figure 6C) after a snow event, it becomes less correlated with the metals and base cations. Thus, contaminant mobilization is highly correlated with base cations and metals during the rising limb of a specific conductance pulse but not the falling limb, which can remain elevated for weeks afterwards (Kaushal, Likens Gene E., *et al.*, 2019). This may be due to ongoing mobilization of base cations after specific conductance and Na+ begin to decrease. The main grouping of base cations and trace metals (Ca2+, K+, Mg2+, Cu, Mn, and Sr2+, circled in Figure 6D) remain correlated while both Na+ and specific conductance are anti-correlated. Mn concentrations indicated that metals are mobilized up to 24 hours after peak stream salinity. These elevated metals concentrations may persist in urban streams for several months before returning to baseline conditions (Kaushal, Likens Gene E., *et al.*, 2019). The mechanism causing the lag times may be related to salt accumulation in sediments or groundwater (Cooper *et al.*, 2014).

2.5.4 Potential Mechanisms of Metal Mobilization

The concentration of metals in stream soils and sediments is likely due to the extent of watershed impervious surface area and proximity of roadways to streams. Heavy metals are a common pollutant deposited by motor vehicles (Adams *et al.*, 2009). Metals are often ionically bonded in colloids or ligands and therefore can also be mobilized through base cation exchange. The linear relationship between specific conductance and Cu may be caused by indirect mobilization of organic matter present in stream sediments and adjacent soils (often in the form of colloids) (Amrhein *et al.*, 1992; Nelson *et al.*, 2009; Norrström and Jacks, 1998). Cu has also been shown to associate with oxides and edge sites of clay silicate minerals (McBride, 1994; Nelson *et al.*, 2009). Mobilization of Mn due to road salting may be due to cation exchange through the formation of Cl- complexes and other geochemical processes. The amount of organic matter present, pH and redox conditions also may facilitate mobilization (Granato *et al.*, 1995; Wen, 2012a). Metals are generally less biologically available if they are complexed and more biologically available when dissolved (John and Levanthal, 1995). To research the possibility of Mn and Cu being contaminants within the road salt applied, daily loads of Mn and Cu were plotted against daily loads of Na+ in Supplemental Figure 2.7. Best fit lines were mostly logarithmic in nature with Na+ increasing faster than the metals. This leads us to believe there is little additional of Mn or Cu found in the salt applied. The relationship observed may be controlled by a single high concentration point however so further research should be conducted to rule out this possibility. Cation and metal mobilization using lab grade NaCl has been shown in previous work however (Haq *et al.*, 2018; Kaushal, Likens Gene E., *et al.*, 2019)

2.5.5 Specific Conductance as a Proxy for Chemical Cocktails in Road-Salt Impacted Streams

Simple linear regression models of specific conductance and metals showed promise for developing Mn and Cu proxies. NSE appears to be higher for Cu than Mn but both are within acceptable ranges for a natural system as are RMSE values ranging from 0.009 to 0.05. Adding additional data (from targeted snow event sampling), which populates the dataset with higher concentrations of both specific conductance and mobilized metals in response to road salt use, also appears to help overall model validation. Interestingly, the areas of the timeseries in which the model is the least accurate occur immediately after snowfall events where observed metals concentrations remain elevated after specific conductance has decreased to pre-snow event levels (Figure 5). This temporal lag time has been noted in other studies as well (e.g. (Kaushal, Likens Gene E., *et al.*, 2019)), with metals remaining elevated for up to a month after a storm. Difficulty modeling post storm metal values are also suggested in Table 4 with low RMSE and NSE values for data collected 24 hours after a salinization event. Datasets in Figure 3 are somewhat skewed towards lower concentrations with only a few winter storms captured at or near their maximum specific conductance. Additional hourly sampling data was collected before and during the peak of a storm at Sligo Creek (Supplemental Figure 2.3) which helps illustrate that the slopes derived in Figure 3 are valid and not simply being controlled by the sparse high values. Data collection during storms is challenging as specific conductance can increase by >1000 µS/cm per hour during a storm necessitating extremely high sampling frequencies or lab experiments to cover the gaps in the data. More research should be done just prior to, during, and after winter snowstorms to better constrain proxy models and account for metals release and biogeochemical mechanisms contributing to lag times in metals concentrations returning to baselevel following road salt events. A larger dataset would also allow for developing regression relationships based on weather, discharge, precipitation and/or season. Monitoring of a more “natural” catchment would also be beneficial to determine what baseline metal mobilization is without anthropogenic salt application. Data from urban water sheds with differing amounts of deicing salts applied could also help illuminate how much of the metals flux is originating from cation exchange in sediments vs. metals flux from motor vehicle particulate. It appears that specific conductance may not be a simple proxy for metal concentration. A more complex model integrating time dynamics of mobilization may be needed to account for the lag times discovered. Metal mobilization can be predicted with some precision with the current model but it's return to baselevel is not well constrained.

2.5.6 Future Monitoring Implications

Information on the concentrations and compositions of chemical cocktails will be key to identifying management strategies for this anthropogenic legacy. Specific conductance in streams is a robust proxy for Cl- concentrations in multiple studies (Corsi *et al.*, 2010; Daley *et al.*, 2009; Haq *et al.*, 2018; Moore *et al.*, 2020; Oswald *et al.*, 2019; Perera *et al.*, 2013; Robinson and Hasenmueller, 2017; Snodgrass *et al.*, 2017; Trowbridge *et al.*, 2010), but the potential for specific conductance to serve as a proxy for multiple base cations and trace metals in urban streams has not been thoroughly investigated until recently (Haq *et al.*, 2018; Kaushal, Likens Gene E., *et al.*, 2019; Kaushal *et al.*, 2020; Löfgren, 2001; Morel *et al.*, 2020), and less is known regarding applications of sensors to develop proxies. Our analysis suggests that proxies can be developed to predict concentrations of base cations and trace metals from sensors and characterize seasonal shifts in chemical mixtures or cocktails. Specific conductance sensors are becoming relatively inexpensive to install, and could be distributed across many sites, allowing for much higher frequency monitoring over larger spatial areas than grab sampling or automated water samplers. More research is needed to evaluate proxy relationships across sites spanning a wider gradient of environmental conditions and applications, to manage the causes and consequences of FSS. In addition, it is difficult to obtain high-resolution elemental data from expensive and labor-intensive ICP analyses in routine monitoring of streams and during hydrologic events compared to analyses of nutrients and carbon. When additional data is available, more complex models may also be used which create different regressions for baseline and storm events conditions and incorporate insights gained from the literature on concentration-discharge (C-Q) relationship variability. For example, the C-Qquick-slow model shows particular promise as it is able to consider the possibility that C-Q relationships vary across seasons (Minaudo *et al.*, 2019). Nonlinear empirical modeling may also be explored as similar studies have been conducted relating phosphorus concentrations to turbidity and discharge measurements (Minaudo *et al.*, 2017; Stutter *et al.*, 2017; Villa *et al.*, 2019).

Chapter 3: Stormwater Best Management Practices: Experimental Evaluation of Chemical Cocktails Mobilized by Freshwater Salinization Syndrome

3.1 Abstract

Freshwater Salinization Syndrome (FSS) refers to the suite of physical, biological, and chemical impacts of salt ions on the degradation of natural, engineered, and social systems. Impacts of FSS on mobilization of chemical cocktails has been documented in streams and groundwater, but little research has focused on the effects of FSS on stormwater best management practices (BMPs) such as: constructed wetlands, bioswales, ponds, and bioretention. However emerging research suggests that stormwater BMPs may be both sources and sinks of contaminants, shifting seasonally with road salt applications. We conducted lab experiments to investigate this premise; replicate water and soil samples were collected from four distinct stormwater feature types (bioretention, bioswale, constructed wetlands and retention ponds) and were used in salt incubation experiments conducted under six different salinities with three different salts ($NaCl$, $CaCl_2$, and $MgCl_2$). Increased salt concentrations had profound effects on major and trace element mobilization, with all three salts showing significant positive relationships across nearly all elements analyzed. Across all sites, mean salt retention was 34%, 28%, and 26% for Na^+, Mg^{2+} and Ca^{2+} respectively, and there were significant differences among stormwater BMPs. Salt type showed preferential mobilization of certain elements. $NaCl$ mobilized Cu, a potent toxicant to aquatic biota, at rates over an order of magnitude

greater than both $CaCl_2$ and $MgCl_2$. Stormwater BMP type also had a significant effect on elemental mobilization, with ponds mobilizing significantly more Mn than other sites. However, salt concentration and salt type consistently had significant effects on mean concentrations of elements mobilized across all stormwater BMPs ($p<0.05$), suggesting that processes such as ion exchange mobilize metals mobilize metals and salt ions regardless of BMP type. Our results suggest that decisions regarding the amounts and types of salts used as deicers can have significant effects on reducing contaminant mobilization to freshwater ecosystems.

3.2 Introduction

Freshwater Salinization Syndrome (FSS) is an emerging global pollution problem with both human health and environmental risks (Cañedo-Argüelles *et al.*, 2013; Kaushal *et al.*, 2005; Kaushal, Reimer, Mayer, Shatkay, Maas, Nguyen, Boger, Yaculak, Doody, Pennino, Bailey, Galella, Weingrad, Collison, Wood, Haq, Johnson, *et al.*, 2022; Kaushal, Likens, *et al.*, 2018b, 2019; Thorslund *et al.*, 2021). FSS occurs when anthropogenic sources of salt ions, like deicers, mining waste, fertilizers, sewage, and weathering of concrete raise the salinity and alkalinity of freshwater (Galella *et al.*, 2021; Kaushal *et al.*, 2017; Kaushal, Likens, *et al.*, 2018b). FSS has increasingly affected temperate areas of the United States and Europe over the past century corresponding to increased road salt use (Corsi *et al.*, 2010; Johnson and Stets, 2020; Kaushal, Reimer, Mayer, Shatkay, Maas, Nguyen, Boger, Yaculak, Doody, Pennino, Bailey, Galella, Weingrad, Collison, Wood, Haq, Johnson, *et al.*, 2022; Kaushal, Likens, *et al.*, 2019). For example, road salt sales in the US have increased from 164,000 tons in 1940 to over 22 million tons in 2019 (Abolfazli and

Strom, 2022). In temperate regions, extremely high salinity is sometimes caused by road salting during winter precipitation events (Galella *et al.*, 2021; Kaushal *et al.*, 2005; Moore *et al.*, 2020). Elevated salinity from FSS can act to corrode infrastructure, increase aquatic fauna mortality, and destabilize soil aggregate structures (Green *et al.*, 2008c; b; Mahrosh *et al.*, 2014; Kaushal, Likens, *et al.*, 2018b). In urban streams, high salinity can mobilize major and trace elements. Positive correlations have been found between specific conductance and mobilization of base cations and trace metals like Cu, Sr^{2+}, and Mn (Amrhein *et al.*, 1992; Galella *et al.*, 2021; Kaushal, Likens, *et al.*, 2019; Löfgren, 2001, p. 200). Ion exchange is thought to be amajor driver of contaminant mobilization, but redox reactions and Na^+ dispersion of colloids likely also play a role (Kaushal, Gold, *et al.*, 2018; Kinsman-Costello *et al.*, 2022). Increases in the magnitude and frequency of road salt pulses may also lead to the retention and release of multiple contaminants from urban stormwater Best Management Practices (BMPs)which are ubiquitous in urban landscapes (Kaushal, Reimer, Mayer, Shatkay, Maas, Nguyen, Boger, Yaculak, Doody, Pennino, Bailey, Galella, Weingrad, Collison, Wood, Haq, Johnson, *et al.*, 2022). Stormwater BMPs, also known as green stormwater infrastructure or structural BMPs, are generally designed with the goal of reducing soil erosion, attenuating peak runoff from impervious surfaces, and increasing groundwater connectivity (Loperfido *et al.*, 2014; Yu *et al.*, 2013). Previous research has shown that stormwater BMPs can be both sources and sinks of various elements, changing seasonally with road salt application (Barbier *et al.*, 2018).

A recent study estimates that between 2016 and 2036, the US will spend $19.2 billion (US) on stormwater infrastructure (Throwe *et al.*, 2020). Modern stormwater BMPs such as bioretention cells and constructed wetlands often act to retain nutrients and attenuate peak discharge (Collins *et al.*, 2010; Davis, 2008; Passeport *et al.*, 2013). Though the efficacy of nutrient removal and flood prevention varies from site to site, there is generally a net positive effect of stormwater BMPs on contaminant retention (Davis, 2008; Koch *et al.*, 2014). Less is known, however, about the effectiveness of stormwater BMPs for retaining the chemical cocktails mobilized by FSS (Kaushal, Mayer, *et al.*, 2022; Kaushal, Reimer, Mayer, Shatkay, Maas, Nguyen, Boger, Yaculak, Doody, Pennino, Bailey, Galella, Weingrad, Collison, Wood, Haq, Johnson, *et al.*, 2022). Chemical cocktails are an anthropogenic consequence of FSS, defined by an increase in the mobilization of inorganic and organic chemicals combinations both chronically and acutely due to salt pollution (Kaushal, Gold, *et al.*, 2018). Specifically in this research we will focus on chromatographic chemical cocktails (ions mobilized and retained on soil exchange sites) and reactive chemical cocktails (nutrients and redox sensitive elements) (Kaushal, Gold, *et al.*, 2018). Because salinization mobilizes chemical contaminants from sediments (Duan and Kaushal, 2015; Haq *et al.*, 2018; Kaushal, Likens, *et al.*, 2019), these salt ions may unintentionally affect the functioning of stormwater BMPs to release harmful ions and metals (Barbier *et al.*, 2018; Semadeni-Davies, 2006; Williams *et al.*, 2016).

Ion exchange in soils and sediments is a major driver of chemical cocktail mobilization during FSS, but changes in redox conditions, pH, and solubility, enhanced microbial activity, complexation, and others process likely play a role

(Kaushal, Mayer, *et al.*, 2022; Kaushal *et al.*, 2021; Kaushal, Likens, *et al.*, 2018b). Anthropogenic inputs of Na^+, Ca^{2+}, Mg^{2+}, and K^+ ions contribute to freshwater salinization across land uses (Kaushal *et al.*, 2017; Moore *et al.*, 2017). Positively charged metal ions such as Cu, Mn, Sr^{2+}, and Hg are often ionically bonded to negatively charged exchange sites on colloid particles in sediment and soil. Monovalent and divalent base cations, often introduced through road salting, act to displace metals and other cations into solution (Galella *et al.*, 2021; Kaushal, Likens, *et al.*, 2019; Morel *et al.*, 2020). Metals are also often transported as aqueous complexes with salt ions, forming metal-ligand bonds (Gaillardet *et al.*, 2003). Chloro-complexation may also play a role in mobilization as Cl^- can increase Cd^{2+} and Pb solubility (Kaushal, Likens, *et al.*, 2019). Combinations of road salts may be more harmful than using only NaCl. For example, a 3:2 ratio of $CaCl_2$ to NaCl (by weight), commonly used in road salting, was shown to mobilize greater quantities of As, Pb and Hg, from exposed soils than did NaCl alone (Sun *et al.*, 2015).

In addition to other salt ions and trace metals, FSS has also been shown to mobilize nutrients and organic matter (Green *et al.*, 2008a; Haq *et al.*, 2018; Inamdar *et al.*, 2022). As salt ions accumulate in soils, ammonium, nitrate, and organic nitrogen can be mobilized by ion exchange and other processes influencing relative proportions of inorganic *vs.* organic forms (Green *et al.*, 2008a; Hale and Groffman, 2006). The process of nitrification and denitrification and other forms of microbial activity may be also affected due to changes in pH (Green *et al.*, 2008a; Hale and Groffman, 2006). As a result, leaching of nitrate to local waterways increases in salt-impacted soils (Green *et al.*, 2008a). Road salt can also affect organic matter mobility, particularly when using NaCl (Green *et al.*, 2008c). Organic matter naturally helps maintain soil structure and aggregate stability (Peinemann *et al.*, 2005). Increased soil aggregate stability may be caused by the cation exchange capacity (CEC) of the organic matter present, the preference of Ca^{2+} ion exchange sites over Na^{+}, and the ability of soil organic matter to donate protons (Peinemann *et al.*, 2005). Ca^{2+} and Mg^{2+} help bind organic matter, but when mobilized through base cation exchange with Na^{+} from road salting, soil aggregate structure can begin to fail, mobilizing organic matter (Green *et al.*, 2008c; b). Initially, increases in salinity act to temporarily disperse organic matter, as soil aggregates break apart (Green *et al.*, 2008c; b). If this increased salinity becomes chronic,soil pH can decrease, howeer. Through the mobile anion effect (this is when negatively charged ions move through the soil profile), bonded base cations can be mobilized along with anions, exhausting buffering capacity) (Green *et al.*, 2008c; b). Elevated concentrations of NaCl, $CaCl_2$, and $MgCl_2$ in streams in response to road salting can also increase flocculation of suspended sediments and soils (Abolfazli and Strom, 2022), leading to larger soil aggregates, increased deposition, and compromising benthic ecosystems (Abolfazli and Strom, 2022). Flocculation increases with ion concentrations and is caused by cations (particularly divalent and multivalent cations) decreasing the thickness of the double layer (the two layers of charge surrounding an object), allowing for the attraction force to overcome the repulsion force, forming aggregates (Abolfazli and Strom, 2022).

Because stormwater BMPs are ubiquitous in urban landscapes (and also key features along urban hydrologic flowpaths (Kaushal and Belt, 2012)), it is critical to understand how these features are affected by FSS and how contaminant mobilization impacts urban water quality. With many different design strategies available, we seek to understand how different stormwater BMPs mobilize or retain chemical cocktails during road salting events and how different road salt types influence the chemical cocktails released. This research quantifies how different salt ions, salt concentrations, and stormwater BMPs affect the mobilization of carbon, nutrients, and major and trace elements. Our study aims to provide a better understanding of mobilization thresholds and the behavior of salts in stormwater BMPs. We assess whether these stormwater management features are potential salinity management tools or if salt adversely affects their function. Stormwater BMPs at the University of Maryland, College Park, Maryland, USA, 38°59'9.53"N, 76°56'33.21"W were chosen for this study. Bioretention cells, bioswales, wetlands, and ponds were chosen as sampling sites to test a variety of different stormwater BMPs (Table 5).

Table 5. Stormwater BMP Characteristics

Table 5: Characteristics of stormwater management BMPs sampled in this study. Samples were collected at the University of Maryland College Park 38°59'9.53"N, 76°56'33.21"W.

Site	Feature Area (m^2)	Drainage Area (m^2)	Year Constructed	Sediment Matrix
Bioswale #1	165	2,500	2017	Mulch and porous soil
Bioswale #2	175	2,500	2017	Mulch and porous soil
Bioretention #1	10	30,000	2006	Organic-rich soil
Bioretention #2	225	30,000	2003	Mulch and porous soil
Wetland #1	1,100	25,500	2001-2002	Sand / silt / clay
Wetland #2	2,400	4,200	1989-1994	Silt / clay
Pond #1	3,500	25,000	2002-2005	Silt / clay
Pond #2	700	6,000	<1988	Silt / clay

We hypothesize that salt type, salt concentration, and stormwater BMP type influence the mobilization of chemical cocktails from stormwater BMP sediments into aqueous form (Barbier *et al.*, 2018; Burgis *et al.*, 2020; Gill *et al.*, 2017; Kaushal, Reimer, Mayer, Shatkay, Maas, Nguyen, Boger, Yaculak, Doody, Pennino, Bailey, Galella, Weingrad, Collison, Wood, Haq, Johnson, *et al.*, 2022; Knox *et al.*, 2021; Maas *et al.*, 2021; McGuire and Judd, 2020; Semadeni-Davies, 2006; Snodgrass *et al.*, 2017). We hypothesize that different salt types will preferentially mobilize different major and trace elements, increasing salt concentration will mobilize greater concentrations of major and trace elements (until a potential threshold is reached), and stormwater BMP type will influence retention of major and trace elements. Our results have implications for guiding decisions regarding the amounts and types of road salt ions used and their potential to reduce contaminant mobilization in the environment.

3.3 Methods

3.3.1 Experimental Design of Salinization Experiments

For this study we sampled 8 separate stormwater BMPs consisting of pairs of stormwater BMP site types (bioretention cell 1 and 2, bioswale 1 and 2, wetland 1 and 2, and pond 1 and 2). The stormwater BMPs were all located within the Uinversity of Maryland College Park Campus but separate from each other hydrologically. Salt incubations of sieved sediment and unfiltered water from each stormwater BMP were prepared with three different salt types, NaCl, $CaCl_2$, and MgCl2. Six different treatment levels were chosen with salt quantities being normalized to 1, 2.5, 5, and 10 g Cl^-/L for each salt type, along with Milli-Q and stream water blanks. Each site had a duplicate sample prepared for each salt concentration including Milli-Q and stream water blanks. Every sampling site nominally had 12 samples prepared per salt type or 36 samples in total. When all sampling sites are included, 288 samples were prepared in total but 4 accidently became cross-contaminated and could not be used for further analysis, meaning n = 284. The quantity of salt added is not subtracted from subsequent ICP-OES analysis results. For clarity a graphic of the experimental design used in this study is included in supplemental material (Supplemental Figure 3.1)

3.3.2 Site Descriptions for Stormwater Management BMPs:

The stormwater BMPs sampled during this study were located on the University of Maryland College Park campus, in the Paint Branch watershed nested within the broader Anacostia River watershed. Soils, water quality, stormwater management, and hydrology within the Paint Branch watershed have been described extensively in our previous papers (Haq *et al.*, 2018; Kaushal, Reimer, Mayer, Shatkay, Maas, Nguyen, Boger, Yaculak, Doody, Pennino, Bailey, Galella, Weingrad, Collison, Wood, Haq, Johnson, *et al.*, 2022; Kaushal, Likens, *et al.*, 2019; Wood *et al.*, 2022) and elsewhere (Davis, 2008; Davis *et al.*, 2009, 2011; DiBlasi *et al.*, 2009; Jones and Davis, 2013). Four types of stormwater BMPs (bioretention cells, bioswales, wetlands, and ponds) were sampled, in pairs for a total of eight sampling sites (Table 5). Bioretention features are characterized by a base of sand, soil, or other type of organic media that treats stormwater while also allowing for infiltration, topped by mulch, vegetation, and an area for runoff pooling and overflow (Davis *et al.*, 2009). Bioswales are similarly constructed except they are usually sloped to convey water through the system efficiently (ASLA, 2022). Constructed wetlands are often characterized by a base liner, topped with soil, sand, gravel, or other organic material with shallow standing water, an assemblage of hydrophilic plants and planned surface and subsurface flow (Davis, 1995). Retention wet ponds are often built to store water, prevent flooding, and reduce peak storm discharge. In Maryland retention ponds are often 1.8-2.4 m deep with accommodations for anticipated flooding (10 and 100 year) and adequate overflow spillways (Schueler and Claytor, 2009). Current regulations require ponds to have vegetative cover, but older structures may be concrete lined. (Schueler and Claytor, 2009). Henceforth, we refer to the sites as: Bioretention #1 and #2, Bioswale #1 and #2, Wetland #1 and #2, and Pond #1 and #2. Sites were chosen based on similar characteristics. Some sites were ephemeral and four (Bioswales #1 and #2, and Bioretention #1 and #2) had no surface water when sampled. For these sites, water from nearby Paint Branch and Campus Creek were collected. Surface water for the remaining four sites was collected *in-situ* from the stormwater BMPs.

Bioswales #1 and #2 were constructed in 2017 to help manage runoff from new building construction and a new ~2,500 m^2 parking lot. Three bioswales were constructed but the two most similar in size were sampled for this study (Figure 7).

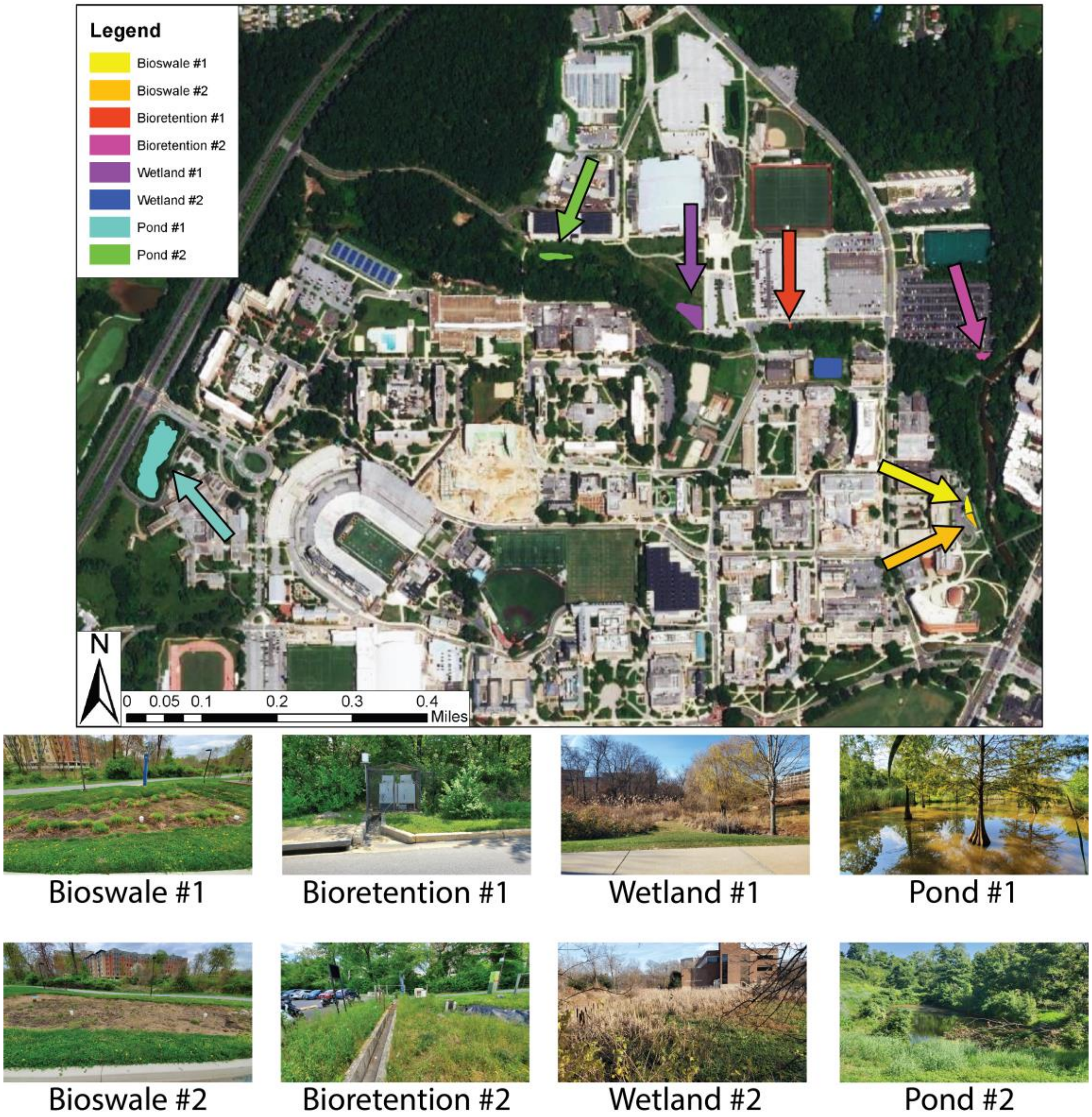

Figure 7. Stormwater Management Features

Stormwater management features sampled across the UMD campus. Duplicate bioswale, bioretention, wetland, and pond sites were selected.

Cells (the discreet vegetated units which facilitate filtration, storage, and groundwater connection) were constructed of a top layer (3-8 cm) of mulch overlaying a porous soil matrix (Davis *et al.*, 2011). Water tolerant species were planted in this area to promote evapotranspiration and slow overland flow of runoff.

Bioretention site #1 and #2 were built three years apart from one another. Bioretention #1 was constructed in 2006 to help drain a neighboring ~30,000 m^2 parking lot. The site is the smallest of the stormwater BMPs sampled, with a 10-m concrete inlet collecting runoff from the parking lot and an outlet discharging into Campus Creek. Organic-rich soil with overlaying grasses was present in the conduit. Bioretention #2, built in 2003 to treat runoff from a 2,000 m^2 parking lot (Davis *et al.*, 2011), contains two separate, parallel cells which originally contained porous soil covered with a 3-8 cm layer of decomposed hardwood mulch (Davis *et al.*, 2011). In order to increase biological diversity, evapotranspiration, and pollutant uptake, trees, shrubs, and grasses were planted (Davis *et al.*, 2011).

Wetland #1 was constructed and Wetland #2 was accidental (an unintentional artefact of management) (*sensu* Maas et al. 2021). During 2001 and 2002, Wetland #1 was installed to help control runoff from a 17,000 m^2 indoor stadium facility at the University of Maryland (UMD) and neighboring 8,500 m^2 parking lot. Wetland #1 contains two parallel cells containing individual water inlets, each with a ponded section with boulders and cobbles to help reduce erosion and a shallow marsh area populated with wetland flora. Wetland #2 was originally designed as a runoff pond sometime between 1989 and 1994 to capture runoff from four neighboring buildings on the UMD campus and three small parking lots. After ~30 years of gradually infilling through slack water sedimentation, the site has transitioned to a heavily vegetated wetland with <10% open water.

Ponds #1 and #2 were similar in design but differed in age. Pond #1 was constructed between 2002 and 2005 to accept drainage from the UMD's 25,000 m^2 School of Music building complex. The site contains a riparian buffer planted around the lake's border to reduce its temperature and limit overland flow. The oldest site sampled was Pond #2, constructed prior to 1988 and further altered in 2001. Pond #2 has high banks and high-water depth, with abundant wetland flora and fauna (*e.g.* amphibians).

3.3.3 Salinization Experiments to Determine Mobilization of Chemical Cocktails

Sediment samples were collected along the hydrologic flowpaths of stormwater BMPs. Individual samples were homogenized in the field and later subdivided into replicate batches for use in salinization incubations. Similar to our previous methods in Haq *et al.* (2018), Duan and Kaushal (2015), and Kaushal *et al.* (2022), ~1-kg of sediment was removed from each site with a clean plastic trowel and placed into a new zip-top bag. Metal tools were not used so as to not introduce additional metals to the sediment. At least two liters of surface water were also collected (*via* acid-washed HPDE Nalgene bottles; no headspace). If no surface water was available within the site itself, the closest neighboring body of water was used as a collection point. Both sediment and water samples were put in a chilled cooler for transport back to the laboratory and chilled at $4^{o}C$ (Haq *et al.*, 2018). In order to increase homogeneity, the sediment samples were sieved through a 4-mm sieve and the fines were utilized for incubation analysis (Duan and Kaushal, 2015; Haq *et al.*, 2018). Sixty grams of sediment fines and 100 mL of unfiltered stream water from each site were added to duplicate acid-washed glass Erlenmeyer flasks. The vertical water column created therein simulates a vertical water column with both a sediment-water and water-air interface.

The common road salts NaCl, $MgCl_2$, and $CaCl_2$ were used to create aqueous salt treatments for this study. Salt quantities were normalized to Cl^- concentration, with concentrations of 1, 2.5, 5, and 10 g Cl^-/L added to stream water and ultra-high purity Milli-Q water (pH 7), for a total of six treatment levels (Table 6).

Table 6. Salt Additions Normalized to Chloride

Quantity of NaCl, $CaCl_2$, and $MgCl_2$ added to unfiltered stream water for each incubation.

Salt Introduced	0 g Cl^-/L	1 g Cl^-/L	2.5 g Cl^-/L	5 g Cl^-/L	10 g Cl^-/L
NaCl	0.0	1.6	4.1	8.2	16.5
$CaCl_2$	0.0	1.6	3.9	7.8	15.7
$MgCl_2$	0.0	1.3	3.4	6.7	13.4

The range of salinities were selected based upon the peak salinity readings within the Washington DC and Baltimore MD metro areas, with the highest concentration of added Cl^- being just over half that of seawater. Long-term chloride concentrations in Baltimore streams reached above 5 g/L (Kaushal *et al.*, 2005) and, in wetlands and ponds, Cl^- concentrations high as 13.5 g/L were observed (Hintz and Relyea, 2019).

All sediment aliquots for each site were incubated together with their duplicates within 12 hours of field collection. Flasks were loosely capped with an aluminum foil shield used to block out any ambient light during incubation. Flasks were placed on a shaking table and slowly agitated for 24 hours at a room temperature of ~20°C. Agitation during incubation simulated water flow through the stormwater BMP features. Post-incubation, water was carefully removed from the flask using a pipette to avoid undue disturbance to the sediment. Water was immediately filtered through an ashed 0.7-micron glass fiber filter and stored in a refrigerator at 4°C or frozen for later analysis. A portion of the filtered incubation water was diluted to < 0.5g Cl^- and acidified in a 60 mL acid-washed HDPE Nalgene bottle to a concentration of 0.5% metal grade nitric acid. Acidification made the sample shelf stable at room temperature for 6 months and allowed for later analysis via inductively coupled plasma optical emission spectrometry ICP-OES (Environmental Monitoring Systems Laboratory, 1996).

3.3.4 Sampling a Stormwater Management Feature During a Snow Event

An opportunity to study real world chemical cocktail formation in response to road salt applications in a stormwater BMP presented itself during the winter months of this study. In order to corroborate our incubation results, an ISCO 3700 water sampler was used to sample the surface water of Wetland #2 during a snow event (and road salt applications) between 1/28/22 and 1/29/22 (Teledyne, 2022). Samples were immediately collected and kept chilled at 4°C until filtered through an ashed 0.7-micron glass fiber filter. A 60 ml aliquot of the sample was transferred to an acid-washed HDPE Nalgene bottle and acidified to a concentration of 0.5% metal grade nitric acid. Acidification made the sample shelf stable at room temperature for 6 months and allowed for later analysis via inductively coupled plasma optical emission spectrometry ICP-OES (Environmental Monitoring Systems Laboratory, 1996).

3.3.5 Water Chemistry Analyses

Base cation and trace metal concentrations in the acidified water samples were measured via ICP-OES on a Shimadzu Elemental Spectrometer (ICPE-9800; Shimadzu, Columbia, Maryland, USA). Base cation measurements were analyzed in radial mode (across a plasma flame), and trace metals measurements, were analyzed in axial mode (down plasma flame). The instrument was calibrated to the range of trace metals that are commonly observed in urban streams via the utilization of an Inorganic Ventures standard.

Dissolved organic carbon (DOC), measured as non-purgeable organic carbon, dissolved inorganic carbon (DIC) and total dissolved nitrogen (TDN) were measured using a Shimadzu Total Organic Carbon Analyzer (TOC-V CPH/CPN) total nitrogen module, TNM-1 (Haq *et al.,* 2018).

3.3.6 Statistical methods

In order to elucidate the relationships between salt application and elemental mobilization, linear regressions were performed in Microsoft Excel (Figure 8 and Table 7) with Cl^- concentration as the independent variable and elemental concentration in mg/L as the dependent variable. Retention of Na^+, Ca^{2+}, and Mg^{2+} was determined by calculating the concentration of Na^+, Ca^{2+}, and Mg^{2+} added to the incubation aliquots in mg/L and subtracting the concentration (in mg/L) measured after 24 hours of incubation. The quantity retained (mg/L) was plotted against the initial concentration added (Figure 9) to indicate how much of the cation added is sorbed onto colloids and other sediment particles.

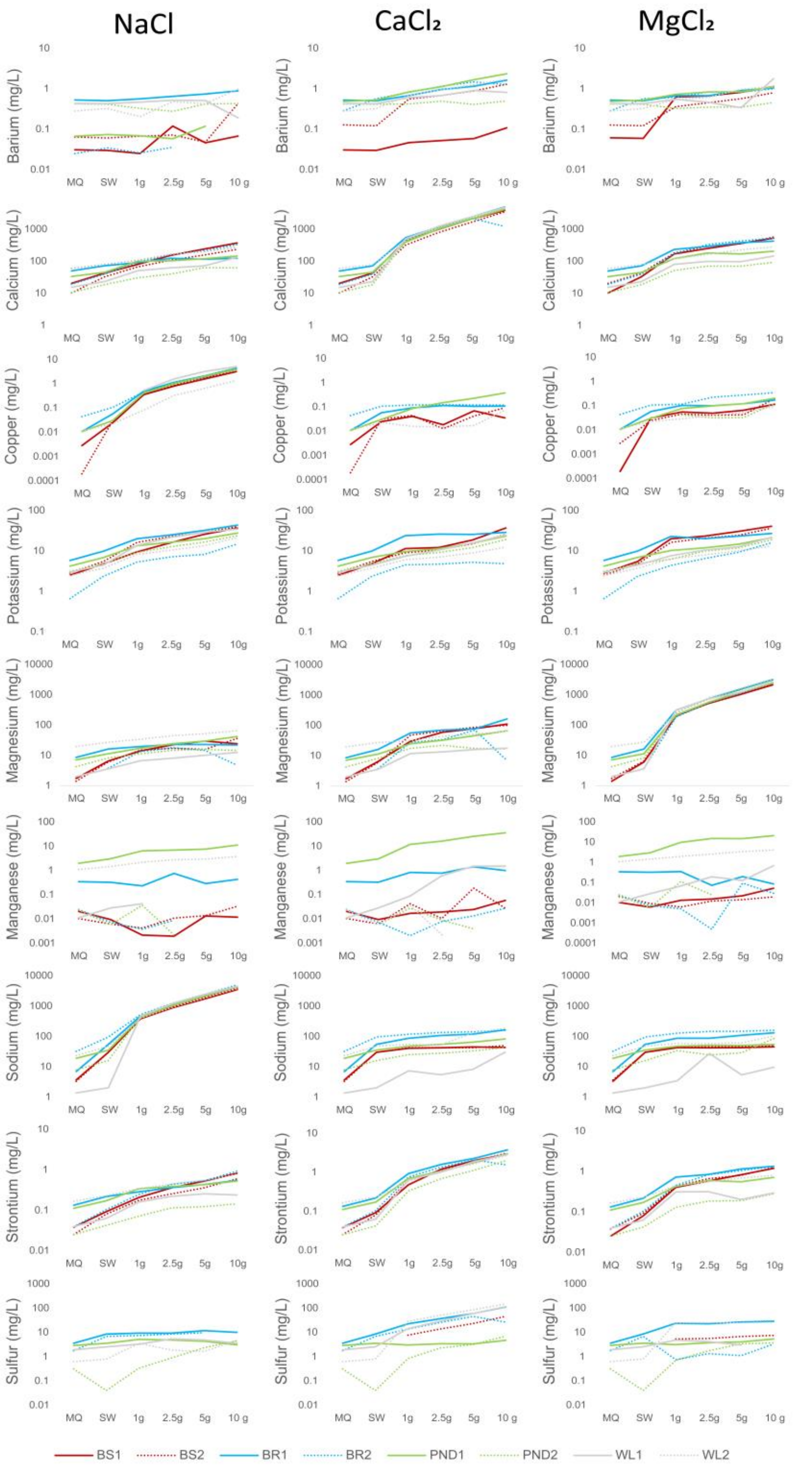

Figure 8. Elemental Mobilization

Elements mobilized by salt type and concentration. Scales are matching between salt types to better illustrate changes in mobilization by salt type. For visual clarity, the Y axis is plotted logarithmically to allow for easy comparison between sub-plots.

Table 7. R^2 Results – Elemental Concentration / Cl^- Concentration

Linear regression analysis of elemental concentration to Cl^- concentration added in incubations. R^2 results are color coded from white to green with green indicating high R^2 and white indicating low R^2. Significant cells are shown in bold typeface (p-values <0.05).

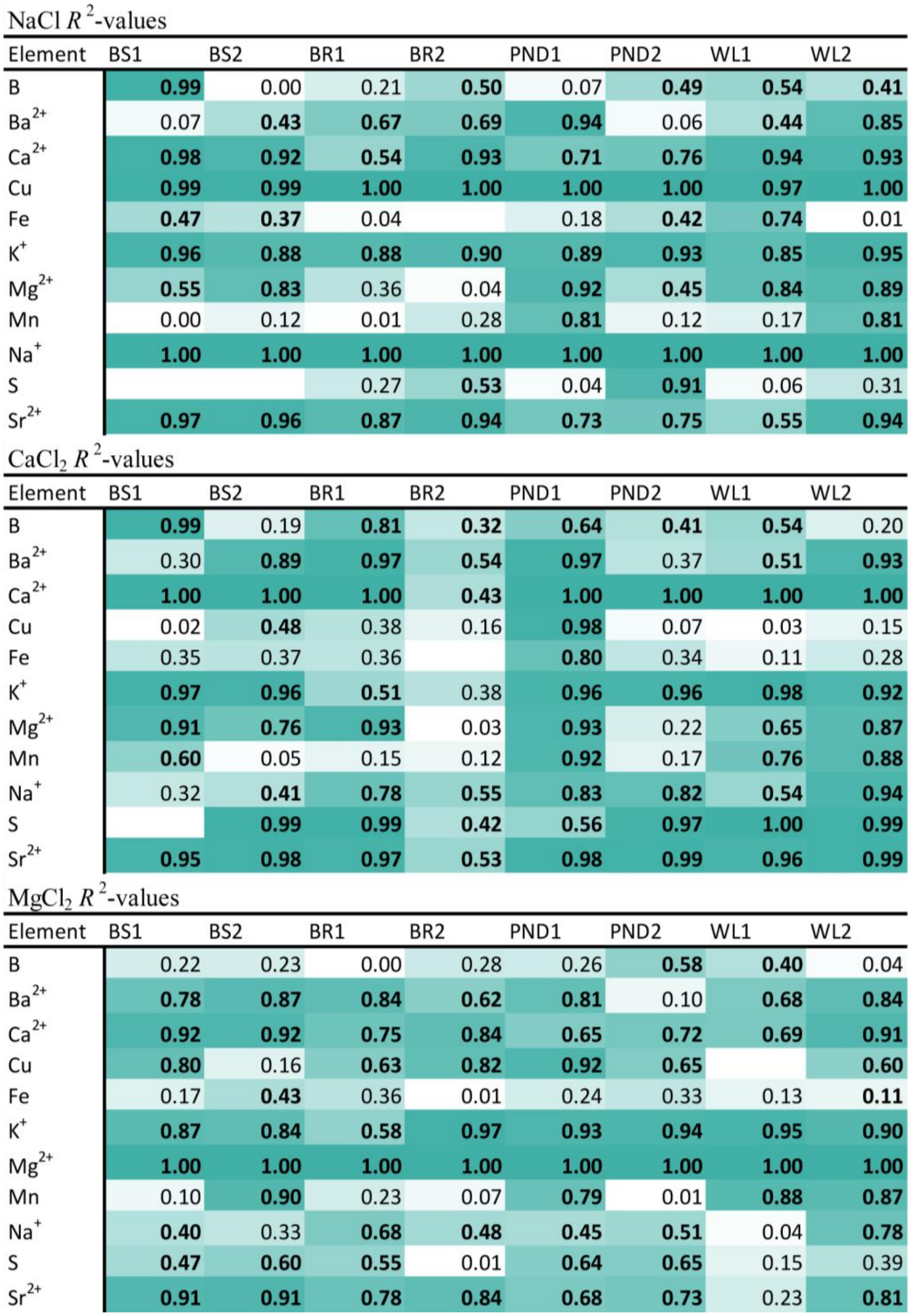

NaCl R^2-values

Element	BS1	BS2	BR1	BR2	PND1	PND2	WL1	WL2
B	**0.99**	0.00	0.21	**0.50**	0.07	**0.49**	**0.54**	**0.41**
Ba^{2+}	0.07	**0.43**	**0.67**	**0.69**	**0.94**	0.06	**0.44**	**0.85**
Ca^{2+}	**0.98**	**0.92**	**0.54**	**0.93**	**0.71**	**0.76**	**0.94**	**0.93**
Cu	**0.99**	**0.99**	**1.00**	**1.00**	**1.00**	**1.00**	**0.97**	**1.00**
Fe	**0.47**	**0.37**	0.04		0.18	**0.42**	**0.74**	0.01
K^+	**0.96**	**0.88**	**0.88**	**0.90**	**0.89**	**0.93**	**0.85**	**0.95**
Mg^{2+}	**0.55**	**0.83**	0.36	0.04	**0.92**	**0.45**	**0.84**	**0.89**
Mn	0.00	0.12	0.01	0.28	**0.81**	0.12	0.17	**0.81**
Na^+	**1.00**	**1.00**	**1.00**	**1.00**	**1.00**	**1.00**	**1.00**	**1.00**
S			0.27	**0.53**	0.04	**0.91**	0.06	0.31
Sr^{2+}	**0.97**	**0.96**	**0.87**	**0.94**	**0.73**	**0.75**	**0.55**	**0.94**

$CaCl_2$ R^2-values

Element	BS1	BS2	BR1	BR2	PND1	PND2	WL1	WL2
B	**0.99**	0.19	**0.81**	**0.32**	**0.64**	**0.41**	**0.54**	0.20
Ba^{2+}	0.30	**0.89**	**0.97**	**0.54**	**0.97**	0.37	**0.51**	**0.93**
Ca^{2+}	**1.00**	**1.00**	**1.00**	**0.43**	**1.00**	**1.00**	**1.00**	**1.00**
Cu	0.02	**0.48**	0.38	0.16	**0.98**	0.07	0.03	0.15
Fe	0.35	0.37	0.36		**0.80**	0.34	0.11	0.28
K^+	**0.97**	**0.96**	**0.51**	0.38	**0.96**	**0.96**	**0.98**	**0.92**
Mg^{2+}	**0.91**	**0.76**	**0.93**	0.03	**0.93**	0.22	**0.65**	**0.87**
Mn	**0.60**	0.05	0.15	0.12	**0.92**	0.17	**0.76**	**0.88**
Na^+	0.32	**0.41**	**0.78**	**0.55**	**0.83**	**0.82**	**0.54**	**0.94**
S		**0.99**	**0.99**	**0.42**	**0.56**	**0.97**	**1.00**	**0.99**
Sr^{2+}	**0.95**	**0.98**	**0.97**	**0.53**	**0.98**	**0.99**	**0.96**	**0.99**

$MgCl_2$ R^2-values

Element	BS1	BS2	BR1	BR2	PND1	PND2	WL1	WL2
B	0.22	0.23	0.00	0.28	0.26	**0.58**	**0.40**	0.04
Ba^{2+}	**0.78**	**0.87**	**0.84**	**0.62**	**0.81**	0.10	**0.68**	**0.84**
Ca^{2+}	**0.92**	**0.92**	**0.75**	**0.84**	**0.65**	**0.72**	**0.69**	**0.91**
Cu	**0.80**	0.16	**0.63**	**0.82**	**0.92**	**0.65**		**0.60**
Fe	0.17	**0.43**	0.36	0.01	0.24	0.33	0.13	**0.11**
K^+	**0.87**	**0.84**	**0.58**	**0.97**	**0.93**	**0.94**	**0.95**	**0.90**
Mg^{2+}	**1.00**	**1.00**	**1.00**	**1.00**	**1.00**	**1.00**	**1.00**	**1.00**
Mn	0.10	**0.90**	0.23	0.07	**0.79**	0.01	**0.88**	**0.87**
Na^+	**0.40**	0.33	**0.68**	**0.48**	**0.45**	**0.51**	0.04	**0.78**
S	**0.47**	**0.60**	**0.55**	0.01	**0.64**	**0.65**	0.15	0.39
Sr^{2+}	**0.91**	**0.91**	**0.78**	**0.84**	**0.68**	**0.73**	0.23	**0.81**

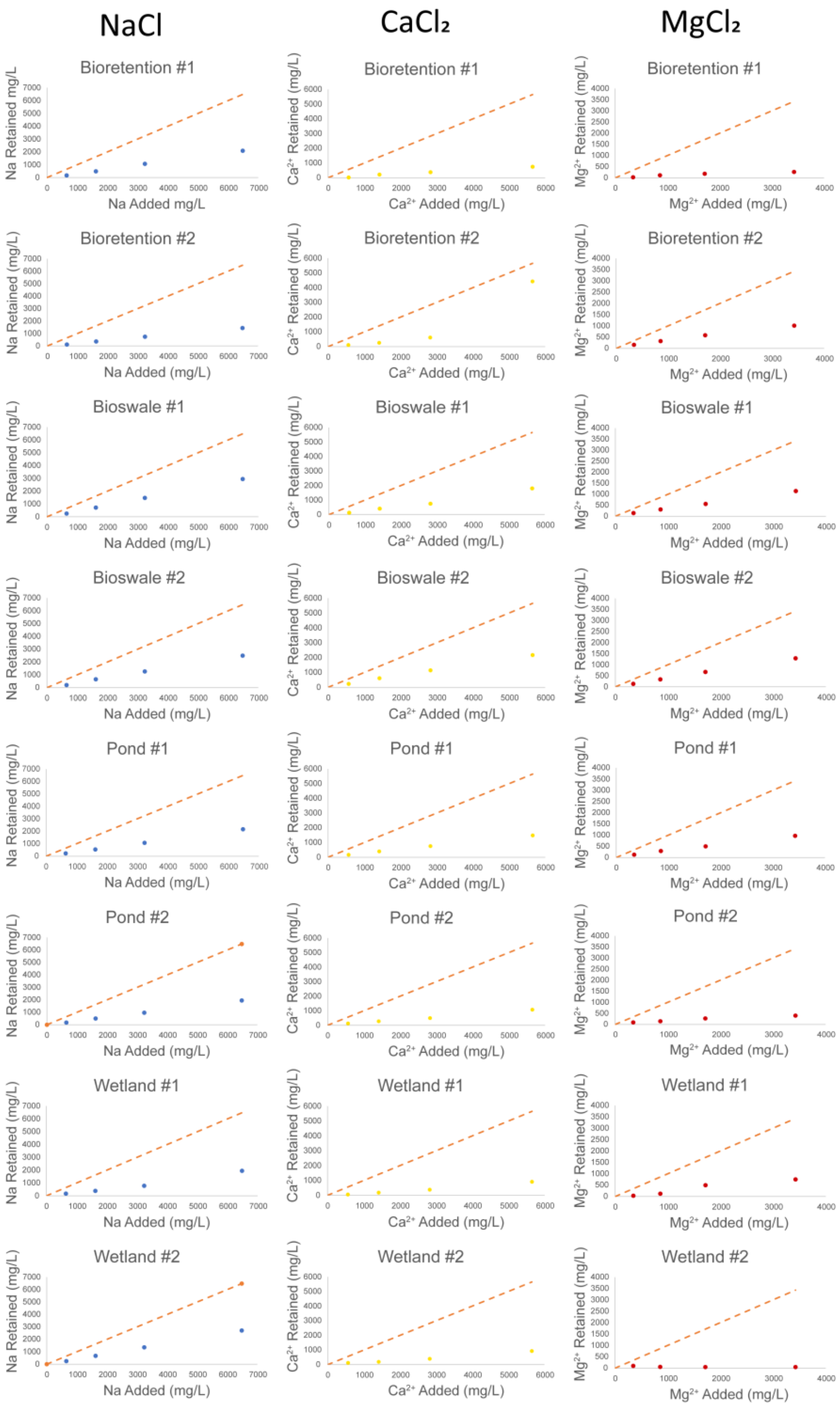

Figure 9. Salt Retention

Na, Ca^{2+}, and Mg^{2+} retention after NaCl, $CaCl_2$, and $MgCl_2$ incubations. The orange dash line indicates 100% adsorption, and the blue, yellow and red circles are the measured values in mg/L.

The dataset was found to be normally distributed using a Quantile – Quantile plot (QQ plot) and density plot of residuals (Supplemental Figure 3.2, 3.3). Three-way analysis of variance (ANOVA) was performed with concentrations of respective elements as dependent variables in models that included all treatments (stormwater BMP type, salt type, or salt concentration levels) as independent variables. Main treatment and interaction effects with alpha level ($p \leq 0.05$) were considered statistically significant and indicating that the major or trace element analyzed increased in concentration (*i.e.,* mobilized) due to stormwater BMP type, salt type, and salt concentration or interactions thereof. For three-way ANOVAs, Tukey's Honestly Significant Difference test was used to make pair-wise comparisons among means for respective treatments (stormwater BMP type, salt type, salt concentration level) and interactions among treatments to determine which BMP type, salt type, salt concentration, or combination thereof influenced elemental mobilization. Data were analyzed using R-Studio, software.

Principal component analysis (PCA) was used to explore multivariate patterns in major and trace element mobilization. The PCA was completed in MATLAB, where datasets were normalized to correct for the different scales of the data used. PCA was used to illustrate the changing correlations between major and trace elements based on salt type used in the incubation. Distinct groupings of elements represent distinct chemical cocktails mobilized by NaCl, $CaCl_2$, and $MgCl_2$; any element within a 90^o angle of one another is considered positively correlated in a PCA analysis, and any element 180^o opposed to one another is non-correlated.

3.4 Results

3.4.1 Retention of Salt Ions among Stormwater BMPs

We calculated retention of Na^+, Mg^{2+} and Ca^{2+} by comparing the known concentration of each cation in the water added to each incubation to the measured concentration in post incubation aliquots. The retention shown in mg/L (Figure 9) indicates how much of the cation is retained on cation exchange sites in the stormwater BMPs sediment. Other biogeochemical reactions may also be at occurring, but we believe cation exchange to be the primary driver of the observed retention. Na^+, Mg^{2+} and Ca^{2+} retention varied based on the type of salt added, salt concentration, and the stormwater BMP sampled. Retention increased with increasing concentration of Na^+, Mg^{2+} and Ca^{2+} added in all but one sampling site. At Wetland #2, Mg^{2+} retention decreased as more was added, 103 mg/L was retained of the initial 342.8 mg/L dose (1g Cl^-/L) and retention decreased to 47.8 mg/L of the initial 3428 mg/L dose (10g Cl^-/L). This may be caused by locally high Mg^{2+} levels present in the sediment at Wetland #2 as elevated Mg^{2+} levels were present in NaCl incubations of the site. Mean Na^+ retention was the highest at 1011 mg/L (34%), likely due to it being monovalent, with divalent Mg^{2+} and Ca^{2+} averaging 690 mg/L (28%) and 357 mg/L (26%) retention, respectively. Using 3-way ANOVA analysis and Tukey's Honestly-Significant-Difference tests, retention was found to be significantly different between salt types. Stormwater BMP type was also found to be a significant factor in retention with bioswale sites significantly retaining the most salt cations (mean retention 914 mg/L) and wetland sites significantly retaining the least salt cations (mean retention 543 mg/L). Bioretention and pond sites retained similar quantities of base cations (mean retention 646 mg/L and 633mg/L respectively) making them statistically indistinct from one another.

Our results showed that cation exchange sites could become saturated at elevated salt levels. In 79% of incubations, base cation retention decreased or plateaued with increasing salt concentration, suggesting that cation exchange sites on colloids and organic matter became saturated. The remaining 21% of incubations showed increasing cation retention with increasing salinity. If saturation is reached on soil exchange sites, the stormwater BMP may no longer be able to reduce the effects of salinization downstream and any metals will be mobilized into solution.

3.4.2 Mobilization of Elements across Salt Concentrations, Salt Types, and Site Types

Significant mobilization was observed in salt ions, metals, DIC, DOC, and TDN across stormwater BMP types, salt concentrations, and salt types (Tables 7, 8, 9, 10, Figure 8).

Table 8. 3-Way ANOVA

Three-way ANOVA analysis data assessing main effects of stormwater BMP type, salt type and salt concentration on resulting elemental mobilization. Major and trace elemental analysis is shown, along with dissolved inorganic carbon (DIC), dissolved organic carbon as non-purgeable organic carbon (DOC), and total dissolved nitrogen (TDN). Significant p values are denoted by bold typeface. Lower p-values and higher F-ratios have greater significance.

A

	BMP Type			Salt Type			Salt Concentration		
Variable	N	F-ratio	p-value	N	F-ratio	p-value	N	F-ratio	p-value
B	284	38.795	**<0.001**	284	5.295	**0.006**	284	3.838	**0.002**
Ba^{2+}	284	38.67	**<0.001**	284	27.826	**<0.001**	284	37.97	**<0.001**
Ca^{2+}	284	1.522	0.21	284	619.158	**<0.001**	284	235.919	**<0.001**
Cu	284	1.466	0.225	284	321.924	**<0.001**	284	101.24	**<0.001**
Fe	284	21.078	**<0.001**	284	2.049	0.13143	284	1.23	0.29609
K^{+}	284	19.132	**<0.001**	284	12.86	**<0.001**	284	120.436	**<0.001**
Mg^{2+}	284	5.487	**0.00119**	284	2214.832	**<0.001**	284	699.21	**<0.001**
Mn	284	26.152	**<0.001**	284	2.424	0.09105	284	3.949	**0.00191**
Na^{+}	284	8.078	**<0.001**	284	5305.091	**<0.001**	284	1578.654	**<0.001**
$Sr2^{+}$	284	22.656	**<0.001**	284	377.479	**<0.001**	284	282.989	**<0.001**
DIC	82	1232.88	**<0.001**	82	32.09	**<0.001**	82	33.05	**<0.001**
DOC	82	1051.47	**<0.001**	82	24.972	**<0.001**	82	7.247	**<0.001**
TDN	82	130.305	**<0.001**	82	16.089	**<0.001**	82	22.533	**<0.001**

B

	BMP TYPE:Salt			BMP TYPE:Treatment			Salt:Treatment			BMP TYPE:Salt:Treatment		
Variable	N	F-ratio	p-value	N	F-ratio	p-value	N	F-ratio	p-value	N	F-ratio	p-value
B	284	5.45	**<0.001**	284	3.464	**<0.001**	284	1.632	0.099	284	1.657	0.022
Ba^{2+}	284	3.471	**0.003**	284	0.492	0.943	284	3.643	**<0.001**	284	0.641	0.927
Ca^{2+}	284	4.682	**<0.001**	284	1.552	0.09	284	159.525	**<0.001**	284	2.214	**<0.001**
Cu	284	0.641	0.697	284	0.411	0.975	284	89.056	**<0.001**	284	0.383	0.999
Fe	284	3.265	**0.00431**	284	0.588	0.88273	284	1.836	0.05608	284	1.149	0.2805
K^{+}	284	2.537	**0.02158**	284	3.406	**<0.001**	284	2.55	**0.00632**	284	0.592	0.95587
Mg^{2+}	284	7.728	**<0.001**	284	2.218	**0.00678**	284	656.652	**<0.001**	284	3.621	**<0.001**
Mn	284	1.789	0.10261	284	2.339	**0.00408**	284	0.489	0.8964	284	0.332	0.99967
Na^{+}	284	6.223	**<0.001**	284	3.262	**<0.001**	284	1479.792	**<0.001**	284	2.504	**<0.001**
$Sr2^{+}$	284	1.615	0.144	284	3.724	**<0.001**	284	74.651	**<0.001**	284	0.816	0.741
DIC	X	X	X	82	39.41	**<0.001**	82	3.61	**0.001**	X	X	X
DOC	X	X	X	82	10.91	**<0.001**	82	1.363	**<0.001**	X	X	X
TDN	X	X	X	82	7.472	**<0.001**	82	1.043	**<0.001**	X	X	X

Table 9. Tukey's Test – Salt

Tukey's Honestly-Significant-Difference test was used to compare mean elemental mobilization in the three-way ANOVAs across different salts (NaCl, $CaCl_2$, $MgCl_2$). Mean mobilization rates for a given major or trace element share a common letter in the post-hoc column when they are not statistically different from one another (*p*>0.05).

Salt	**Mean mg/L**	**SE**	**Post-hoc**	**Mean mg/L**	**SE**	**Post-hoc**	**Mean mg/L**	**SE**	**Post-hoc**
	Barium			**Boron**			**Calcium**		
NaCl	0.422	0.029	a	0.933	0.266	a	100.106	8.235	a
$CaCl_2$	0.710	0.053	b	0.720	0.241	ab	1294.752	152.265	b
$MgCl_2$	0.601	0.032	b	0.224	0.069	b	173.952	15.994	a
	Copper			**Iron**			**Potassium**		
NaCl	1.175	0.150	a	4.031	1.230	a	14.985	1.172	a
$CaCl_2$	0.054	0.007	b	2.488	0.854	a	11.151	0.868	a
$MgCl_2$	0.072	0.008	b	1.557	0.528	a	12.568	0.987	a
	Magnesium			**Manganese**			**Sodium**		
NaCl	17.856	1.423	a	1.166	0.250	a	1280.582	153.306	a
$CaCl_2$	35.826	3.533	a	2.496	0.689	a	55.831	4.922	b
$MgCl_2$	791.744	99.690	b	1.803	0.463	a	53.085	4.409	b
	Strontium			**DIC**			**DOC**		
NaCl	0.280	0.022	a	20.836	2.650	a	26.267	3.438	a
$CaCl_2$	1.107	0.105	b	17.418	0.610	a	5.737	0.601	b
$MgCl_2$	0.472	0.041	a	16	1.144	a	14.922	1.706	ab
	TDN								
NaCl	6.394	0.792	a						
$CaCl_2$	3.896	0.361	b						
$MgCl_2$	7.164	0.871	a						

Table 10. Tukey’s Test – BMP Type

Tukey’s Honestly-Significant-Difference test was used to make pair-wise comparisons among mean elemental mobilization in the three-way ANOVAs across BMP type (Bioswale, Bioretention, Pond, Wetland). Mean mobilization rates for a given major or trace element share a common letter in the post-hoc column when they are not statistically different from one another (*p*>0.05).

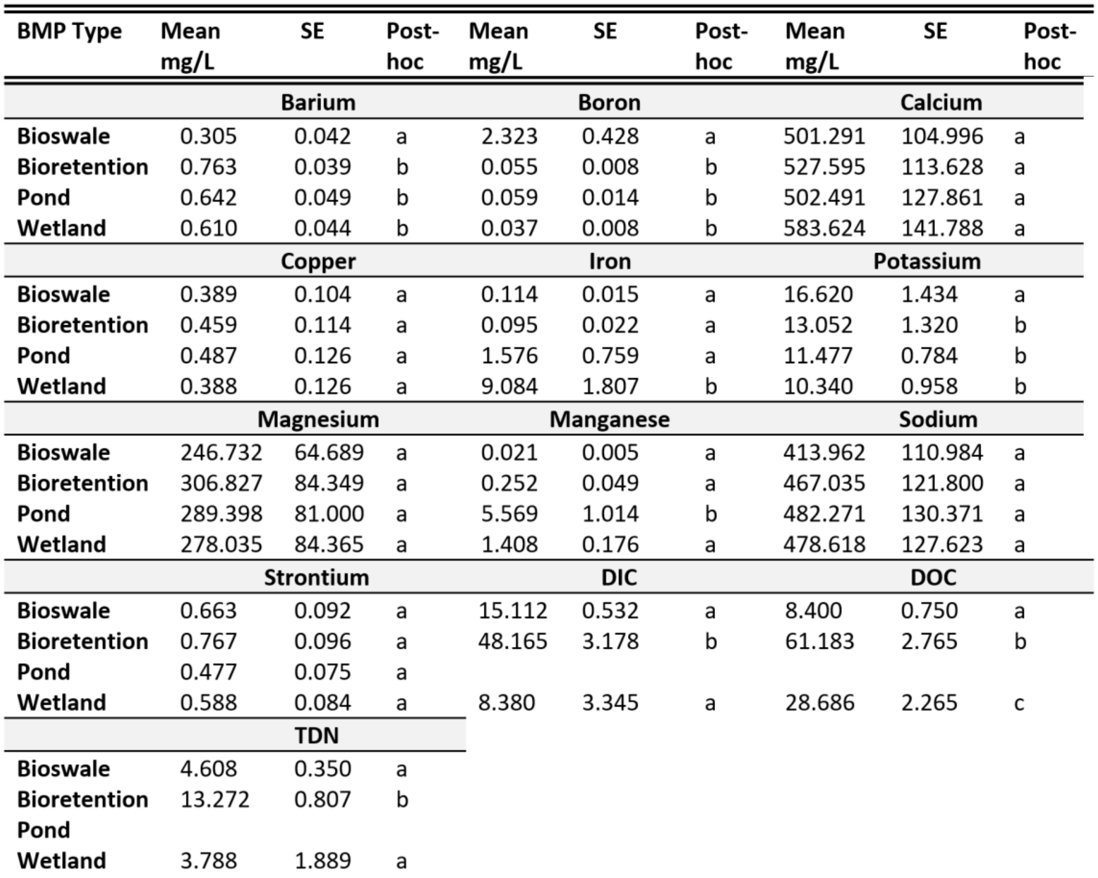

BMP Type	Mean mg/L	SE	Post-hoc	Mean mg/L	SE	Post-hoc	Mean mg/L	SE	Post-hoc
	Barium			**Boron**			**Calcium**		
Bioswale	0.305	0.042	a	2.323	0.428	a	501.291	104.996	a
Bioretention	0.763	0.039	b	0.055	0.008	b	527.595	113.628	a
Pond	0.642	0.049	b	0.059	0.014	b	502.491	127.861	a
Wetland	0.610	0.044	b	0.037	0.008	b	583.624	141.788	a
	Copper			**Iron**			**Potassium**		
Bioswale	0.389	0.104	a	0.114	0.015	a	16.620	1.434	a
Bioretention	0.459	0.114	a	0.095	0.022	a	13.052	1.320	b
Pond	0.487	0.126	a	1.576	0.759	a	11.477	0.784	b
Wetland	0.388	0.126	a	9.084	1.807	b	10.340	0.958	b
	Magnesium			**Manganese**			**Sodium**		
Bioswale	246.732	64.689	a	0.021	0.005	a	413.962	110.984	a
Bioretention	306.827	84.349	a	0.252	0.049	a	467.035	121.800	a
Pond	289.398	81.000	a	5.569	1.014	b	482.271	130.371	a
Wetland	278.035	84.365	a	1.408	0.176	a	478.618	127.623	a
	Strontium			**DIC**			**DOC**		
Bioswale	0.663	0.092	a	15.112	0.532	a	8.400	0.750	a
Bioretention	0.767	0.096	a	48.165	3.178	b	61.183	2.765	b
Pond	0.477	0.075	a						
Wetland	0.588	0.084	a	8.380	3.345	a	28.686	2.265	c
	TDN								
Bioswale	4.608	0.350	a						
Bioretention	13.272	0.807	b						
Pond									
Wetland	3.788	1.889	a						

Results from the three-way ANOVA indicated that stormwater BMP type was a significant factor in major and trace element mobilization, with B, Ba^{2+}, Fe, K^+, and Mg^{2+} Mn, Na^+, Sr^{2+}, DIC, DOC, and TDN concentrations all significantly related to the type of stormwater BMP sampled (Tables 8 and 10). Significantly less DIC, DOC, TDN, and Ba^{2+}, and more B and K^+ were mobilized in bioswale incubations than in the other stormwater BMP types (Table 10). Significantly more Mn was mobilized at the pond sites (Table 10). Significantly more DIC, DOC, and TDN was mobilized at Bioretention #1 and #2 sites than other features studied. Even within a stormwater BMP type, there was sometimes large variation in mobilization response, possibly due to differences in pH, organic matter, clay content, soil type, or anthropogenic pollution sources (Kaushal, Reimer, Mayer, Shatkay, Maas, Nguyen, Boger, Yaculak, Doody, Pennino, Bailey, Galella, Weingrad, Collison, Wood, Haq, Johnson, *et al.*, 2022). For example, significantly more Mn was mobilized in Pond #1 than in Pond #2 across all salts tested (NaCl, $CaCl_2$ and $MgCl_2$).

Salt type had significant treatment effects across all elements except Mn and Fe, causing significantly increased mobilization after incubation with NaCl, $CaCl_2$ and $MgCl_2$ (Table 8 and 5). Preferential mobilization of elements with salt type was observed, the most notable of which was NaCl mobilizing more than 10 times the quantity of Cu than $MgCl_2$ or $CaCl_2$ (Table 9 and Figure 10).

Figure 10. Average Cu Mobilization by Salt Type

Comparison of Cu mobilized by different salt treatments. NaCl treatments mobilized Cu at a rate more than an order of magnitude higher than $CaCl_2$ or $MgCl_2$. The EPA's Cu limit for drinking water is shown by the yellow line at 1.3 mg/L (US EPA, 2015c; d).

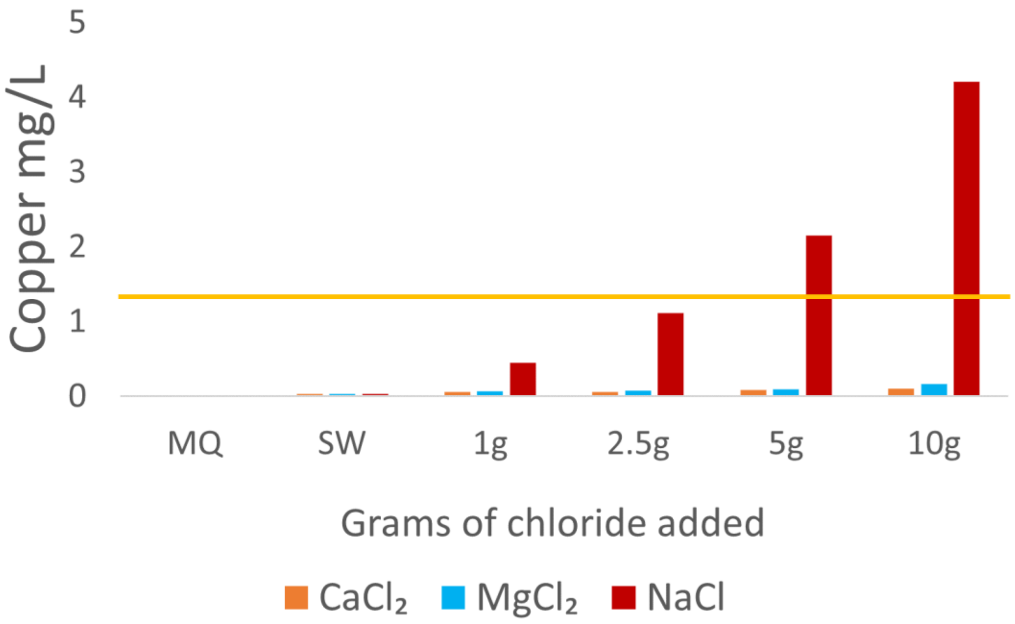

NaCl also mobilized significantly less Ba and significantly more B, DOC, and TDN than other Salts. $CaCl_2$ also mobilized significantly more (2.4 times more Sr^{2+} than $MgCl_2$ and 4.1 times more Sr^{2+}) than NaCl (Table 9). $CaCl_2$ also mobilized significantly less DOC than other salts tested. Increasing salt concentration significantly increased mobilization of every analyte other than Fe, regardless of salt type tested (Table 8 and 5).

3.4.3 PCA Results Show Formation of Chemical Cocktails

Principal Component Analysis (PCA) results showed distinct patterns of elemental mobilization across salt type and concentration (Figure 11 A-C). When plotted by salt type, the X-axis explained ~ 40 - 60% of variance and the Y-axis explained ~20% of the variance for all three plots. NaCl, $CaCl_2$, and $MgCl_2$ incubations all exhibited correlation between Na^+, Ca^{2+}, Mg^{2+}, K^+, Cu, and Sr^{2+} as they were clustered within 90^o (Figure 11 A-C). Among the NaCl, $CaCl_2$, and $MgCl_2$ incubations, Mn was the only element not considered correlated, possibly due to mobilization through redox reactions. $CaCl_2$ mobilized Sr^{2+} most readily (Figures 3 and 4) with Ca^{2+} and Sr^{2+} being tightly clustered regardless of the salt used for the incubation. The clustering between Sr^{2+} and Ca^{2+} is noted in Figure 11 A-C with a blue circle. Cu and Na also showed a similar clustering, denoted with a red circle (Figure 4 A). Increased salt concentrations show heightened mobilization of chemical cocktails in Figure 12. NaCl, $MgCl_2$ and $CaCl_2$ incubations at Bioswale, Bioretention, and Pond sites (respectively) all showed greater clustering and correlation between Na^+, Ca^{2+}, Mg^{2+}, K^+, Cu, and Sr^{2+} at “high” concentration incubations (2.5 to 10 g/L salt) than at “low” concentration incubations (Milli-Q to 1 g/L salt).

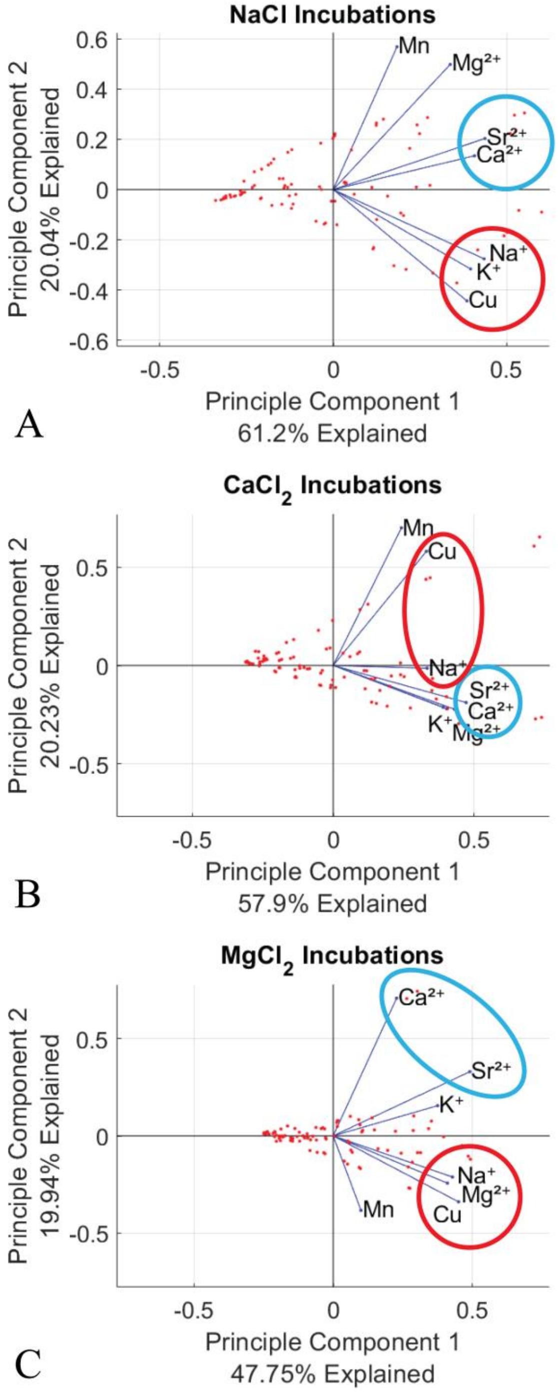

Figure 11. PCA Analysis – Salt Type

PCA plots showing chemical cocktails mobilized by different salts. All results indicate chemical cocktail dispersion with 6 of the 7 elements analyzed being correlated with the Na, Ca^{2+}, or Mg^{2+} added during incubations. Figure 4A shows NaCl incubation results, which illustrate Sr-Ca and Cu-Na co-mobility. Figure 4B shows $CaCl_2$ incubation results illustrating Sr-Ca and Cu-Na co-mobility. Figure 4C shows $MgCl_2$ incubation results illustrating Sr-Ca co-mobility.

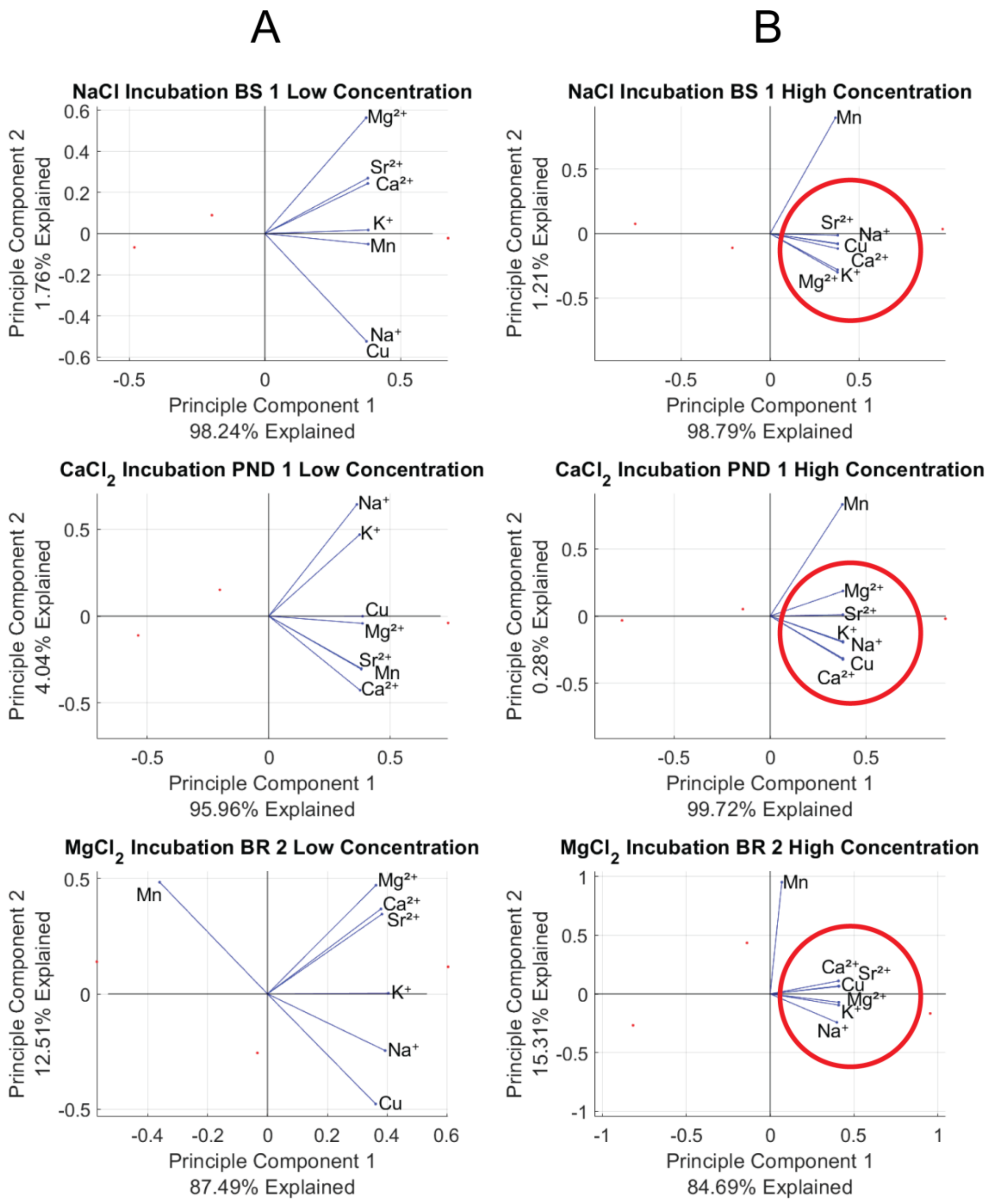

Figure 12. PCA Analysis - Concentration

PCA plots showing chemical cocktail mobilization at low (Milli-Q to 1 g/L) and high (2.5 - 10 g/L) concentrations for NaCl, $CaCl_2$ and $MgCl_2$. Bioswale 1, Bioretention 2, and Pond 1 are used as examples to show this phenomenon is not isolated to one stormwater BMP. The formation of chemical cocktails is highlighted by red circles in the high concentration PCAs.

3.5 Discussion

All stormwater BMP types showed elemental mobilization by simulated road salting. This demonstrates that chemical cocktails could be formed in stormwater BMPs under elevated salinity, potentially effecting areas downstream. Increased salt concentration led to increased mobilization of all elements tested except for Fe (Table 8 and Table 7). Fe is often more readily mobilized through redox reactions instead of base cation exchange, explaining its lack of significance. Mn can also be mobilized by redox reactions similarly to Fe, but Mn has been shown to also be mobilized by cation exchange, especially if initial soil pH is low (Wen, 2012b). Furthermore, B, Ba^{2+}, Ca^{2+}, Cu, K^+, Mg^{2+}, Mn, Na^+, Sr^{2+}, DIC, DOC, and TDN all showed increased mobilization with increased concentration over all salt types (Table 8, Table 9 and Figure 8). Site type influenced mobilization of key elements with significantly less DIC, DOC, TDN, and Ba^{2+}, and more B and K^+ mobilized in bioswale incubations than in the other stormwater BMP types (Table 10). Increased retention of nitrogen and organic matter may be due to site composition or potentially age as the bioswales are the youngest site in the study by over a decade. Significantly more DIC, DOC, and TDN was mobilized at Bioretention #1 and #2 than other features studied. As these sites drain the largest area into smallest stormwater BMP footprint, they may have diminished CEC (as evidenced by their significantly diminished retention compared to bioswale sites). Previous site history also may play a role in chemical cocktail mobilization as significantly more Mn was mobilized in Pond #1 than in Pond #2, reaching concentrations of up to 36 mg/L.

Incubation results are consistent with field results from Galella *et al*. (2021), which explored chemical cocktail mobilization of Ca^{2+}, K^+, Na^+, Mg^{2+}, Cu, Mn and Sr^{2+} in urban streams using routine sampling and high-frequency sensors. This suggests that urban streams and stormwater BMPs (bioswales, bioretention sites, wetlands and ponds) behave more similarly to one another with respect to base cation source and sink dynamics than has been suggested in previous literature (Barbier *et al.*, 2018; Burgis *et al.*, 2020; Gill *et al.*, 2017; Knox *et al.*, 2021; Maas *et al.*, 2021; Semadeni-Davies, 2006). Stormwater ponds had previously been found to retain metals (Gill *et al.*, 2017; Knox *et al.*, 2021) but at a decreased efficiency (~50% summer performance) in the winter after roadsalt input (Semadeni-Davies, 2006). Stormwater ponds were also found to mobilize base cations after road salting events (Barbier *et al.*, 2018).Though stormwater BMPs do offer excellent conditions for decreasing peak discharge and organic matter and nutrient pollution, stormwater BMPs may be sources rather than sinks of metals and cations during road salting events (Kaushal et al. 2022 a, b), potentially leading to increased salt and chemical cocktail contamination of surface and groundwater (Burgis *et al.*, 2020; Kaushal, Likens, *et al.*, 2019; Maas *et al.*, 2021).

3.5.1 Variations in Ion Retention and Release among Stormwater BMPs

Our results suggest that stormwater BMPs have a high capacity for retaining salt ions. Na^+ was retained significantly more than Ca^{2+} or Mg^{2+} across all stormwater BMP types (Supplemental Table 3.1). The elevated Na^+ retention measured may be caused by its smaller ionic radius, Na^+ dispersion, and flocculation (Green *et al.*, 2008b; Kaushal, Likens, *et al.*, 2019). Diminishing retention with increasing salt concentration indicates that cation exchange sites were being exhausted and less salt was retained (Figure 9). BMP Type also affected retention significantly with biowsale sites retaining the most salt, followed by bioretention, pond and wetland sites. Bioswale sites retained significantly more cations (on average 141% more) than bioretention sites. This may be due to differences in construction or site age as the bioswale sites sampled are the youngest studied by more than a decade.

While they are an effective sink of Na^+, Mg^{2+} and Ca^{2+}, through cation exchange, stormwater BMPs are also a simultaneous source of other base cations and metals (Figure 8) (Kaushal, Reimer, Mayer, Shatkay, Maas, Nguyen, Boger, Yaculak, Doody, Pennino, Bailey, Galella, Weingrad, Collison, Wood, Haq, Johnson, *et al.*, 2022). Other studies indicate that there is significant retention of various base cations and metals in stormwater ponds (Barbier *et al.*, 2018; Semadeni-Davies, 2006), wetlands (Gill *et al.*, 2017; Knox *et al.*, 2021), accidental wetlands (Maas *et al.*, 2021), bioswales and bioretention features (Burgis *et al.*, 2020), but less work has directly analyzed the impacts of salt ions on ion exchange and release of contaminants (Kaushal et al. 2022). The potential for retention or release of contaminants can be influenced by site-specific characteristics, such as a hypersaline layer developing only in deeper sections of stormwater ponds (Semadeni-Davies, 2006), or wetlands delaying peak discharge and therefore lessening peak salinity (Maas *et al.*, 2021). Below, we discuss potential impacts of these characteristics on retention and release of salts observed in this study.

While we couldn't measure all factors contributing to retention in the lab and the field, groundwater storage could be an important mechanism for salt retention (Cooper et al. 2014), and we observed elevated salt concentrations in the stormwater BMP that persisted over time in the field (Figure 13).

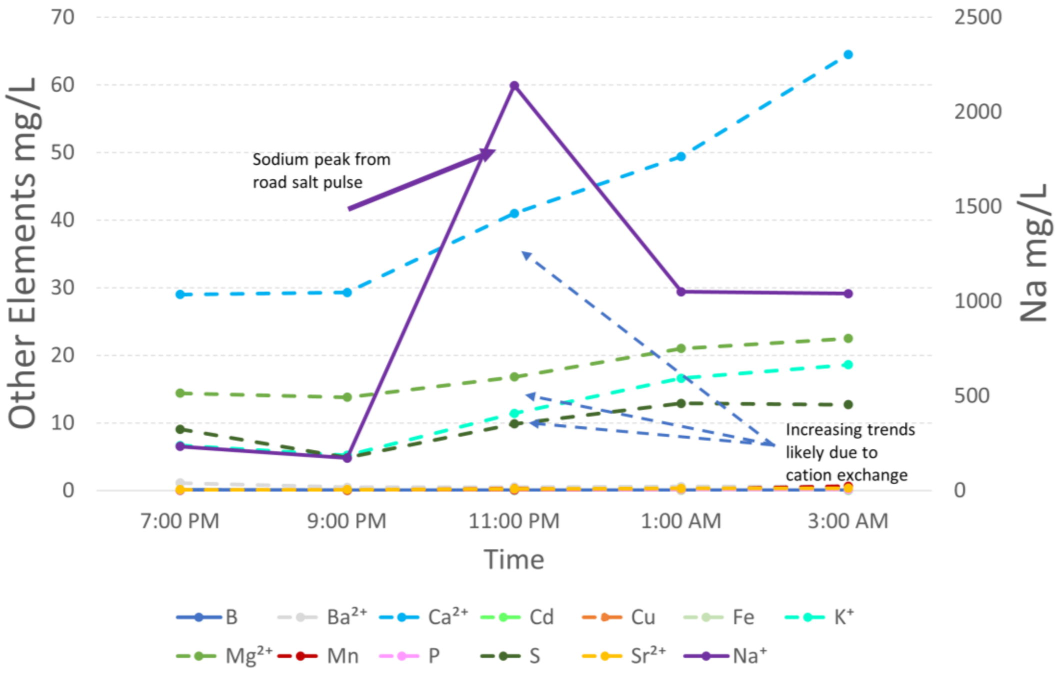

Figure 13

Winter storm event sampling conducted at Wetland #2 from 1/28/22 through 1/29/22. Sampling was conducted during a snowstorm where road salting occurred on the University of Maryland College Park campus. Base cation exchange is thought to drive the elemental mobilization seen after the peak Na^+ concentration (2140 mg/L) was reached.

Field data during and after actual road salt events can be less common in the literature due to the difficulty of winter sampling. Increased groundwater infiltration is a design strategy implemented at all stormwater BMPs studied, which suggested that similar groundwater plumes may also be present. When wetland soils were experimentally flushed with 2.5–5 g Cl/L NaCl, soils retained 3.6–41% of the added Cl, and there were also significant positive relationships between soil organic matter (SOM) and Cl^- (McGuire and Judd, 2020). The proposed mechanism for this retention is the formation of organic Cl^- compounds (McGuire and Judd, 2020) which can occur biotically or abiotically, but microbially derived organic Cl^- compounds were the most likely source (McGuire and Judd, 2020). Most Na^+, Mg^{2+}, and Ca^{2+} retention results were broadly similar in this study across stormwater BMP types and salt concentrations (Figure 9). Stormwater ponds in Maryland yielded higher Cl^- concentrations in both the winter and summer months, indicating that such ponds are the source of NaCl rich-groundwater plumes, with groundwater Cl^- concentrations reaching up to 421 mg/L due to increased groundwater connectivity (Cooper *et al.*, 2014; Snodgrass *et al.*, 2017).

Though not studied directly by this research, retention time and the intensity and duration of road salt application each winter may also play a critical role in determining how long before stormwater BMPs exchange sites become completely saturated (Barbier *et al.*, 2018; Burgis *et al.*, 2020). Exchange site saturation was observed at Wetland #2 and nearly all sites exhibited diminishing percent cation retention at 10 g Cl/L incubations. Desorption of cations during the spring may take months to reach pre-roadsalt exposure levels.Retention ponds in France showed that 91% of the salt adsorbed during the winter was removed by March 1st, despite Ca^{2+} levels reaching 503.65 mg/L (Barbier *et al.*, 2018). Bioswales and bioretention sites also showed similar trends, temporarily reducing effluent surface loads during a snow storm by 82% and 76%, but retaining little Na^+ long-term (up to 200 mg/kg in the summer) (Burgis *et al.*, 2020). As road salt applications are seasonal in temperate climates, freshwater (with low salinity) from spring and summer precipitation typically desorbs accumulated salt ions from stormwater BMPs. Cation retention followed by chemical cocktail mobilization may explain the complicated sink (Figure 9) / source (Figure 8) dynamics found in our study.

3.5.2 FSS Impacts Function of Stormwater BMPs

Our results showed that different types of salt ions have the potential to affect patterns and processes in stormwater BMPs relevant to soil structure and hydrological and biogeochemical functions. Currently, watershed restoration strategies employ stormwater BMPs to slow and store urban runoff, enhance infiltration and hydrologic residence times, and boost biogeochemical functions related to contaminant retention and removal (Davis, 2008; Koch *et al.*, 2014; Maas *et al.*, 2021). However, increased salinization can reduce infiltration capacity and the ability for urban runoff to percolate through stormwater BMPs (Behbahani *et al.*, 2021). In addition, ion exchange sites in soils can become saturated with Na^+ and other ions and shift stormwater BMPs from contaminant sinks to sources (McGuire and Judd, 2020; Snodgrass *et al.*, 2017). Finally, increased salinization can alter microbial and plant processes and influence rates of biogeochemical processes related to contaminant retention in stormwater BMPs (Kim and Koretsky, 2013). Below, we explore how salts can influence infiltration rates, ion exchange and saturation of exchange sites, and microbial and plant processes.

Stormwater BMPs appear to provide a complex combination of positive and negative effects for their associated watersheds (*e.g.*, we found retention of cations but release of other elements). Peak discharge and nutrients are generally reduced, but cations, metals, and organic matter can be mobilized during road salting events (as observed in this study) (Figures 8, 9, and 12; Tables 8, 9, and 10) (Davis, 2008; Koch *et al.*, 2014). At high salt concentrations, metals can reach levels that are harmful to both freshwater biota and humans (Kondakis *et al.*, 1989; Mahrosh *et al.*, 2014). Accidental and designed wetlands may decrease peak salinity downstream but may also funnel surficial water contamination directly into groundwater aquifers (Maas *et al.*, 2021; Palta *et al.*, 2017). Stormwater BMPs offer more environmental benefits than cement culverts and buried streams, but further study must be conducted regarding risks associated with freshwater salinization (Kaushal et al. 2021, 2022a, b). If salt use continues or increases, the quantity of metals released may begin to decrease as colloids become depleted of metals with constant base cation exchange and flushing downstream (Fernandez *et al.*, 2003). Evidence of exchangeable metal depletion may be present in the Wetland #2 site, one of the oldest sites in the study at ≥30 years old, which mobilized less Cu than any other site, especially during NaCl incubation (Figure 8). Further work should investigate the factors influencing cation exchange capacity in stormwater BMPs and elucidate the role of organic carbon *vs.* clays.

Our results suggest that FSS can alter organic matter in stormwater BMPs similar to other studies (Kaushal et al. 2022 a, b); this may have implications for changes in soil aggregate structure, erosion potential, and infiltration rates. Our study found that concentrations of DOC increased in response to initial stages of salinization, significantly from salinization with Na^+, consistent with changes in solubility and destruction of soil aggregates due to Na^+ dispersion and loss of cation bridging from Ca^{2+} and Mg^{2+} in sodic soils (Figure 8, Table 9) (Green *et al.*, 2008c; b; Abolfazli and Strom, 2022; Norrstrom and Bergstedt). In sodic or saline-sodic soils with exchangeable sodium percentages > 15 and an exchange of Na^+, replacing Ca^{2+} or Mg^{2+} soil aggregates break up, hydraulic conductivity decreases and colloid mobility increases. Changes in pH can also influence this process though it was not recorded in this study. Our results also showed some rapid declines in DOC concentrations at higher levels of salinization at Bioretention #1 and Wetland #1, before reaching a threshold (between 2.5 and 5 g Cl^-/L) and once again increasing. This may indicate flocculation of soil particles at higher salinities (Figure 8) (Abolfazli and Strom, 2022). At high concentrations ≥ 947 µS/cm flocculation is thought to occur due to a decrease in the thickness of the double layer. As the double layer shrinks, this allows for the repulsion force to be overcome by the attraction force and aggregates form (Abolfazli and Strom, 2022). Loss of soil aggregates can lead to increased erosion in stormwater BMPs and mobilization of contaminants bound to sediments, similar to increased erosion in other salinized soils (Behbahani *et al.*, 2021). Increased flocculation at higher levels of salinity can lead to clogging of soils and sediments in stormwater BMPs and reductions in infiltration capacity similar to other salinized soils (Abolfazli and Strom, 2022). Much previous work in other salinized soils has shown that the amounts and types of salt ions can impact soil aggregate structure, hydraulic conductivity, and infiltration rates (Green *et al.*, 2008c; b; Snodgrass *et al.*, 2017; Abolfazli and Strom, 2022).

The effectiveness of different stormwater BMPs to retain contaminants is also related to abiotic factors such as CEC of soils and sediments (Green *et al.*, 2008b; Peinemann *et al.*, 2005). Different stormwater BMPs have been shown to have CEC ranging from 2.9 meq/100g soil to 25.91 meq/100g soil (Behbahani *et al.*, 2021; Davis *et al.*, 2001). We observed significant differences in retention of Na^+, Ca^{2+}, and Mg^{2+} and trace metals in the different stormwater BMPs in this study, possibly due to differences in CEC across stormwater BMPs, landscape position, age and pollution history (Rieuwerts *et al.*, 1998). In older stormwater BMPs receiving high levels of pollution like Pond #1, cation exchange sites may become occupied with metals such as Mn (Figure 9 and Figure 8), becoming more susceptible to mobilization of contaminants (McGuire and Judd, 2020; Snodgrass *et al.*, 2017). Stormwater BMPs may also show potential for retaining Na^+ and other cations even into the summer as was seen in previous work by this research group (Galella *et al.*, 2021) and others (McGuire and Judd, 2020; Snodgrass *et al.*, 2017). Stormwater BMPs saturated with Na^+ may have significantly decreased capacity to serve as contaminant sinks in urban watersheds and landscapes. We observed that a) maximum salt ion retention usually occurred at the lowest concentrations (1g Cl^-/L), b) decreasing as Cl^- concentration increased, indicating that exchange sites were becoming exhausted as greater quantities of cations were added. Na^+ had significantly higher retention than Ca^{2+} or Mg^{2+}, likely due to cations in soil aggregates (Figure 9). Differences in retention thresholds among sites may have also been due to changes in organic matter content and quality of the sediments, or differences in CEC of the soils. These variables should be included in future research on this topic.

FSS can influence the function of stormwater BMPs by altering biogeochemical processes, like encouraging the growth of fungal and microbial mats which may in turn mobilize Fe and Mn into the environment (though only Mn mobilization was observed in this study) (Kim and Koretsky, 2013). Previous work suggests that microbial activity can be influenced by factors influenced by FSS. For example, microbial biomass and activity were positively correlated with organic carbon, total nitrogen, pH, moisture content, total petroleum hydrocarbons, and watershed area ratio (a ratio of the area draining into the feature to the area of the stormwater BMP itself) (Deeb *et al.*, 2018). We observed a statistically significant increase in TDN with increased salt concentrations for all salts tested (NaCl, $CaCl_2$, and $MgCl_2$). The ions that produced the largest increases in TDN were Mg^{2+} and Na^+. Na^+ mobilized concentrations up to 17 mg/L likely because it is monovalent and can more easily mobilize NH_4^+. Duckworth & Cresser (1991) noted that high Na^+ inputs flush ammonium ions from their exchange sites, also reducing retention from atmospheric sources (Duckworth and Cresser, 1991). Elevated ammonium concentrations in waterways affected by FSS have also been attributed to a combination of dissimlatory nitrate reduction to ammonium (DNRA) and ammonification with associated diminished nitrification (Inamdar *et al.*, 2022). Changes in pH due to displacement of H^+ by Na^+ and alkalinization over time have also been observed (Green *et al.*, 2008c; a; b). Nitrification and denitrification can be enhanced at slightly elevated pH and N cycles may be altered based on availability of

Ca^{2+} and calcareous soils (Green *et al.*, 2008c; a; b). Increased salinization has the potential influence the N cycle of stormwater BMPs and further research needs to look at this in more depth at the watershed scale (Collins *et al.*, 2010; Passeport *et al.*, 2013).

3.5.3 Thresholds for Aquatic Life and Formation of Chemical Cocktails in Stormwater BMPs

In this study, we measured specific conductance in stormwater management features > 8000 uS/cm, well above EPA thresholds of 230 uS/cm for aquatic life in the Mid-Appalachian region (EPA, 2011). Targeted sampling conducted during a winter storm at Wetland #2 revealed extremely high concentrations of Na^+, up to 2140 mg/L (Figure 13) triggering mobilization of major and trace elements similar to our laboratory incubation experiments. As was expected in stormwater BMPs, the salinity levels in Wetland #2 were higher than were ever recorded in urban streams in the area. The levels of salinization used in our study were within ecologically relevant ranges reported for other systems. Salt concentrations as low as 217−445 mg Cl^-/L have caused shifts in species composition, particularly plankton and benthic organisms, towards more salt tolerant species, which may in turn lead to eutrophication due to a combination of reduced grazing pressure from zooplankton and a release of nutrients, particularly phosphorus from lake sediments (Hintz and Relyea, 2019).

Our results also showed increasing trends of major and trace elements with increasing salt concentrations contributing to the formation of chemical cocktails.

Chemical cocktails of salt ions, metals, and nutrients also increased in concentration with increasing salinization. Mobilization of major and trace elements was not uniform across the different salts used in incubations. PCA and ANOVA results showed significant co-mobilization of Cu and NaCl (Figures 4 and 5). At every concentration tested, NaCl incubations mobilized Cu at concentrations more than an order of magnitude greater than $MgCl_2$ and $CaCl_2$ (Figure 10). For example, averaged results for samples incubated with 10g/L Cl mobilized 0.11 mg/L of Cu for $CaCl_2$ incubations, 0.17 mg/L Cu for $MgCl_2$ incubations and 4.21 mg/L Cu for NaCl incubations. Elevated Cu concentrations are likely due to Na^+ dispersion of organic matter rich colloids. Cu is dispersed from sediment particle layers into suspension when Na^+ concentrations are elevated (Kinsman-Costello *et al.*, 2022). Sr^{2+} also showed significant co-mobilization with CaCl, mobilizing more than double the concentration compared to the other salts studied. This is likely due to the shared charges of Ca^{2+} and Sr^{2+}.

Although stormwater BMPs may not contain as many species as natural ecosystems, they can be important urban habitats (Snodgrass *et al.*, 2008; Van Meter *et al.*, 2011). Increased major ion concentrations can directly cause detrimental effects on freshwater biota (Clements and Kotalik, 2016; Hintz and Relyea, 2019). Insects, when exposed to concentrations of aqueous $NaHCO_3$, $MgSO_4$, and NaCl ranging from 60 to 300 μS/cm, had lower metabolic rates and abundance than control populations (Clements and Kotalik, 2016). With local specific conductance levels surpassing 1,000 μS/cm nearly every winter in urban streams surrounding the study site, it is likely that salinity alone is negatively affecting aquatic food webs. Certain species of zooplankton (*Daphnia pulex*) can develop cross-tolerance to different deicers (Hintz *et al.*, 2019). For example, those species tolerant of height concentrations of NaCl were also tolerant of elevated $MgCl_2$ and $CaCl_2$ (Hintz et al., 2019). However, salt-tolerant species reproduced more slowly than less tolerant species (Hintz *et al.*, 2019). Rainbow trout fry showed no negative impacts when exposed to $MgCl_2$ up to 3000 mg/L, but did show reduced growth when exposed to NaCl at 3000 mg Cl^-/L and $CaCl_2$ at 860 mg Cl^-/L (Hintz and Relyea, 2017a). Atlantic salmon embryos exhibited larval deformities when exposed to NaCl concentrations $\geq$ 5000 mg/L combined with Cu at (10 μg Cu/L) (Mahrosh *et al.*, 2014). These deformities were not present when embryos were exposed to solely NaCl concentrations $\geq$ 5000 mg/L although there was increased egg mortality (Mahrosh *et al.*, 2014). The synergistic detrimental effects of NaCl and Cu when combined illustrate the importance of studying chemical cocktails as a whole instead of focusing on individual elements one at a time. Incubations for this study contained up to 16,500 mg/L of added NaCl and 15,700 mg/L of added $CaCl_2$, chosen to be within a realistic range of salinities expected at the stormwater BMPs selected (Table 6), far exceeding the thresholds established for aquatic ecosystem harm (Hintz and Relyea, 2017a). More work needs to investigate the effects of salinization on contaminant mobilization and toxicity to aquatic life.

3.5.4 Impacts of Alternative Road Salt Ions Compared with NaCl

A key component of the present study was to compare the impacts of different common road salt ions on retention and release of multiple elements. We found significant differences in retention and release of chemical cocktails, but it is important to place these results within context when considering management implications. The effectiveness of different types of salt ions as deicers is dependent on temperature. For example, NaCl is capable of melting snow and ice to as low as -9.4^{o}C, but $MgCl_2$ and $CaCl_2$ melt snow and ice to -20.6 ^{o}C and -31.7 ^{o}C, respectively (Diamond Crystal, 2017; Kissner, 2012a; b). $CaCl_2$ was found to be the most effective deicer to use on snow and ice, followed by $MgCl_2$ (Kołodziejczyk and Ćwiąkała, 2009). Our results show that site type usually had less of an effect than salt concentration and salt type on the mobilization of metals, nutrients, and carbon (Tables 8, 9, and 10). Regardless of stormwater BMP, the amount and type of road salt applied is the most significant factor controlling major and trace element mobilization (Table 8 and Figure 8). Na^+, being monovalent, often mobilizes major and trace elements differently from divalent Ca^{2+} and Mg^{2+} (Table 9). If $CaCl_2$ is used as a deicer instead of NaCl, it may be possible to apply less total road salt and still achieve road safety due to $CaCl_2$'s lower melting temperature and greater efficacy (Kołodziejczyk and Ćwiąkała, 2009). Ca^{2+} and Mg^{2+} also contribute to water hardness, often reducing the toxicity of certain metals (Ebrahimpour *et al.*, 2010). Ca^{2+} and Mg^{2+} may also have less detrimental effects on soil aggregate stability than Na^+ (Green *et al.*, 2008c; b). Depending on the contaminant of concern (e.g. Cu) and environmental issues (soil erosion), the use of alternative deicers other than NaCl could reduce the overall quantity of salt used while still maintaining safe roadway travel. Currently cost is a major obstacle restricting the use of alternative salts, as

NaCl is the least expensive deicer option in the United States (Tiwari and Rachlin, 2018).

3.5.5 Scientific Limitations of Study and Path for Future Research

Though every effort was made to perform a robust assessment of the effects of FSS on chemical cocktail mobilization, some limitations still exist. Though replicate stormwater BMPs were sampled they were all within a geographically limited area which could be expanded in future studies. Mobilization of nitrogen and possible redox reactions are often associated with changes in the pH of water and sediment. pH data would have been a useful additional data source which should be considered for future similar studies. The organic matter content of sediment samples collected should also be explored in future studies as it may help better define the differences in retention and release observed at different stormwater BMPs. A more in-depth analysis of sediment particle size makeup would also help better describe retention and release mechanisms. Analysis of biological communities in stormwater BMPs before and after road salting events would also be helpful to determinge what the impacts of FSS are on both flora and fauna.

3.6 Conclusion

Salt concentration, salt type, and, to a lesser extent, site type determines the composition and concentrations of chemical cocktails released from stormwater BMPs. Increasing the concentration of NaCl, $CaCl_2$, or $MgCl_2$ in stormwater BMP water and sediment samples mobilizes chemical cocktails or major and trace elements in a linear fashion for certain elements (Cu, K, and Sr^{2+}) (Figure 8). Different salts show increased mobilization, with NaCl mobilizing Cu at concentrations more than an order of magnitude more than $CaCl_2$, or $MgCl_2$, and $CaCl_2$ preferentially mobilized Sr^{2+}. Concentrations of mobilized elements exceeded water quality standards for certain metals such as Cu and Mn (US EPA, 2015b; d). Results showed that the amounts of salt ions had significant effects on mobilization of a wide variety of contaminants including nutrients, other salt ions, and metals. The amounts of road salts applied to impervious surfaces during winter months and the amounts of salt loadings from other potential sources is not closely tracked. More work on calibrating and tracking road salt application rates is necessary to reduce risk from excess Na^+, Mn, and Cu.

Our research also suggests that there are important interactions between salt ions and mobilization of carbon, nitrogen, and metals from stormwater BMPs. Though the dataset is incomplete due to an instrument malfunction, positive relationships were observed between NaCl, $CaCl_2$, $MgCl_2$ and DOC and TN at bioswale sites (Supplemental Figure 3.4). Inorganic carbon has mixed results with both increasing and decreasing trends observed across bioswale, bioretention, and wetland sites (Supplemental Figure 3.4). Strategic efforts to minimize biogeochemical interactions that mobilize contaminants of concern (below concentration thresholds determined from this study) can be used to better inform goals for meeting total maximum daily loads (TMDLs). Our results also showed that the types of salt ions impacted contaminant mobilization potentials. This information may be used to guide selection of alternative deicers based on biogeochemical interactions and potential water quality impacts. Our results also showed that different stormwater BMPs can retain significant amounts of salts and that salt type and site type influence their retention potential (Figure 8). The extremely saline environments present in stormwater BMPs that we observed after road salting (up to 2140 mg/L Na^+) elevate the risk of formation of groundwater chemical cocktail plumes, especially because many stormwater BMPs both increase groundwater connectivity and generate unique chemical cocktails. For example, elevated Cl^- from chemical cocktail plumes may still be detectable 15 km away from the stormwater BMP that generated them (Snodgrass *et al.*, 2017). Further research will be needed to determine if other mobilized elements may be transported and over what distances. Overall, our results suggest that reducing the level of salt ions significantly reduces the mobilization of contaminants from sediments to streams. Our results also clearly show that selecting different types of salt ions can have significantly different effects on mobilizing contaminants. The amounts and types of salt ions need to be considered explicitly in watershed management and restoration strategies to more effectively reduce risk to human health and the environment.

Our results highlight the complexity of stormwater BMPs and their roles in contaminant retention and release under varying environmental conditions. Incubation results and field measurements suggest that the stormwater BMPs studied behaved as contaminant sources rather than sinks during road salting events, similar to the urban streams studied in Galella et al. (2021). The environmental benefits of nutrient storage and peak storm discharge reduction offered by stormwater BMPs contrasts with the unintended consequences of chemical cocktail mobilization after road salting (Davis, 2008; Koch *et al.*, 2014). This is further complicated by the potential of stormwater BMPs to generate groundwater chemical cocktail plumes (Snodgrass *et al.*, 2017). Though NaCl is often the most cost-effective deicer available, the use of brines, $MgCl_2$ and $CaCl_2$ should be considered as an alternative, especially in environmentally fragile areas or where fisheries are affected by Cu pollution. Further research on alternative deicers is needed, as their full effect on the food web, particularly on zooplankton is still not fully known (Hintz *et al.*, 2022).

Chapter 4: Freshwater Salinization Syndrome Alters Nitrogen Transport in Urban Watersheds

4.1 Abstract

Anthropogenic salt inputs have increasingly impacted many urban streams in the U.S. for more than a century. Urban stream salinity is often chronically elevated and punctuated by episodic salinization events, which can last hours to days after snowstorms and the application of road salt. Here we investigated the impacts of freshwater salinization on total dissolved nitrogen (TDN) and NO_3^- / NO_2^- concentrations and fluxes across time in six urban watersheds in the Baltimore-Washington D.C. metropolitan region of the Chesapeake Bay region. Concentrations of TDN, NO_3^- / NO_2^- and specific conductance (SC) were monitored in five urban streams, and there was targeted storm event sampling and high-frequency sensor data at select sites. Results suggested that episodic salinization from road salt applications quickly extracted and mobilized watershed stores of (TDN) through ion exchange, and other geochemical and biological processes. Urban streams had elevated concentrations of TDN and NO_3^- / NO_2^- and specific conductance concentrations that peaked during and after winter road salt events, and then declined. There were significant linear relationships between TDN concentrations and SC at multiple sites over time. Hourly mass fluxes of TDN in streams were also found to be elevated during winter months with peaks coinciding with road salting events. Targeted winter snow event sampling and high-frequency sensor data suggested plateaus in NO_3^- /

NO_2^- and TDN concentrations at the highest peak levels of SC during road salt events between 1,000 and 2,000 µS/cm, which possibly indicated source limitation of TDN after extraction and mobilization of watershed nitrogen reservoirs by road salt ions. Our results suggest that there can be thresholds in the transport and transformation of nitrogen in watersheds, which impact patterns in concentrations and hourly fluxes in urban streams across time. FSS may alter the timing of nitrogen delivery to sensitive receiving waters during winter months when biological uptake is lowest and enhance the transport of N to sensitive receiving waters.

4.2 Introduction

Freshwater salinization syndrome (FSS) has been observed throughout North America and Europe over the past century (Kaushal *et al.*, 2005; Kaushal, Gold, *et al.*, 2018). FSS refers to the suite of biophysical impacts triggered by increased salt ions in the environment. In temperate areas, anthropogenic salt inputs are thought to be the primary driver of FSS, with chronically elevated salinity punctuated by acute episodic salinization events caused by road salt application (Galella *et al.*, 2021). For example, U.S. sales of road salt have increased 147-fold from 149,000 metric tons in 1940 to nearly 22 million metric tons in the winter of 2017-2018 (Jackson and Jobbágy, 2005; Pecher *et al.*, 2019). This trend is a result of larger and more severe winter storms triggered by ongoing anthropogenic climate change (Pecher *et al.*, 2019). Changing land use is also a factor, with impervious surface cover increasing across the United States largely due to increased suburbanization (Vogler and Vukomanovic, 2021). FSS is relevant because it can cause alterations in contaminant mobility, biodiversity and the quality of drinking water in urban watersheds (Corsi *et al.*, 2010; Galella *et al.*, 2021; Haq *et al.*, 2018; Hintz *et al.*, 2022; Hintz and Relyea, 2019). Road salting in temperate regions has been shown to mobilize nutrients such as nitrogen and phosphorus, organic matter, and other ions (Na^+, Ca^{2+}, Mg^{2+}, K^+, Cu, Mn, Sr^{2+}) (Galella *et al.*, 2021; Haq *et al.*, 2018; Kaushal, Gold, *et al.*, 2018; Kaushal, Reimer, Mayer, Shatkay, Maas, Nguyen, Boger, Yaculak, Doody, Pennino, Bailey, Galella, Weingrad, Collison, Wood, Haq, Newcomer-Johnson, *et al.*, 2022). Mobilization of nitrogen during and after road salting events in urban watersheds is not well understood. In this study, we use a combination of routine monitoring, winter storm event data and high-frequency sensor data collected before, during, and after winter road salt events to understand temporal trends in nitrogen mobilization in urban watersheds.

Anthropogenically enhanced nitrogen loads often lead to eutrophication in urban waterways and coastal receiving waters (Howarth and Marino, 2006; Kaushal *et al.*, 2008; Testa *et al.*, 2018). Nitrogen is often a limiting nutrient and can trigger the growth of phytoplankton and harmful algal blooms (Howarth and Marino, 2006). Decomposition of organic matter from eutrophication causes dissolved oxygen levels to diminish, creating hypoxic (dissolved oxygen < 2 ml/L), conditions incompatible with life for many marine organisms (Diaz and Rosenberg, 2008). Benthic and demersal organisms which live at or near the bottom of a water body are particularly susceptible to eutrophication as deeper waters are often most affected by elevated nitrogen levels (Testa *et al.*, 2018). Both flora and fauna can also be affected by eutrophication, leading to habitat loss, changes in ecological structure, and alterations to phytoplankton composition (Howarth *et al.*, 2000).

While nitrogen transport in urban watersheds has been well studied, the role of FSS impacts on watershed N transport and transformation has received relatively less attention (*e.g.*, Hale and Groffman 2006, Duan and Kaushal 2015, Haq et al., 2018), and there is little knowledge of FSS impacts on watershed N transport. Nitrogen concentrations in urban streams can be elevated by sewage leaks, atmospheric deposition, and fertilizers (Kaushal *et al.*, 2011). Our current understanding suggests that the ability of urban streams to retain and transform nitrogen may be diminished by: decreased hydrologic connectivity between streams and "hot spots" of N retention in urban riparian zones (Groffman *et al.*, 2003), increased hydrologic flashiness and decreased hydrologic residence times (Pennino *et al.*, 2016), headwater stream burial and channelization of streams (Alberts *et al.*, 2017; Elmore and Kaushal, 2008; Pennino *et al.*, 2014), and decreased biological uptake of N following storms and scouring of biofilms (Kaushal, Gold, *et al.*, 2018). Overall, there may be an increased supply of N in urban streams that exceeds biological demand (Wollheim *et al.*, 2018). Although many biophysical factors have been studied regarding N transport and transformation in urban watersheds, the potential role of FSS in influencing the N cycle has been less studied, but it may represent a disturbance in some urbanized watersheds (Kaushal *et al.*, 2005).

Freshwater salinization can enhance N transport from soils to streams *via* ion exchange, changes in solubility of organic nitrogen, and changes in biogeochemical processes. Ion exchange causes Na^+ as well as other base cations including Ca^{2+},

Mg^{2+}, and K^+ to desorb positively charged NH_4^+ from sediments and negatively charged colloids (Ardón *et al.*, 2013; Kinsman-Costello *et al.*, 2022; Rysgaard *et al.*, 1999; Seitzinger *et al.*, 1991). This process causes increased mobilization of reactive N into urban watersheds during episodic salinization associated with road salting. Salt ions are in fact so efficient at mobilizing nutrients that in standard lab tests, salts like NaCl and KCl are used to extract NH_4^+, NO_3^-, and aluminum from soil samples (Kachurina *et al.*, 2000; Shuman and Duncan, 1990). Other salt ions mobilize elements *via* cation exchange (e.g. ammonium), anion exchange (e.g. nitrate), solubility changes (*e.g.*, dissolved organic nitrogen) (Haq *et al.*, 2018; Herbert *et al.*, 2015). NaCl, a common deicer, can also act to mobilize ammonium through cation exchange and sodium dispersion (Compton and Church, 2011; Duckworth and Cresser, 1991; Green *et al.*, 2008a; Kim and Koretsky, 2011). The positive charge of ammonium allows it to be sorbed onto negatively charged colloid particles in soils and sediments (Nieder *et al.*, 2011). Influxes of base cations (Na^+, Ca^{2+}, and Mg^{2+}), can then displace ammonium through base cation exchange, mobilizing ammonium into the water column (Duckworth and Cresser, 1991; Kim and Koretsky, 2011). In addition, salt ions can influence the solubility of organic nitrogen (Green *et al.*, 2008a). Some studies have indicated that increased salinity can mobilize dissolved organic nitrogen (DON) from soil and plant matter (Steele and Aitkenhead-Peterson, 2013). There can also be “salting in” effects, which alter organic matter quality and solubility (Kaushal, Reimer, Mayer, Shatkay, Maas, Nguyen, Boger, Yaculak, Doody, Pennino, Bailey, Galella, Weingrad, Collison, Wood, Haq, Newcomer-Johnson, *et al.*, 2022). During “salting in”, the solubility of organic matter is increased as ionic strength elevates (Kaushal, Reimer, Mayer, Shatkay, Maas, Nguyen, Boger, Yaculak, Doody, Pennino, Bailey, Galella, Weingrad, Collison, Wood, Haq, Newcomer-Johnson, *et al.*, 2022). Salt extraction of nutrients may be unintentionally occurring in urban watersheds affected by FSS, but less is known regarding the spatial and temporal extent and patterns.

Winter road salt pulses, which quickly increase stream water salinity, can also alter microbial processes that affect the nitrogen cycle. High osmotic stress and ion-specific toxicity caused by elevated salinity can lead to cell lysis and release of formerly stored inorganic and organic N and labile organic matter (Kaushal, Reimer, Mayer, Shatkay, Maas, Nguyen, Boger, Yaculak, Doody, Pennino, Bailey, Galella, Weingrad, Collison, Wood, Haq, Newcomer-Johnson, *et al.*, 2022; Kinsman-Costello *et al.*, 2022). Hydrologic systems that have been chronically exposed to FSS may evolve microbial communities distinct from those in more natural watersheds (Lancaster *et al.*, 2016). These microbial communities are often adapted to elevated salinities (Hale and Groffman, 2006; Kinsman-Costello *et al.*, 2022; Lancaster *et al.*, 2016).

Despite potential mobilization mechanisms, N concentrations and fluxes are often variable in their response to road salt application (Duan and Kaushal, 2015; Haq *et al.*, 2018). In prior incubation studies, increased salinity showed a positive relationship with TDN concentration in some study sites, while other sites did not show a clear trend (Duan and Kaushal, 2015; Haq *et al.*, 2018). A possible explanation for this variability may be that the sediment present in some of the sites may have had lower N content due to leaching from repeated previous exposure to elevated salinity levels (Hale and Groffman, 2006; Haq *et al.*, 2018). Freshwater salinization may mobilize available N from watersheds and soils until there is source limitation or a plateau in concentrations at the highest levels of salinity (Galella *et al.*, 2023; Haq *et al.*, 2018). Here we investigate the potential for temporal patterns in the concentrations and mass fluxes of nitrogen to be exacerbated by FSS at the watershed scale. Specifically, we analyze the effects of winter road salt events, seasonal cycles, and flow paths on watershed salt and nitrogen transport in urban streams.

4.3 Methods

4.3.1 Study Sites

Within the Chesapeake Bay watershed, five study sites were chosen. Sligo Creek and Rock Creek within the D.C. metropolitan area and Scotts Level Branch, Herring Run and Jones Falls within the Baltimore metropolitan area (Figure 14).

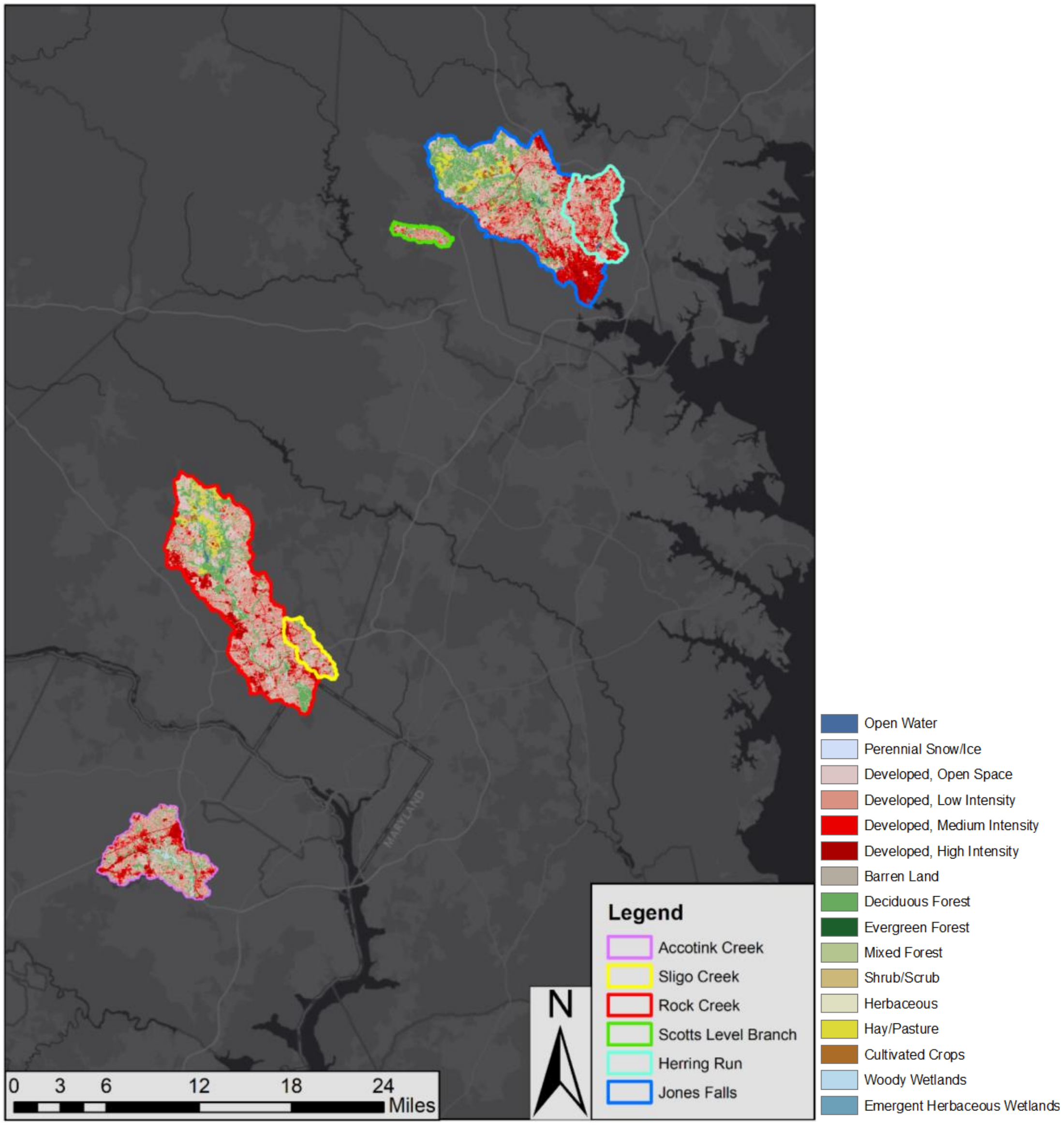

Figure 14. Study Sites

Land use at Herring Run, Jones Falls, Scotts Level Branch, Rock Creek, Sligo Creek, and Gwynns Falls watersheds in the Baltimore, MD and Washington D.C. metro areas.

Urban and suburban land use was the most prevalent at all sampling sites and impervious surface cover varied between 18% and 33%. More detailed site characteristics can be found in Table 11. Riparian buffers are present at all sites but are most pronounced at Rock Creek and least pronounced at Jones Falls, where they become absent within the city of Baltimore where the channel is buried. StreamStats, a USGS based web application, was used to delineate watersheds and the National Land Cover Database provided 30 m resolution land use and impervious surface cover data (“StreamStats,” 2022; “(MRLC),” 2022). Watershed characteristics were visualized with ArcMap 10.8.2.

Table 11. Monitoring Site Characteristics

USGS monitoring site characteristics. The metro area, latitude, longitude, USGS site number and monitoring duration are all listed. Rock Creek, Sligo Creek, Scotts Level Branch, Herring Run and Jones Falls were sampled bi-weekly by our lab group. Accotink Creek data was obtained through the USGS gauge station present.

Study Site	Metro Area	Latitude	Longitude	USGS Site Number	NLCD 2016 Impervious Surface Cover %	Monitoring Duration
Rock Creek	D.C.	38°57'36.6"	77°02'31.4"	1648010	18.35	10/19/2017 - 6/23/2021
Sligo Creek	D.C.	38°59'10.4"	77°00'17.5"	1650800	27.19	10/4/2017 - 6/23/2021
Scotts Level Branch	Baltimore	39°21'41.7"	76°45'42.3"	1589290	22.24	10/4/2017 - 4/15/2021
Herring Run	Baltimore	39°19'04.7"	76°33'18.5"	1585219	32.76	10/26/2017 - 1/3/2019
Jones Falls	Baltimore	39°17'02.8"	76°36'13.1"	1589485	21.28	11/1/2017 - 11/6/2019
Accotink Creek	Virginia	38°48'46"	77°13'43"	1654000	23.4	2/5/2015 - 1/1/2023

4.3.2 Routine Monitoring & High Frequency Monitoring

Routine stream water grab samples were collected at bi-weekly intervals beginning in October 2017 and ending between 2019 and 2021 (Table 11). Samples were collected directly into 125-mL HDPE Nalgene acid-washed sample bottles (Galella *et al.*, 2021). For targeted winter storm event sampling, hourly samples were collected using an automated sampler (ISCO 3700) at Sligo Creek. The automated sampler was used to collect samples before, during and slightly after snowstorm events. Every hour, 300 ml of water was collected and remained on ice (internal reservoir) until the storm subsided and it was safe to retrieve the unit(s) (Galella *et al.*, 2021). Once collected, samples were kept chilled on ice in the field or in a lab fridge kept at 4 ± 2 ºC until analysis (Galella *et al.*, 2021).

All sampling sites were located at USGS gauge stations equipped with high-frequency sensor measurements of discharge and specific conductance (5–15 min) (USGS NWIS, 2020). USGS monitoring stations utilize multiparameter datasondes which take instantaneous measurements. Jones Falls (USGS Gauge Station 1589485), Herring Run (USGS Gauge Station 1585219), Rock Creek (USGS Gauge Station 1648010), Sligo Creek (USGS Gauge Station 1650800) and Scotts Level Branch (USGS Gauge Station 1589290) were monitored continuously for discharge (Q) and specific conductance (SC), whereas Rock Creek was continuously monitored by sensors for SC, Q, and NO_3^-/NO_2^- (USGS NWIS, 2020). Data from Accotink Creek near Annandale, VA (USGS Gauge Station 1654000) was also used in this study as the NO_3^-/NO_2^- sensor at Rock Creek was discontinued in 2019. Accotink Creek was continuously monitored by sensors for SC, Q, and NO_3^-/NO_2^- (USGS NWIS, 2020). SC was reported in microsiemens per centimeter (µS/cm) at 25 °C. SC contact sensors were temperature adjusted (to report at 25 °C) and accurate > 0.5 ± 0.5% of readings, or ±2 µS cm−1 (Gibs *et al.*, 2012; Wagner *et al.*, 2006). Temperature data was collected using a thermistor with an accuracy of ±0.1 °C. Q is measured to an accuracy of the nearest 0.01 ft or 0.2% stage height ("USGS," 2018; Wagner *et al.*, 2006). Instantaneous measurements of NO_3^-/NO_2^-, collected *via* a multiparameter datasonde (USGS NWIS, 2020).

4.3.4 Water Quality Analyses

Once transported to the laboratory, water samples were immediately filtered through an ashed Whatman 0.7-micron glass fiber filter into labeled HDPE Nalgene bottles (Galella *et al.*, 2021). Total dissolved nitrogen (TDN) was analyzed on a Shimadzu total organic carbon analyzer (Shimadzu TOC-V CPH/CPN) total nitrogen module, TNM-1 using a chemiluminescence method (Galella *et al.*, 2021). Calibration of the TOC-V was performed every run (max 80 samples) with a 5 point calibration curve. Blanks were run and checked for accuracy (< 0.5) every 15 samples (Galella *et al.*, 2021). Calibration (internal) standards, as well as external check standards, were used in instrument calibration to determine if results were within the acceptable range of ± 20% of the true value (Galella *et al.*, 2021).

4.3.5 Numerical Analysis and Plotting

MATLAB 2021b was used to generate hysteresis plots. SC in microsiemens per centimeter at 25°C was plotted on the X axis. High frequency storm data collected at Sligo Creek plotted TDN on the Y axis in milligrams per liter. Data collected at Accotink Creek at the USGS monitoring site plotted NO_3^-/NO_2^- on the Y axis. Data from Rock Creek was not used in this analysis due to NO_3^-/NO_2^- sensor cessation in 2019. Four winter precipitation events from 2019 - 2021 were used for hysteresis analysis and a color scale was added to the data points in order to show the temporal nature of the data. Blue data points were taken near the beginning of the precipitation event and yellow data points were collected at the end. Hysteresis loops moving in a clockwise direction indicated that N or NO_3^-/NO_2^- concentrations decreased with increasing SC over the course of the storm. Counterclockwise hysteresis indicated that N or NO_3^-/NO_2^- concentrations increased with increasing SC over the course of the storm.

TDN and NO_3^-/NO_2^- mass fluxes in kg/hr were calculated using the following formula:

(TDN or NO_3^-/NO_2^- concentration in mg/L) X (Q in CFS) X 28.3168 X 60 X 60 / 1,000,000

Where: 28.3168 is liters per cubic foot
60 is seconds per minute
60 is minutes per hour
1,000,000 is milligrams per kilogram

4.4 Results

4.4.1 Seasonal Trends in Routine Sampling Sites and USGS Data

Bi-weekly sampling data revealed the existence of distinct seasonal patterns in streams draining all five watersheds in the Baltimore and Washington D.C. metro areas. Sensor data from the USGS showed that winter road salting could regularly increase SC by more than an order of magnitude over the course of several hours (Table 12, Figure 15). Peaks in TDN concentrations were also elevated during winter months, coinciding with the peaks in SC (Figure 15).

Table 12. Snow Event Sampling Data

Snow event sampling conducted with an ISCO automated water sampler. Samples were all collected at Sligo Creek, proximal to USGS station 1650800 in the Washington D.C. Metro Area.

Snow Event	Sampling Initiated	Sampling Ceased	N	Δ in Specific Conductance μS/cm
1	3/1/2019 20:23	3/2/2019 19:23	24	902 - 1730
2	12/16/2020 10:00	12/18/2020 3:10	33	419 -5130
3	1/25/2021 17:30	1/26/2021 17:00	48	682 - 3850
4	1/31/2021 6:00	2/2/2021 5:00	46	1330 - 12500

All five routine sampling sites had positive relationships between specific conductance and TDN concentrations over time. There were significant positive linear relationships between specific conductance and TDN concentrations at Sligo Creek and Scotts Level Branch. Jones Falls did not have statistically significant relationships between SC and TDN concentrations; this is probably because the site is tidal, which results in highly variable SC readings throughout the year. There were elevated TDN mass fluxes at Rock Creek during 2018, which are likely a result of sewage leaks frequently reported in the area (Fenston, 2022).

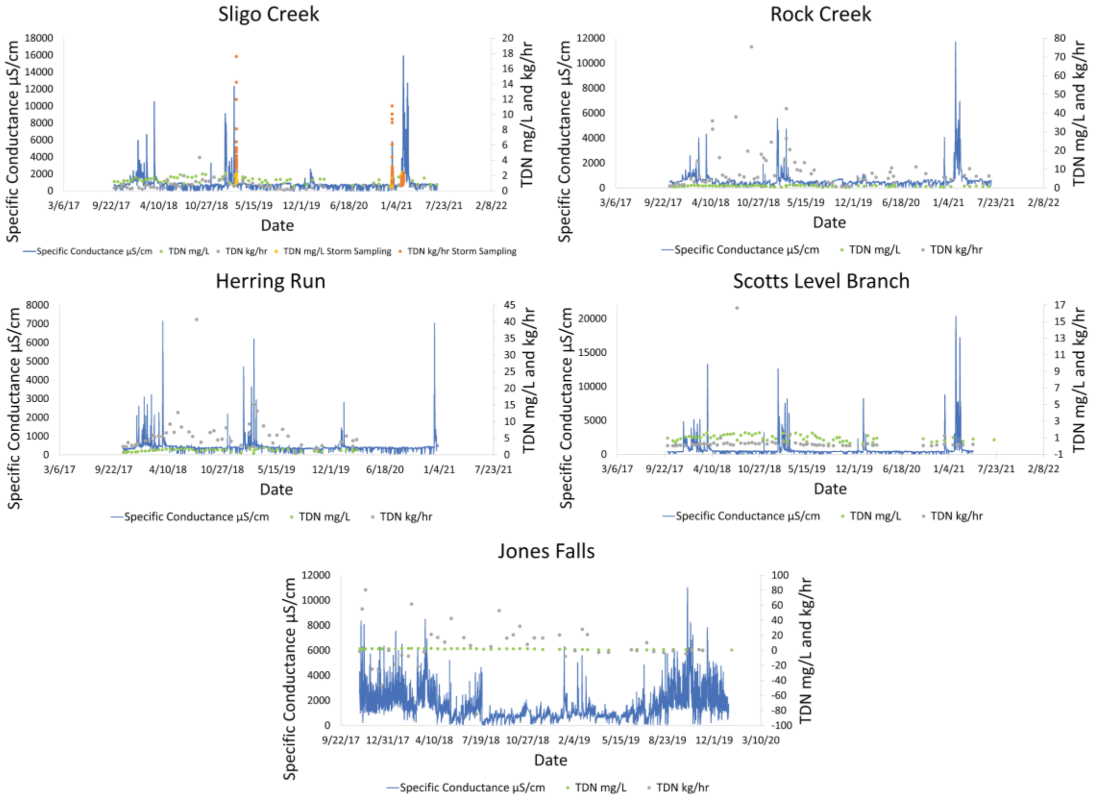

Figure 15. Peaks in TDN Associated with Peaks in Specific Conductance

Peaks in TDN associated with peaks in specific conductance. Rock Creek, Sligo Creek, Herring Run, Scotts Level Branch and Jones Falls were monitored by bi-weekly sampling. Targeted storm sampling data is also included at Sligo Creek. Concentration (mg/L) and flux kg/hr were calculated.

USGS data from Rock Creek and Accotink Creek also showed similar positive relationships between SC and NO_3^-/NO_2^- (Figure 16). Seasonal trends were most apparent when comparing mass fluxes of NO_3^-/NO_2^- with SC at Accotink Creek (Figure 16). Peak SC was always associated with peak mass fluxes of NO_3^-/NO_2^- every winter from 2015 to 2021. Elevated hourly mass fluxes of TDN and NO_3^-/NO_2^- coincided with peaks in SC, which suggested that N concentrations were not significantly diluted by increasing discharge (Figure 15,16).

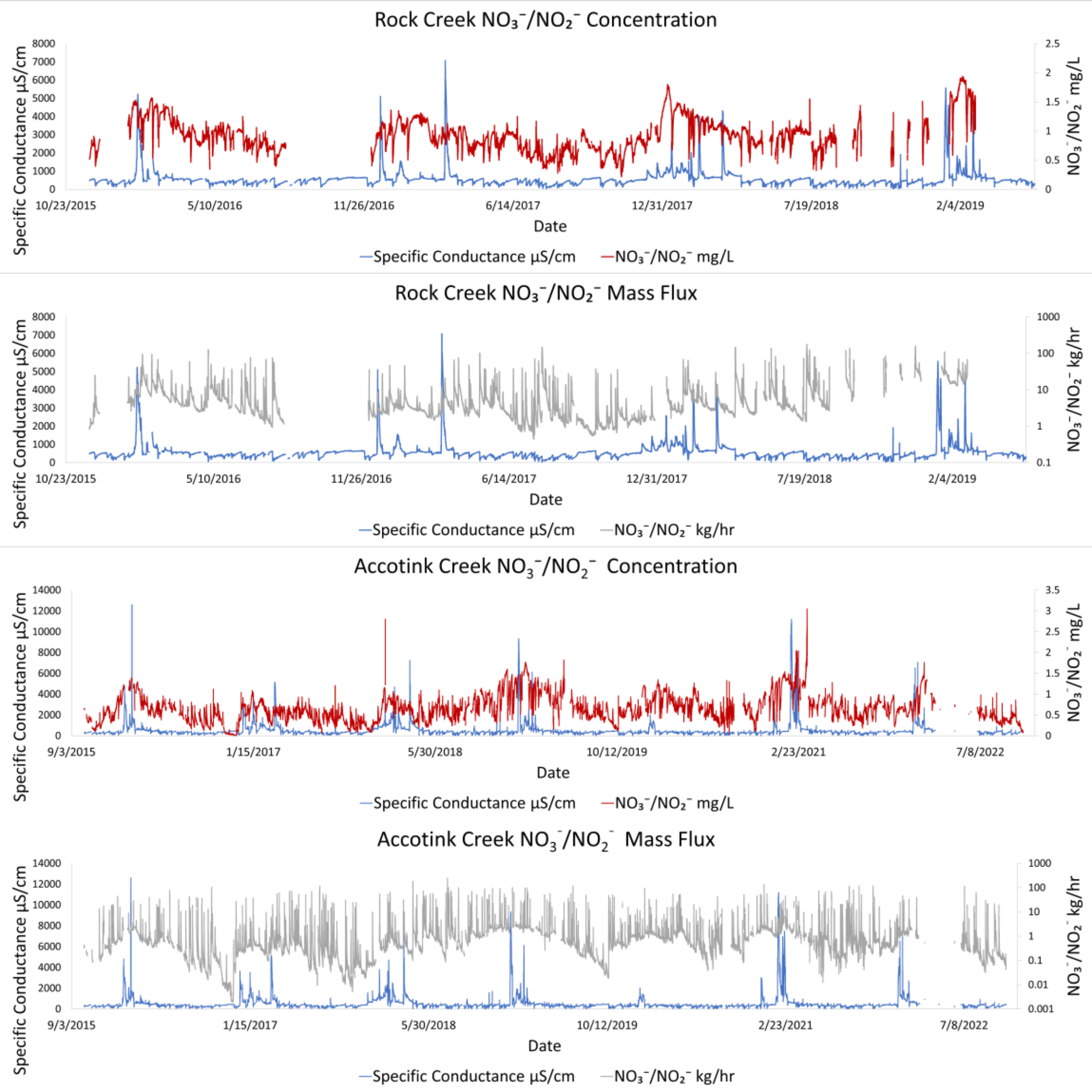

Figure 16. NO_3^-/NO_2^- Peaks Associated with Peaks in Specific Conductance

Peaks in NO_3^-/NO_2^- concentrations associated with peaks in specific conductance. Concentrations of NO_3^-/NO_2^- (mg/L) were measured by high-frequency sensors at Rock Creek and Accotink Creek and hourly fluxes (kg/hr) were calculated from discharge and concentration data.

4.4.2 Targeted Storm Event Sampling of Winter Precipitation (Sligo Creek)

Analysis of high frequency sampling conducted during winter precipitation events illustrated two different trends in NO_3^-/NO_2^- mobilization. When a winter storm was dominated by solid precipitation (snow/sleet) and road salt applications were consistent, concentrations of NO_3^-/NO_2^- decreased with increasing SC. For example, during a snowstorm starting on 1/31/2021NO_3^-/NO_2^- concentration dropped from 2.35 mg/L at the start of the storm to 1.128 mg/L at the end (Figure 17). NO_3^-/NO_2^- . However, hourly mass fluxes consistently increased with increased SC throughout the snowstorm event from 0.82 kg/hr when the storm started to 2.33 kg/hr as the winter storm ceased. Peak SC reached as high as 12,400 µS/cm by the end of the snowstorm event. These observations are consistent across multiple different snowstorms and at both Sligo Creek and Accotink Creek (Figure 17).

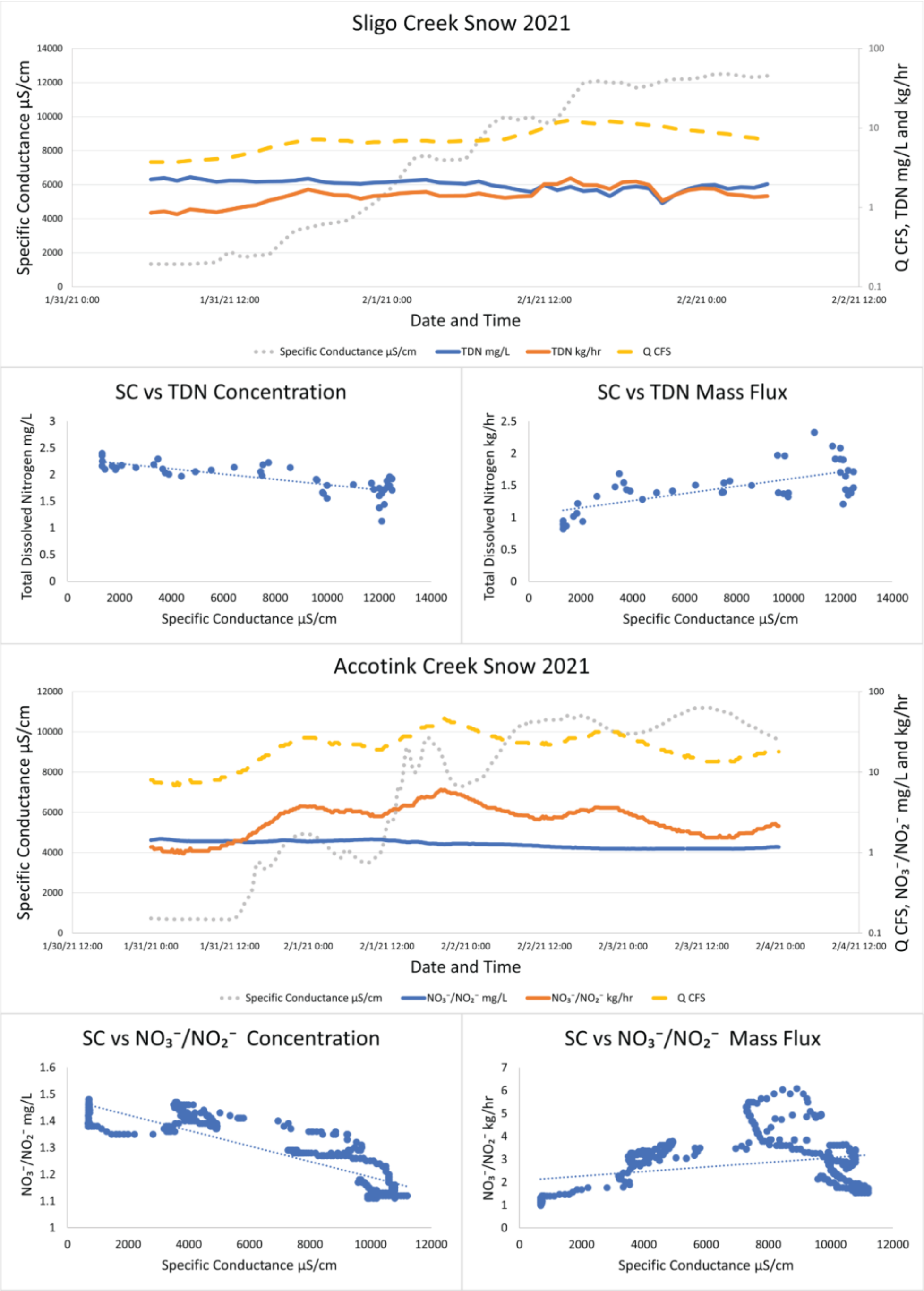

Figure 17. Specific Conductance and Nutrient Trends During Storms

Specific conductance, TDN, NO_3^-/NO_2^-, and discharge trends during two snowstorms at Sligo creek and Accotink Creek. Over the course of the storm, concentration of TDN and NO_3^-/NO_2^- was found to decrease while mass flux was found to increase. TDN data was collected by targeted storm sampling and NO_3^-/NO_2^- data was collected by high frequency sensor measurements.

Interestingly, winter storms which began as snow and then shifted to rain (rain-on-snow events) have different trends. During a rain-on-snow event captured with targeted storm sampling at Sligo Creek (Figure 18), SC quickly peaked at 5,000 µS/cm then sharply decreased, as rain diluted the discharge to 890 µS/cm within three hours. As the rain transitioned back to snow, the SC rose again to 5,000 µS/cm. During this rain-on-snow event, TDN concentrations rose with increased SC from 0.49 mg/L to 1.29 mg/L, but hourly TDN fluxes decreased from 11.1 kg/hr to 2.1 as SC rose.

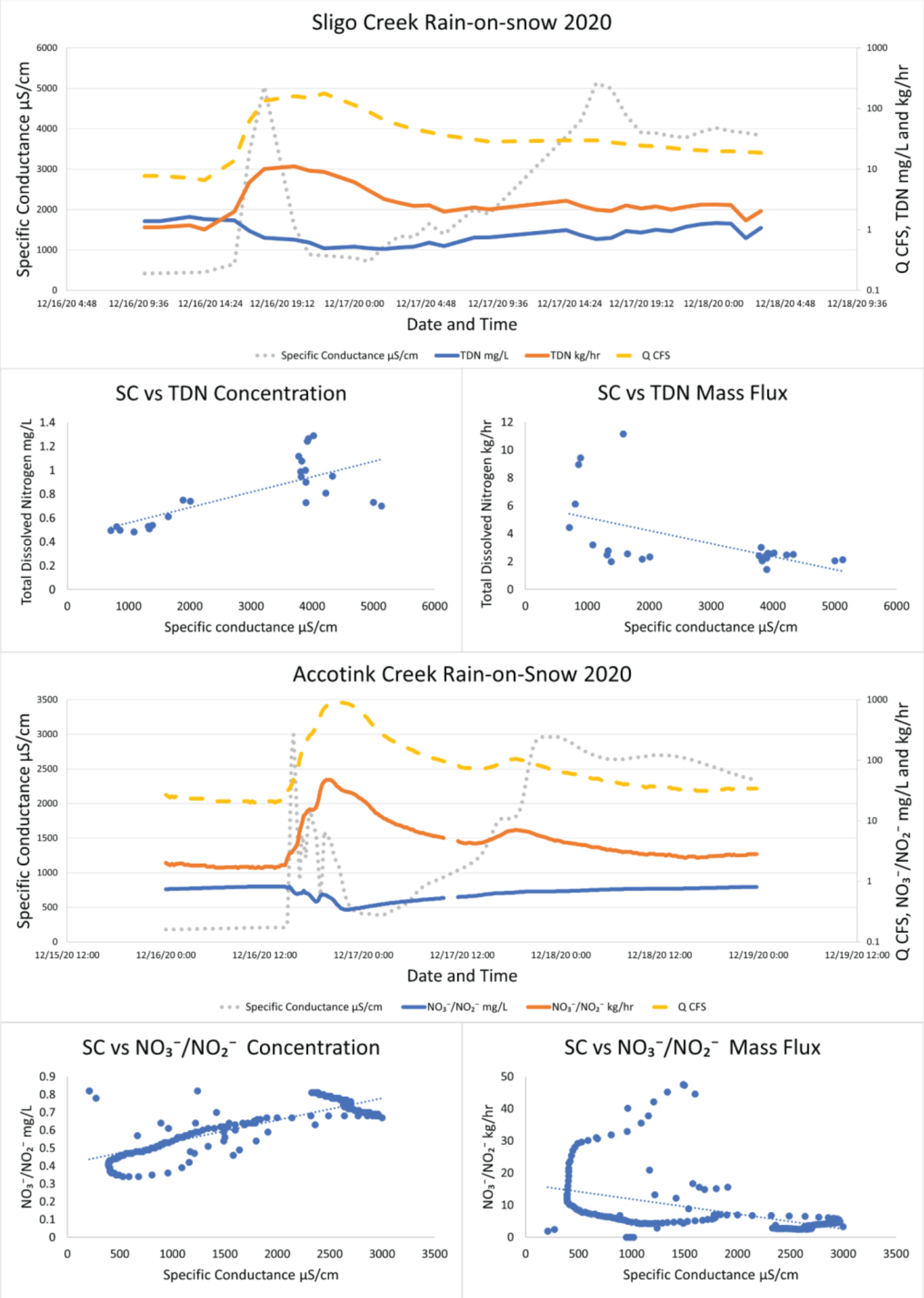

Figure 18. Trends During Rain-On-Snow Events

Specific conductance, TDN, NO_3^-/NO_2^-, and discharge trends during two rain-on-snow storms at Sligo creek and Accotink Creek. Over the course of the storm, concentration of TDN and NO_3^-/NO_2^- was found to increase while mass flux was found to decrease. TDN data was collected by targeted storm sampling and NO_3^-/NO_2^- data was collected by high frequency sensor measurements.

4.4.3 Hysteresis of Nitrogen Concentrations during Winter Snow Events

Hysteresis analyses of rain-on-snow *vs.* snow events revealed distinct patterns of TDN mobilization. Figure 19 shows hysteresis loops from two snow events (indicated with the snowflake symbol) and two rain-on-snow events (indicated with the raindrop symbol). Counterclockwise hysteresis was observed for both rain-on-snow events at Sligo Creek (2019 and 2020), which indicated that TDN concentrations decreased with increasing SC over time. Counterclockwise hysteresis was observed for both snow events recorded at Sligo Creek (2021), which indicated that TDN concentrations increased with increasing SC over time. As expected, results were consistent with those at nearby Accotink Creek, where USGS sensors also measured high-frequency NO_3^-/NO_2^- concentrations. Clockwise hysteresis was observed during both rain-on-snow events and counterclockwise hysteresis was observed during both snowstorms. The 2020 rain-on-snow event at Accotink Creek is unique, as it had both a clockwise and counterclockwise loop present.

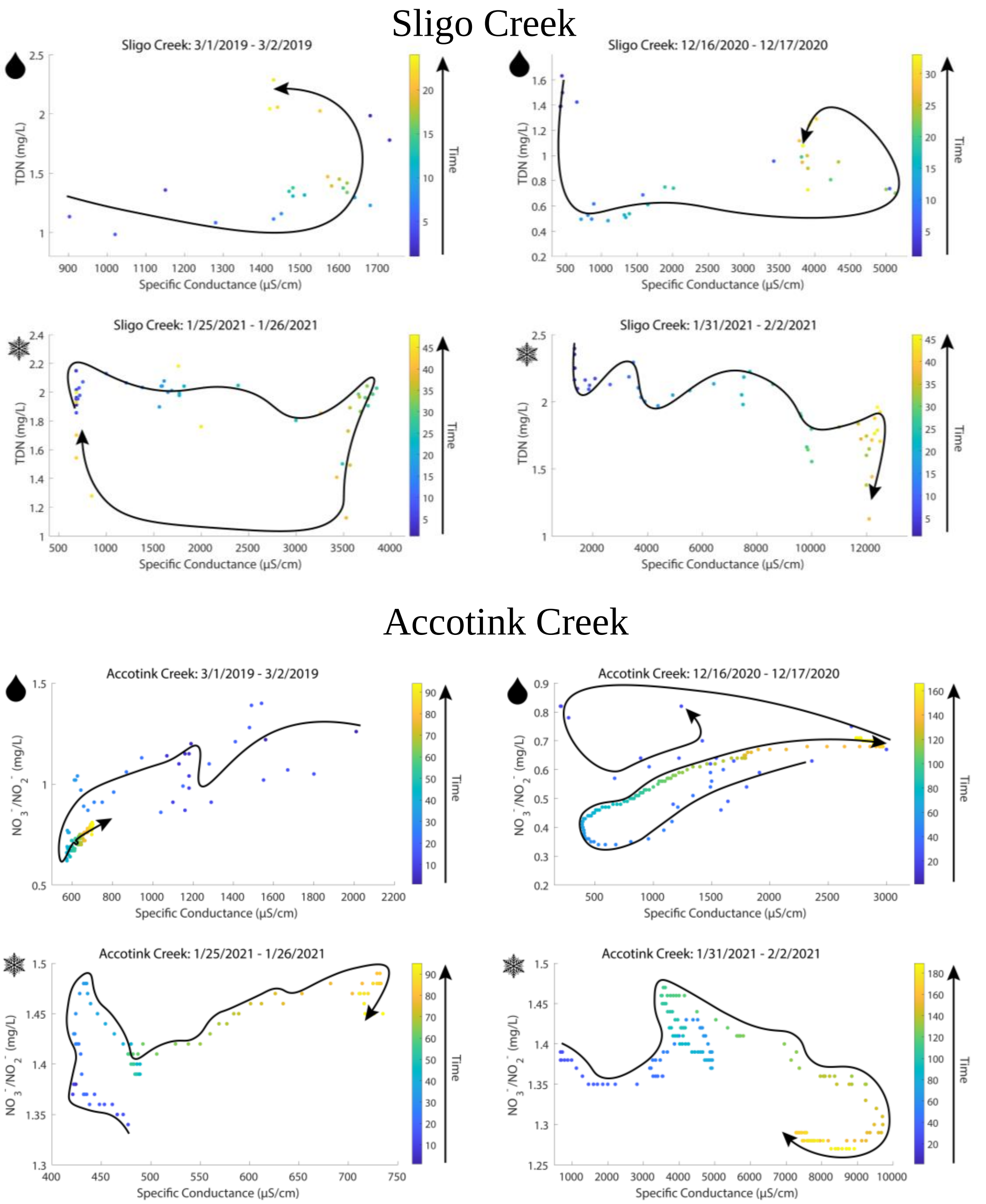

Figure 19. Hysteresis Analysis

Hysteresis loops for snow and rain-on-snow events at Sligo Creek and Accotink Creek. Sligo Creek data recorded TDN concentrations from targeted storm sampling measurements and Accotink data recorded NO_3^-/NO_2^- concentrations from high-frequency sensor measurements. Corresponding high-frequency sensor data for NO_3^-/NO_2^- from Rock Creek during the same time period was not available due to NO_3^-/NO_2^- sensor cessation at that location in 2019. Clockwise loops occurred during snow events and counterclockwise loops occurred during rain on snow events at both sites. Snowflake symbols denote a snow only precipitation event, raindrop symbols denote a rain-on-snow event.

4.4.4 Plateaus in N Concentrations over Time during Road Salt Events

Data from routine and targeted snow event monitoring at Sligo Creek (Figure 20) showed a positive relationship between SC and TDN. The increasing trend between SC and TDN was present until ~ 2,000 μS/cm, where a plateau was reached. A similar pattern was also observed using USGS data from Rock Creek and Accotink Creek, where a positive correlation between SC and NO_3^-/NO_2^- concentrations were observed until a plateau at ~ 1,000 μS/cm as well (Figure 21). Seasonal trends are shown for Rock Creek and Accotink Creek *via* box and whisker plots. Points above the upper quartile marked in red show elevated SC present during the winter months of December through March. Elevated NO_3^-/NO_2^- is also present during the same timeframe of December through March at both Rock Creek and Accotink Creek (Figure 21).

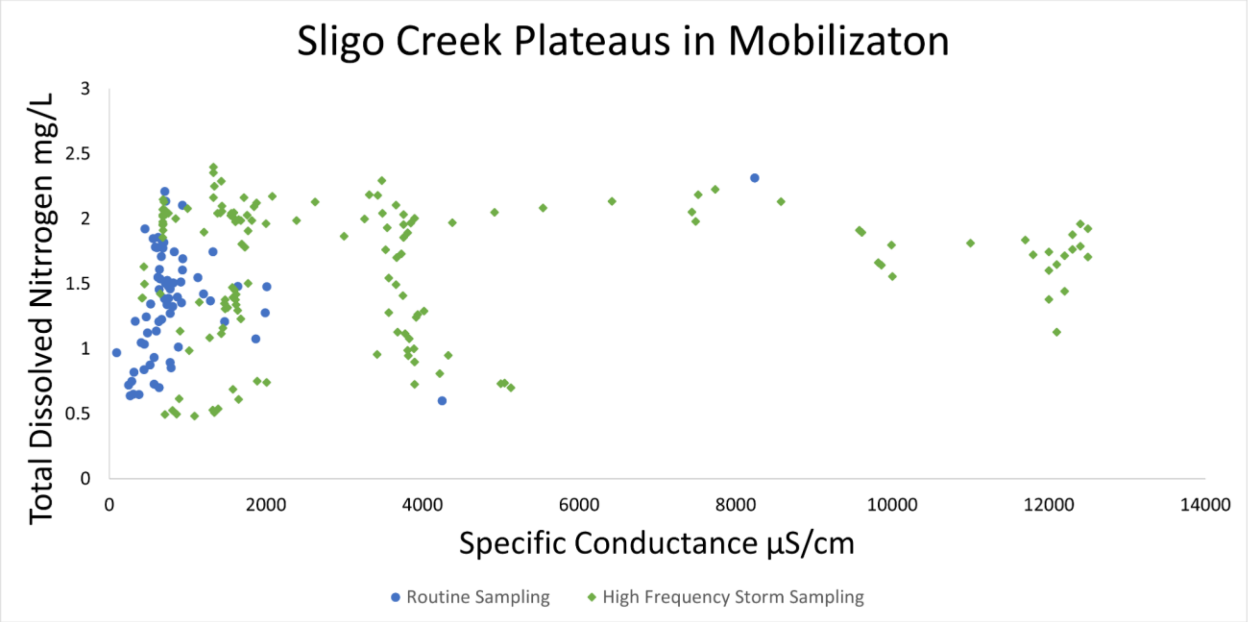

Figure 20. Specific Conductance Plateaus at Sligo Creek

Specific conductance at Sligo Creek. Regular bi-weekly sampling is plotted in blue circles and targeted winter storm event sampling is plotted in green diamonds. A plateau in mobilization is notable at ~2,000 µS/cm where concentrations of TDN stop increasing with increases in specific conductance.

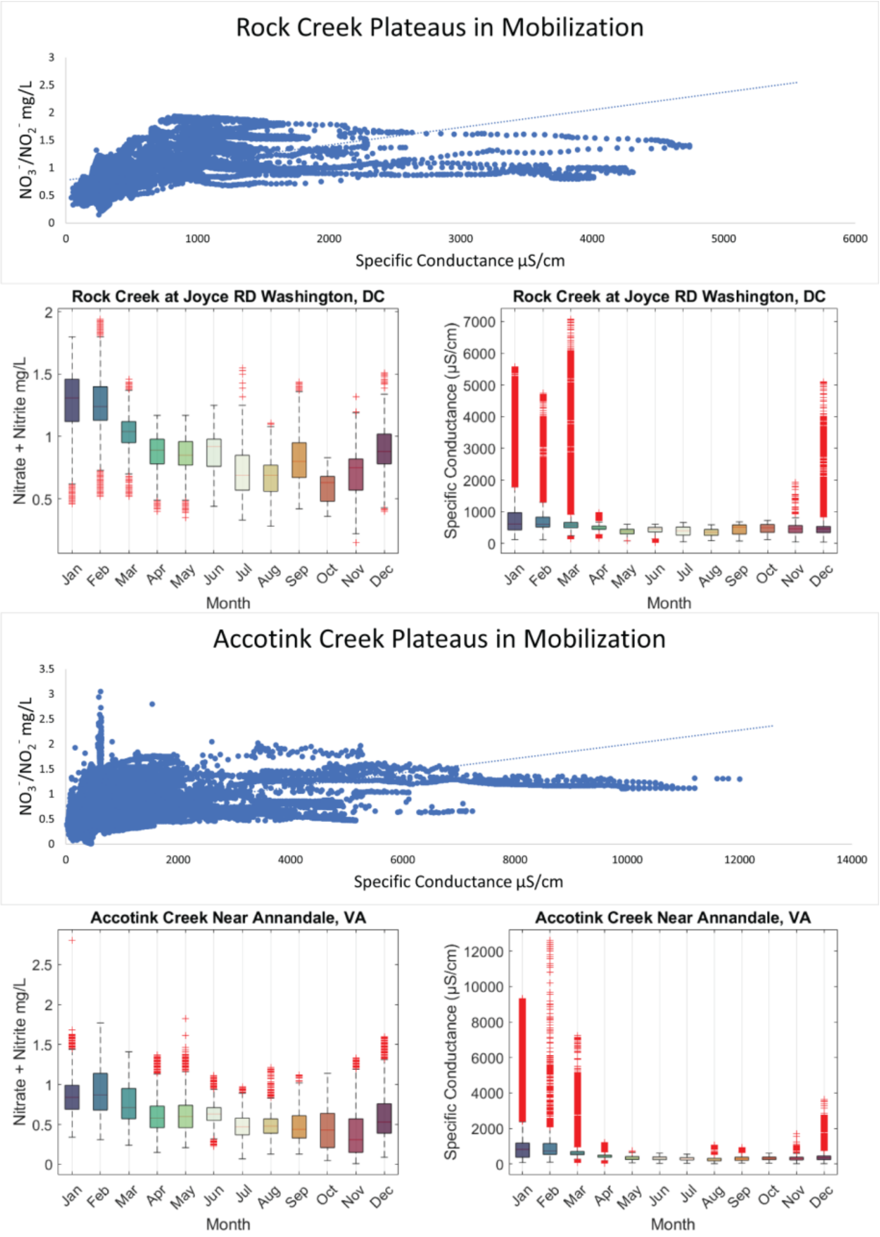

Figure 21. Specific Conductance Plateaus at Rock Creek and Accotink Creek

Figure 21. Specific conductance is plotted against NO_3^-/NO_2^- concentration (mg/L) for Rock Creek and Accotink Creek from high-frequency sensor measurements. Data from Rock Creek and Accotink Creek both show distinctive plateaus in NO_3^-/NO_2^- mobilization at ~1,000 µS/cm. Boxplots show monthly data for both sites where both NO_3^-/NO_2^- and specific conductance peak during the winter and reach a minimum in the autumn.

4.5 Discussion

Our results suggest that FSS can alter the concentrations and fluxes of N transported from urban watersheds. Many studies have evaluated other causes of elevated N transport from watersheds related to atmospheric deposition, land use, management, and other factors (Groffman *et al.*, 2004; Howarth and Marino, 2006; Kinsman-Costello *et al.*, 2022; Mayer *et al.*, 2010). Our work also suggests that relationships between TDN / NO_3^-/NO_2^- concentrations and specific conductance can reveal unique insights into N cycling and transport for urban environments. When targeted winter storm event data and high-frequency sensor data are analyzed (along with routine monitoring data throughout the year), a distinct pattern emerges; there are plateaus in nitrogen concentrations at the highest levels of specific conductance. Up to a certain threshold, the effects of FSS in urban catchments act to elevate both TDN and NO_3^-/NO_2^- concentration as well as hourly mass fluxes. This was observed as seasonal pulses (Figure 15,3, 8) during and after winter storm events (Figure 17, 3.5). Complex biogeochemical interactions can occur, which drive mobilization, transport, and retention of nitrogen. Overall, there were clear patterns in winter pulses of nitrogen concentrations and fluxes in this study, which suggest the importance of reconsidering the importance of water quality monitoring and management during winter months.

4.5.1 FSS and Mobilization of TDN and NO3−/NO2− Pulses

At routine sampling sites, TDN and NO_3^-/NO_2^- concentrations and hourly mass fluxes increased throughout the winter, especially coinciding with winter precipitation events and associated peaks in SC (Figure 15,3). Statistically significant linear relationships between SC and TDN were most apparent at Sligo creek, where targeted winter storm event sampling was conducted; this highlights the importance of integrating storm event or high-frequency temporal sampling in monitoring programs, although this data is often difficult to collect. Average hourly mass fluxes observed at Sligo Creek during routine sampling were 0.8 kg/hr and peaked at 2.5 kg/hr. Targeted winter storm event sampling at Sligo Creek during the 2019 snow event captured hourly TDN mass fluxes reaching a maximum of 17.6 kg/hr (within a one hour of peak SC (2050 µS/cm). Positive SC and TDN relationships were also observed at Rock Creek, Scotts Level Branch and Herring Run. Data from USGS continuous monitoring sensors showed seasonal patterns in NO_3^-/NO_2^- mobilization, with peaks in NO_3^-/NO_2^- concentrations and hourly mass fluxes, which coincided with peaks in specific conductance (Figure 15,16).

Many previous studies have characterized seasonal patterns in nitrogen concentrations in streams. For example, studies from different regions throughout the U.S. have shown that nitrate (NO_3^-) and total dissolved nitrogen peak during winter months, when biological activity is lowest (Johnson and Stets, 2020; Kaushal and Lewis, 2005). However, there are exceptions where stream N concentrations can peak during summer months in some watersheds in warmer regions due to increasing organic matter decomposition, N mineralization, and nitrification (Brookshire *et al.*, 2011; Swank and Vose, 1997). In the Chesapeake Bay watershed, Testa et al. 2018, proposes that there are seasonal cycles to nitrogen loads throughout the year. In spring and early summer there are high NO_3^-, NH_4^+, and particulate nitrogen inputs, a bloom of phytoplankton during the spring and oxygen depletion and NH_4^+ accumulation in the summer (Testa *et al.*, 2018). In late summer and autumn phytoplankton production is reduced and vertical mixing of water columns resumes, replenishing dissolved oxygen and increasing nitrification. This process may explain some of the seasonal cycling observed in this study (Figure 15, 3, 8) but peaks associated with road salting events and positive correlations between specific conductance and NO_3^-/NO_2^- mobilization show that FSS can play a role in nitrogen cycling and transport.

Our watershed monitoring results are consistent with previous laboratory studies that show that salinization can alter N concentrations in soils, streams, and wetlands (Duan and Kaushal, 2015; Green *et al.*, 2008a; Hale and Groffman, 2006; Haq *et al.*, 2018). Lab based incubation analysis on samples collected from the DC and Baltimore metro areas showed increasing mobilization of TDN with increasing salinity at 75% of the sites sampled (Haq *et al.*, 2018). Suburban and urban sites located in the Gwynns Falls watershed showed positive linear relationships with increasing salinization (Supplemental Figure 4.1) (Haq *et al.*, 2018). In addition, impervious surface cover and urban land use have also been linked to total Kjeldahl nitrogen (TKN) mobilization in laboratory salinization experiments. TKN increased in concentration in laboratory incubations, as salinity increased at all sites studied (forested, agricultural, suburban and urban), with the greatest degree of mobilization recorded at urban sites (Duan and Kaushal, 2015). The same trend occurred when mobilization in laboratory salinization incubations was plotted over watershed percent impervious surface cover (% ISC) instead of using land use classifications. Significant positive relationships were discovered between % ISC and TKN concentration (Duan and Kaushal, 2015). Finally, there were variable responses in N mobilization in salinization experiments in stormwater Best Management Practices (BMPs), but there was limited data compared to previous studies. Overall, laboratory results from salinization experiments are consistent with observations of increased concentrations and fluxes of N in watersheds of this study, but results may be complicated based on hydrology, soil characteristics, and land use.

Mobilization of N and NO_3^-/NO_2^- is thought to be driven chemically by a combination of ion exchange (Kachurina *et al.*, 2000; Shuman and Duncan, 1990) and sodium dispersion (Compton and Church, 2011; Duckworth and Cresser, 1991; Green *et al.*, 2008a; Kim and Koretsky, 2011). Cation exchange has also been shown to mobilize NH_4^+ from soils and sediments into solution (Kinsman-Costello *et al.*, 2022). Biological factors like cell lysis due to rapidly changing osmotic stress and ion-specific toxicity may also contribute additional N loading during acute road salting events (Kaushal, Reimer, Mayer, Shatkay, Maas, Nguyen, Boger, Yaculak, Doody, Pennino, Bailey, Galella, Weingrad, Collison, Wood, Haq, Newcomer-Johnson, *et al.*, 2022; Kinsman-Costello *et al.*, 2022). The rates of microbial processes which control nitrogen transformation may also be affected by elevated salinities associated with FSS, increasing leaching of NO_3^- from impacted waterways

(Green *et al.*, 2008a). Some microbial communities in watersheds may become adapted to elevated salinities however, lessening the cell lysis associated with high osmotic stress (Hale and Groffman, 2006). However, more work is necessary to investigate the effects of increased salinization on microbial N cycling.

4.5.2 High Temporal Frequency Sampling and Storm Hysteresis

Different types of winter precipitation can affect TDN and NO_3^-/NO_2^- mobility in urban catchments. High frequency sampling at Sligo Creek and Accotink Creek showed that during solid precipitation events, TDN and NO_3^-/NO_2^- concentrations decreased (clockwise hysteresis) while mass flux increased over time (Figure 16,4). The opposite trends were found during rain-on-snow events, where N and NO_3^-/NO_2^- concentrations increased (counterclockwise hysteresis) while mass flux decreased over time.

During rain-on-snow events, at the point of transition from snow to rain, hourly mass fluxes of TDN and NO_3^-/NO_2^- were significantly higher than at any other point during the storm. These peaks were captured by both high-frequency monitoring by sensors and targeted storm sampling. Initial N mobilization by elevated SC, followed by elevated discharge caused mass fluxes to briefly reach 47 kg/hr NO_3^-/NO_2^- at Accotink Creek (Figure 18). Similar conditions have been recorded in rural forested catchments in Ontario, Canada. During individual rain-on-snow events, as much as 40% of the annual NO_3^- export from the catchment could be mobilized (Eimers *et al.*, 2007). These significant NO_3^- pulses were often followed by depressed pH and alkalinity (Eimers *et al.*, 2007).

After the transition from snow to rain, decreasing specific conductance associated with rainfall may limit the mobilization of TDN into the water column *via hydrologic dilution,* diminished base cation exchange, or decreased osmotic stress on microbial cell membranes (Haq *et al.*, 2018; Kinsman-Costello *et al.*, 2022; Vaughan *et al.*, 2017). We speculate that increased N mass flux with increased SC during snow events may be a result of freshwater and saltwater mixing in the hyporheic zone and mobilization of N from transient storage zones. When a high density gradient is present (saline water mixing with freshwater), the mixing efficiency and reaction area increase, which can elevate NO_3^- production from lysis of microbial cells, ammonification and nitrification, and subsequent transport. (Jiang *et al.*, 2021). However, further research is necessary to determine why N fluxes and concentrations increase due to hydrological and physical and biological mechanisms.

4.5.3 Plateaus in N Concentrations over Time during Road Salt Events

When plotted against SC, TDN and NO_3^-/NO_2^- concentrations have a positive relationship until they reach a plateau. This plateau was found to be at ~ 1,000 μS/cm for NO_3^-/NO_2^- concentrations (Figure 21) and closer to 2,000 μS/cm for N concentrations (Figure 20). Thresholds in N species mobilization by FSS are thought to be caused by the cation exchange capacity (CEC) of the sediments present at these catchments (Sligo Creek, Rock Creek and Accotink Creek). Similar CEC limits were found when examining major and trace element mobilization at urban stormwater BMPs (Galella *et al.*, 2023). Plateaus in N mobilization were also observed in salinization incubation experiments in Haq et al., 2018. Once a cation like Na^+ has mobilized positively charged species like NH_4^+ from all exchange sites available on sediment colloids, the concentration can no longer increase (Duckworth and Cresser, 1991; Kim and Koretsky, 2011). Thresholds in N and NO_3^-/NO_2^- mobilization can also be influenced by biological mechanisms. Recent studies have suggested that over decades of exposure to FSS, microbial communities may become adapted to the high osmotic stress of episodic FSS due to road salting, leading to reduced cell lysis and N dispersion at high salinities (Hale and Groffman, 2006; Kinsman-Costello *et al.*, 2022). These biological factors may also play a role in determining the limits of the plateaus observed.

4.6 Winter Water Quality Implications and Conclusions

Many urban water quality monitoring programs mainly study baseflow and targeted rainstorms during fall, summer, and spring. This means that many important N transport events can be missed during winter snowstorms and episodic road salting in some urban watersheds. Most literature regarding N mobilization focuses on mobilization during rain events but research during the winter months is scarce (Kelly *et al.*, 2019; Mihiranga *et al.*, 2021). More work needs to be done in order to capture more detailed snow event data and thus better understand winter N fluxes and cycling in urban watersheds (Brooks *et al.*, 1997, 1998). Increased fluxes of nitrogen to sensitive, and potentially eutrophic, receiving waters during times of colder temperatures and lower biological uptake could influence downstream transport distances (Testa *et al.*, 2018). Increased salinization could also negatively impact the function of any stream restorations present in the affected catchments, as nutrient retention is usually a stated goal of their construction (Cooper *et al.*, 2014; Kaushal, Reimer, Mayer, Shatkay, Maas, Nguyen, Boger, Yaculak, Doody, Pennino, Bailey, Galella, Weingrad, Collison, Wood, Haq, Newcomer-Johnson, *et al.*, 2022).

Increased winter monitoring may be necessary to help manage TDN mobilization from FSS in some urban watersheds. As there is limited literature on the subject, more data on seasonal trends as well as spatial dynamics of mobilization is needed. High resolution spatial and temporal data is especially important, as certain trends in mobilization are only exposed by very high frequency sampling (≤1 hour resolution) (Figure 20). Debris dams and other sources of organic matter may act as a sink for NO3−, but microbial communities residing in them may take time to adapt to the highly saline environments and the associated osmotic stress present in urban streams (Hale and Groffman, 2006). In the long term, searching for alternatives to NaCl road salt could help alleviate the situation, but it is unclear if $CaCl_2$ or $MgCl_2$ are less harmful at this time (Hale and Groffman, 2006). $CaCl_2$ is more efficient at melting snow and ice than other deicers, so less can be used; however, more research is needed to determine if it would be a suitable alternative (Galella *et al.*, 2023).

Chapter 5: Conclusions and Future Work

5.1 Key Conclusions

FSS and associated chemical cocktails are pervasive in urban watersheds throughout the year. Chronic salinization of groundwater combined with nonpoint pollution from leaky wastewater pipes, weathering of concrete, and the application of fertilizers leads to loosely corelated "summer" cocktails of metals (Cu and Sr^+) and base cations (Na^+, K^+, and Mg^{2+}). During winter road salting events however, when specific conductance can increase by two orders of magnitude in a matter of hours, processes including base cation exchange, the mobile anion effect, chloro-complexation, and high osmotic stress release acute "winter" chemical cocktails of metals (Mn, Cu, Sr^{2+}), base cations (Na^+, Ca^{2+}, Mg^{2+}, K^+), nutrients (TDN), and organic carbon (DOC).

Some chemical constituents of these chemical cocktails like Mn, and Cu have nearly linear response curves with increasing specific conductance, allowing for robust proxies to be developed. The USGS alone monitors over 1,000 streams in the United States for specific conductance at 5-15 minute intervals, allowing for these proxies to be used for real-time monitoring of estimated metal loads across the country. With Mn being a known neurotoxin in humans and Cu being a toxicant to aquatic fauna, monitoring their concentrations is of paramount importance to the health and safety of urban streams.

Stormwater BMPs which are often designed to improve urban watershed health by reducing peak discharge, retaining contaminants, and encouraging groundwater recharge. Acute FSS can turn stormwater BMPs from contaminant sinks to contaminant sources as chemical cocktails of metals (Mn, Cu, Sr^{2+}), base cations (Na^+, Ca^{2+}, Mg^{2+}, K^+), nutrients (TDN), and organic carbon (DOC) become mobilized. Increasing salt concentrations of NaCl, $CaCl_2$ and $MgCl_2$ mobilized statistically significantly (p-value <0.05) higher concentrations of B, Ba^{2+}, Ca^{2+}, Cu, K^+, Mg^{2+}, Mn, Na, Sr^{2+}, DIC, and DOC. Salt type showed preferential mobilization of certain elements. NaCl mobilized Cu, at rates over an order of magnitude greater than both $CaCl_2$ and $MgCl_2$ and $CaCl_2$ mobilized Sr^{2+} at rates over double that of NaCl or $MgCl_2$ incubations. Stormwater BMP type also had a significant effect on elemental mobilization, with ponds mobilizing significantly more Mn than other sites. Stormwater BMP age may also play a factor with significantly more salt being retained in bioswale sites which were more than a decade younger than the other sites sampled.

More in-depth study of nutrient mobilization during road salting events showed that urban streams had elevated concentrations of TDN and NO_3^- / NO_2^- which peaked during and after winter road salt events, and then declined. I found significant linear relationships between TDN concentrations and SC in multiple urban watersheds. Hourly mass fluxes of TDN in streams were also found to be elevated during winter months with peaks coinciding with road salting events. Targeted winter snow event sampling and high-frequency sensor data suggested plateaus in NO_3^- / NO_2^- and TDN concentrations at the highest peak levels of SC during road salt events between 1,000 and 2,000 µS/cm, which possibly indicated source limitation of TDN after extraction and mobilization of watershed nitrogen reservoirs by road salt ions.

As the effects of climate change continue to progress average temperatures may increase but so will the incidence of extreme weather events. Increased evaporation from warmer temperatures coupled with the increased occurrence of strong tropospheric polar vortex events could lead to more severe winter storms and associated road salt use. Prolonged periods of drought could also concentrate and intensify the summer chemical cocktails described above as there will be diminished rainfall to dilute them.

The use of alternative deicers should be explored to help diminish the effects of acute FSS. NaCl is the most prevalent deicer used as it is the most cost-effective option. When environmental costs are considered however, options like brines become more appealing. Similar deicing effects can be achieved when using brines (pickle, beet, etc.) while only introducing a fraction of the salt into urban watersheds. Alternate deicers like $CaCl_2$ and $MgCl_2$ also offer improved ice melting capacity with reduced mobilization of Cu when compared to NaCl. Cu is a potent aquatic toxicant to many freshwater species and its reduction would help to improve the overall health of urban streams affected by FSS. The use of sand or grit should also be investigated but their overuse can have other detrimental effects to urban stream sediment.

Regulating deicer use will likely be a difficult task as it is a zero-sum game. You are trading health and safety of roadways for health and safety of urban watersheds and potentially drinking water supplies. The proliferation of telecommuting may be a potential avenue for regulation to probe as it has been a useful stopgap during COVID lockdowns both for education and business. As groundwater salinity increases year after year in the DC and Baltimore metro area it looks as if deicer use will have to inevitably be regulated, but the timing of implementation is still unknown.

5.2 Future Work

Though every effort was made to conduct complete and comprehensive studies, there are areas which should be investigated in future research. Chemical cocktail mobilization from brine usage should be investigated and compared to mobilization triggered by NaCl, $CaCl_2$ and $MgCl_2$. Many brines like beet brine for example contain organic matter and potential nutrients which may affect urban stream chemistry and contaminant retention / mobilization. They may also enter stream ecosystems more quickly as they are already liquid and dissolution time is not a factor.

Morphological features of sediments should be further investigated, including Fe-Mn concretions and nodules. As there was a temporal delay in Mn mobilization after peak salinization (noted in chapter 1), the behavior these nodules may provide further insight into the effects of changing redox conditions and possible influence of groundwater on the formation of chemical cocktails. More precise evaluation of sediment particle size and organic matter content could help describe what is driving the significant differences observed between stormwater BMP sites in chapter 2.

Data regarding salt application from the Maryland Department Of Transportation (MDOT) and District Department of Transportation (DDOT) would be extremely beneficial to future studies. Though this data wouldn’t be able to account for non-point source pollution from individuals salting their driveways or paths it would represent a good starting point for tracking salt inputs and monitoring movement throughout the environment. Efforts were made to obtain this information for more than a year but the data was never provided.

5.3 Things I’ve learned during my tenure as a graduate student at UMD

Never underestimate the power of nature or people to interfere with field work. Always assume there will be a flood which will wash away instruments downstream and always securely tie them to a nearby tree. Always attach labels inferring that a research site is under video surveillance even if this is not the case. I’ve lost an equal number of samples to vandalism as I have to mother nature. Try to engage with the public when they seem interested in your work (particularly when in the field). You would be surprised how many people are interested in your research especially when it has potential implications for their health and safety. Never let nay-sayers keep you down; as long you keep getting back up they never will.

Appendices

Chapter 2 Supplementary Materials

Supplemental Table 2.1: Statistics for linear regressions found in Figure 4. Percent impervious surface cover is abbreviated as %ISC. This was completed to provide further details and only significant relationships were discussed in the manuscript.

Sligo Creek Synoptic Survey

Analyte	Slope of relationship	P value (Analyte / % ISC)	R^2 Analyte / SC)	Slope
Ca^{2+}	Positive	0.0008	0.62	1.916
Na^+	Positive	0.01	0.44	2.387
Mg^{2+}	Positive	0.01	0.41	0.440
K^+	Positive	0.01	0.45	0.191
DIC	Positive	0.46	0.05	0.198

Supplemental Figure 2.1 Stream discharge from study sites over the same sample collection period as in Figure 2 (“USGS NWIS”). Higher discharge is usually observed in these streams during summer storms in this region with typically smaller precipitation events occurring over the winters.

Rock Creek

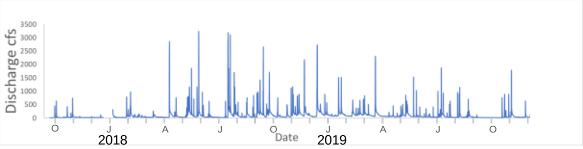

Herring Run

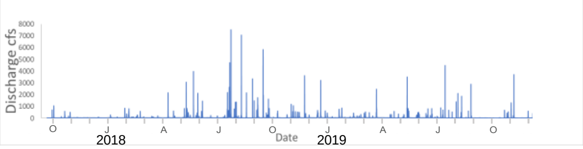

Sligo Creek

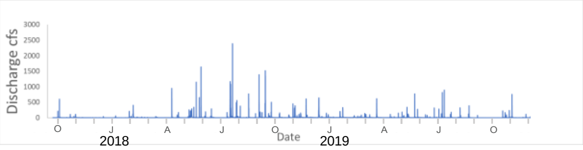

Jones Falls

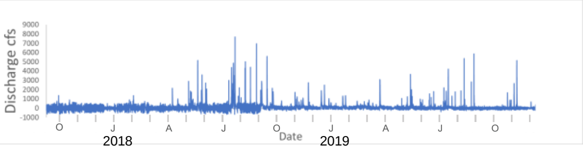

Scotts Level Branch

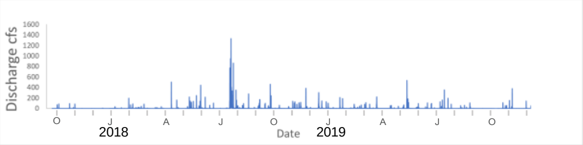

Supplemental Figure 2.2 A-E: Element by element view of data presented in Figure 3 ("USGS NWIS").

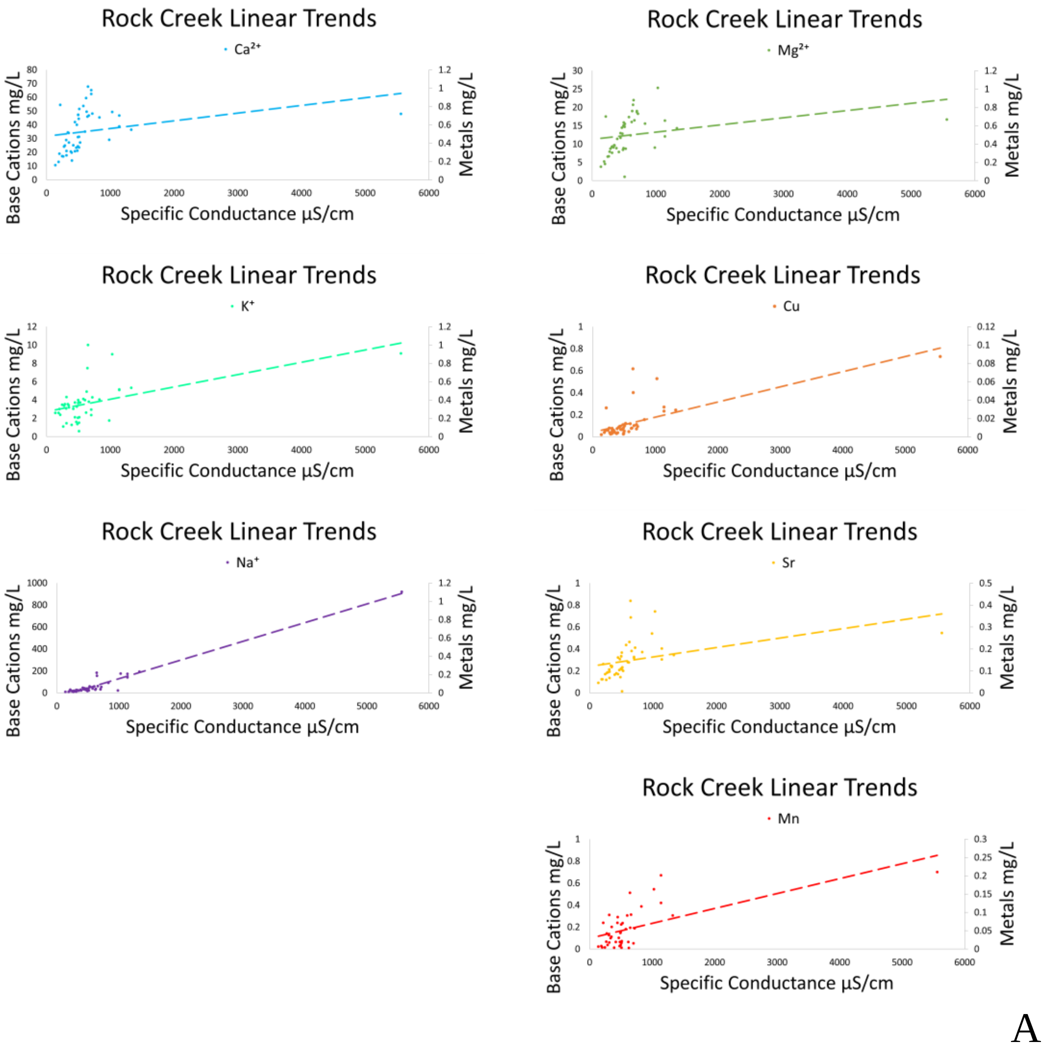

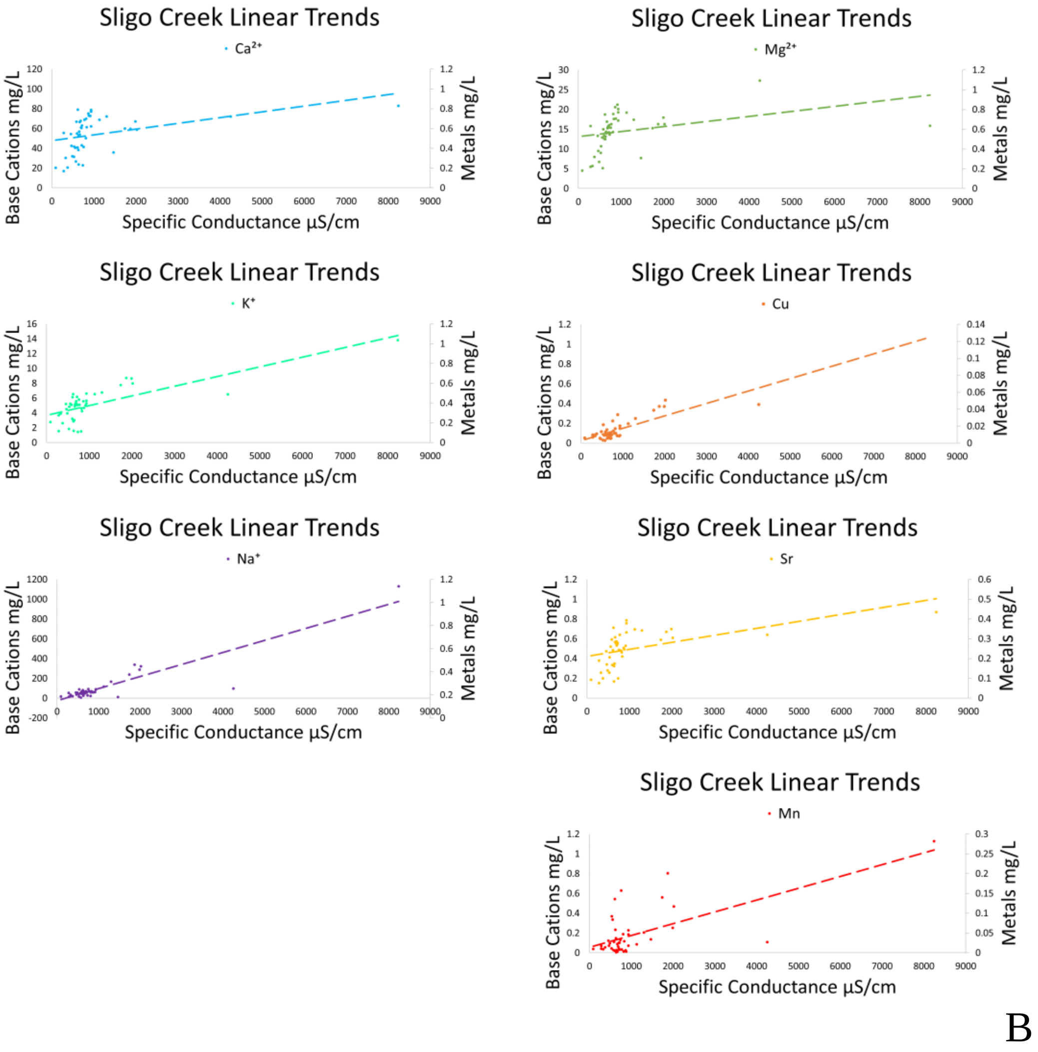
Sligo Creek Linear Trends
Ca²⁺
Base Cations mg/L
Metals mg/L
Specific Conductance µS/cm
Sligo Creek Linear Trends
Mg²⁺
Base Cations mg/L
Metals mg/L
Specific Conductance µS/cm
Sligo Creek Linear Trends
K⁺
Base Cations mg/L
Metals mg/L
Specific Conductance µS/cm
Sligo Creek Linear Trends
Cu
Base Cations mg/L
Metals mg/L
Specific Conductance µS/cm
Sligo Creek Linear Trends
Na⁺
Base Cations mg/L
Metals mg/L
Specific Conductance µS/cm
Sligo Creek Linear Trends
Sr
Base Cations mg/L
Metals mg/L
Specific Conductance µS/cm
Sligo Creek Linear Trends
Mn
Base Cations mg/L
Metals mg/L
Specific Conductance µS/cm
0 1000 2000 3000 4000 5000 6000 7000 8000 9000
B

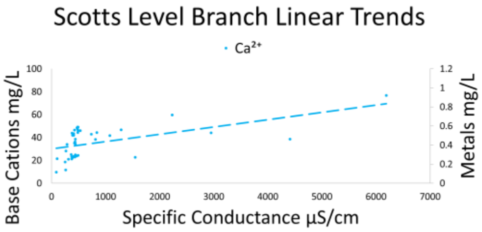
Scotts Level Branch Linear Trends
Ca²⁺
Base Cations mg/L
0
20
40
60
80
100
Metals mg/L
0
0.2
0.4
0.6
0.8
1
1.2
0
1000
2000
3000
4000
5000
6000
7000
Specific Conductance µS/cm

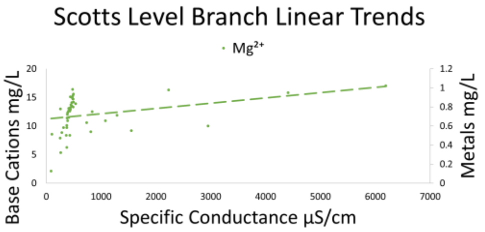
Scotts Level Branch Linear Trends
Mg²⁺
Base Cations mg/L
0
5
10
15
20
Metals mg/L
0
0.2
0.4
0.6
0.8
1
1.2
0
1000
2000
3000
4000
5000
6000
7000
Specific Conductance µS/cm

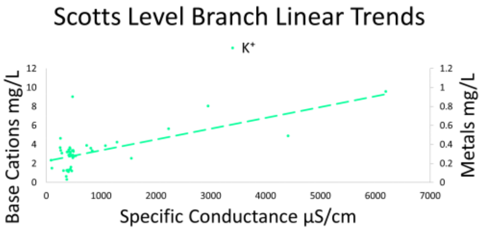
Scotts Level Branch Linear Trends
K⁺
Base Cations mg/L
0
2
4
6
8
10
12
Metals mg/L
0
0.2
0.4
0.6
0.8
1
1.2
0
1000
2000
3000
4000
5000
6000
7000
Specific Conductance µS/cm

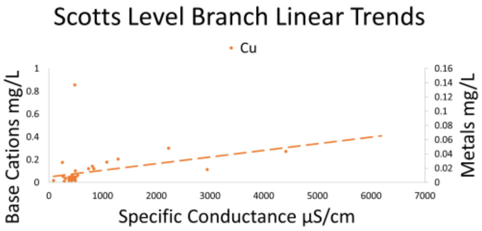
Scotts Level Branch Linear Trends
Cu
Base Cations mg/L
0
0.2
0.4
0.6
0.8
1
Metals mg/L
0
0.02
0.04
0.06
0.08
0.1
0.12
0.14
0.16
0
1000
2000
3000
4000
5000
6000
7000
Specific Conductance µS/cm

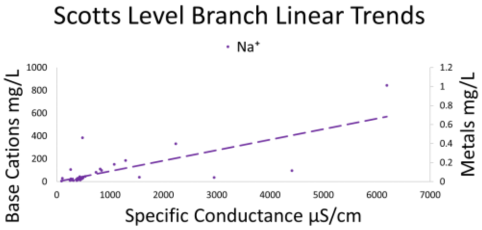
Scotts Level Branch Linear Trends
Na⁺
Base Cations mg/L
0
200
400
600
800
1000
Metals mg/L
0
0.2
0.4
0.6
0.8
1
1.2
0
1000
2000
3000
4000
5000
6000
7000
Specific Conductance µS/cm

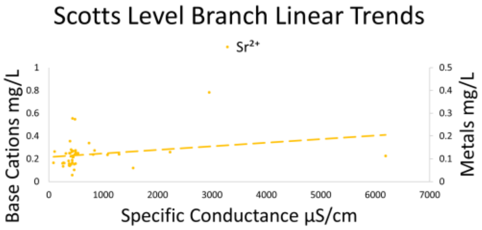
Scotts Level Branch Linear Trends
Sr²⁺
Base Cations mg/L
0
0.2
0.4
0.6
0.8
1
Metals mg/L
0
0.1
0.2
0.3
0.4
0.5
0
1000
2000
3000
4000
5000
6000
7000
Specific Conductance µS/cm

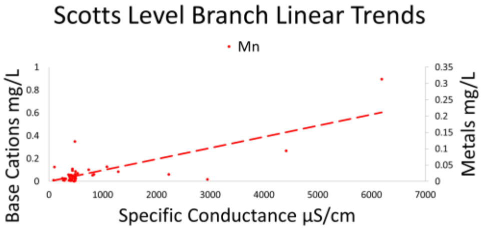
Scotts Level Branch Linear Trends
Mn
Base Cations mg/L
0
0.2
0.4
0.6
0.8
1
Metals mg/L
0
0.05
0.1
0.15
0.2
0.25
0.3
0.35
0
1000
2000
3000
4000
5000
6000
7000
Specific Conductance µS/cm

C

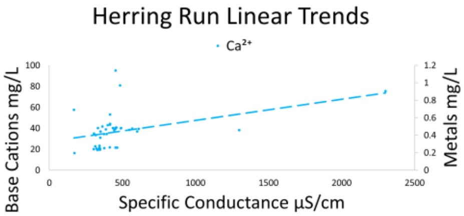
Herring Run Linear Trends
Ca²⁺
Base Cations mg/L
100
80
60
40
20
0
Metals mg/L
1.2
1
0.8
0.6
0.4
0.2
0
0
500
1000
1500
2000
2500
Specific Conductance µS/cm

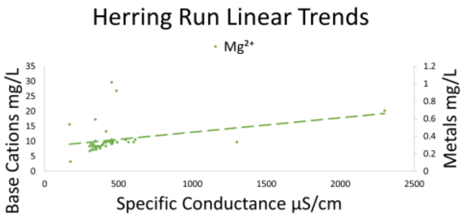
Herring Run Linear Trends
Mg²⁺
Base Cations mg/L
35
30
25
20
15
10
5
0
Metals mg/L
1.2
1
0.8
0.6
0.4
0.2
0
0
500
1000
1500
2000
2500
Specific Conductance µS/cm

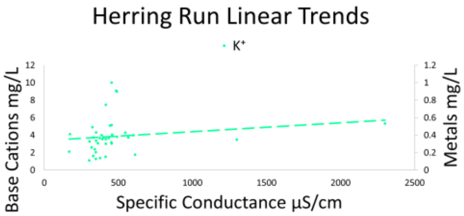
Herring Run Linear Trends
K⁺
Base Cations mg/L
12
10
8
6
4
2
0
Metals mg/L
1.2
1
0.8
0.6
0.4
0.2
0
0
500
1000
1500
2000
2500
Specific Conductance µS/cm

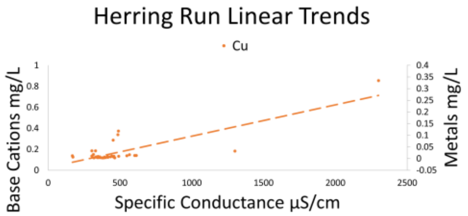
Herring Run Linear Trends
Cu
Base Cations mg/L
1
0.8
0.6
0.4
0.2
0
Metals mg/L
0.4
0.35
0.3
0.25
0.2
0.15
0.1
0.05
0
-0.05
0
500
1000
1500
2000
2500
Specific Conductance µS/cm

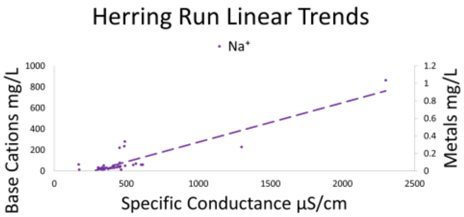
Herring Run Linear Trends
Na⁺
Base Cations mg/L
1000
800
600
400
200
0
Metals mg/L
1.2
1
0.8
0.6
0.4
0.2
0
0
500
1000
1500
2000
2500
Specific Conductance µS/cm

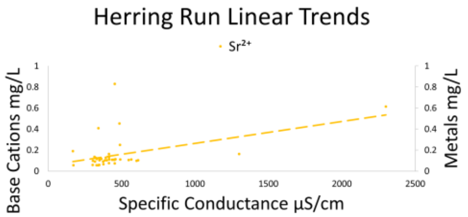
Herring Run Linear Trends
Sr²⁺
Base Cations mg/L
1
0.8
0.6
0.4
0.2
0
Metals mg/L
1
0.8
0.6
0.4
0.2
0
0
500
1000
1500
2000
2500
Specific Conductance µS/cm

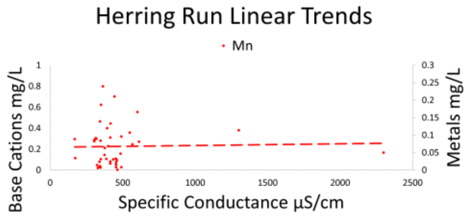
Herring Run Linear Trends
Mn
Base Cations mg/L
1
0.8
0.6
0.4
0.2
0
Metals mg/L
0.3
0.25
0.2
0.15
0.1
0.05
0
0
500
1000
1500
2000
2500
Specific Conductance µS/cm

D

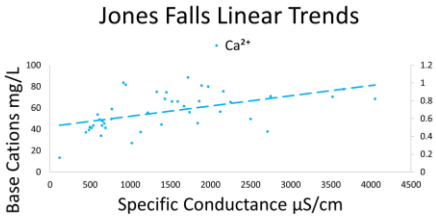
Jones Falls Linear Trends
Ca²⁺
Base Cations mg/L
0
20
40
60
80
100
Metals mg/L
0
0.2
0.4
0.6
0.8
1
1.2
0
500
1000
1500
2000
2500
3000
3500
4000
4500
Specific Conductance µS/cm

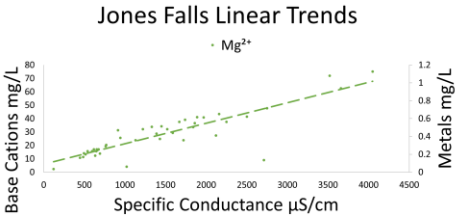
Jones Falls Linear Trends
Mg²⁺
Base Cations mg/L
0
10
20
30
40
50
60
70
80
Metals mg/L
0
0.2
0.4
0.6
0.8
1
1.2
0
500
1000
1500
2000
2500
3000
3500
4000
4500
Specific Conductance µS/cm

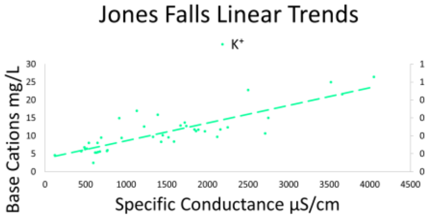
Jones Falls Linear Trends
K⁺
Base Cations mg/L
0
5
10
15
20
25
30
Metals mg/L
0
0.2
0.4
0.6
0.8
1
1.2
0
500
1000
1500
2000
2500
3000
3500
4000
4500
Specific Conductance µS/cm

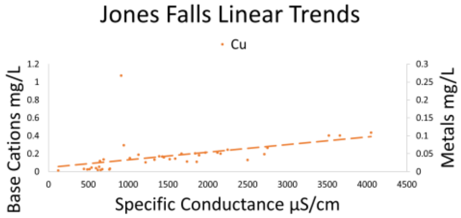
Jones Falls Linear Trends
Cu
Base Cations mg/L
0
0.2
0.4
0.6
0.8
1
1.2
Metals mg/L
0
0.05
0.1
0.15
0.2
0.25
0.3
0
500
1000
1500
2000
2500
3000
3500
4000
4500
Specific Conductance µS/cm

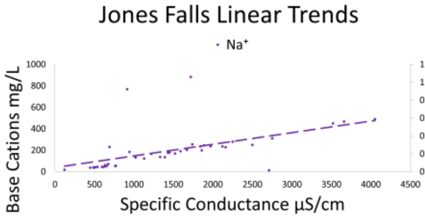
Jones Falls Linear Trends
Na⁺
Base Cations mg/L
0
200
400
600
800
1000
Metals mg/L
0
0.2
0.4
0.6
0.8
1
1.2
0
500
1000
1500
2000
2500
3000
3500
4000
4500
Specific Conductance µS/cm

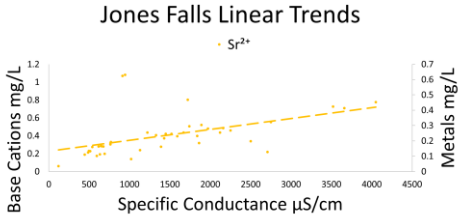
Jones Falls Linear Trends
Sr²⁺
Base Cations mg/L
0
0.2
0.4
0.6
0.8
1
1.2
Metals mg/L
0
0.1
0.2
0.3
0.4
0.5
0.6
0.7
0
500
1000
1500
2000
2500
3000
3500
4000
4500
Specific Conductance µS/cm

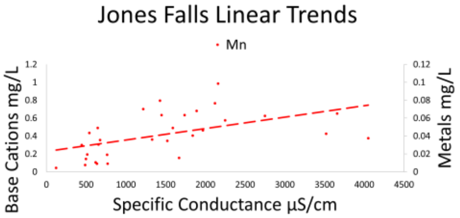
Jones Falls Linear Trends
Mn
Base Cations mg/L
0
0.2
0.4
0.6
0.8
1
1.2
Metals mg/L
0
0.02
0.04
0.06
0.08
0.1
0.12
0
500
1000
1500
2000
2500
3000
3500
4000
4500
Specific Conductance µS/cm

E

Supplemental Figure 2.3: Linear trends for Sligo Creek including data from high frequency sampling during peak specific conductance. This figure illustrates that trends are consistent over a wider range of specific conductance values than illustrated in Figure 3 (“USGS NWIS”). This can also be observed in Figure 3 at Jones Falls to some degree as its tidal, brackish nature allows for a wider range of salinities to be captured.

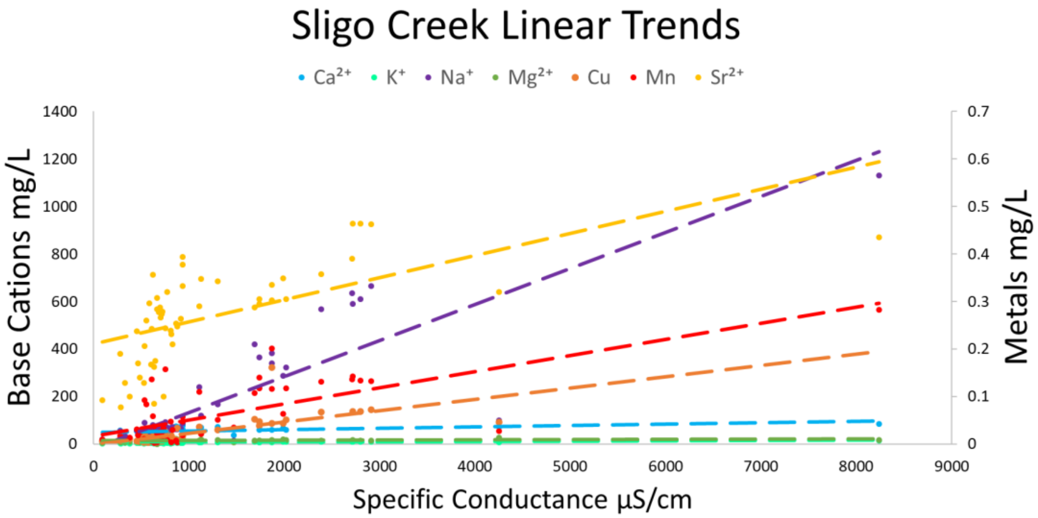

Supplemental Figure 2.4: A-B Discharge integrated daily loads of major and trace elements compared to daily specific conductance for Rock Creek and Sligo Creek ("USGS NWIS"). This was explored as an alternate method for deriving relationships to predict daily loads instead of only concentrations plotted against specific conductance. Unfortunately, relationships were less clear and became even more bimodal due to large changes in loads during hydrologic events; streamflow can be flashy in these urban stream and discharge can vary by orders of magnitude whereas concentrations of ions typically vary several-fold.

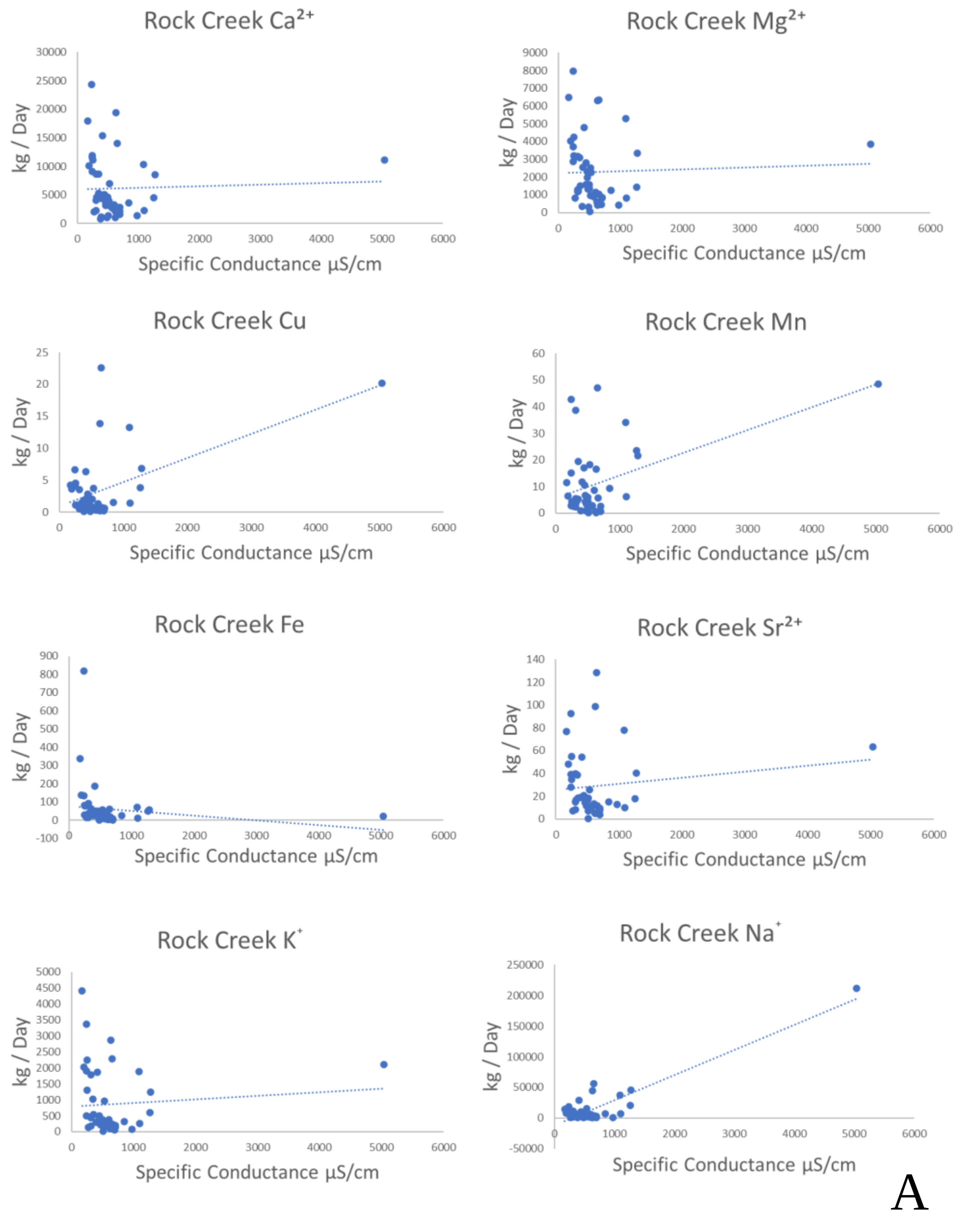

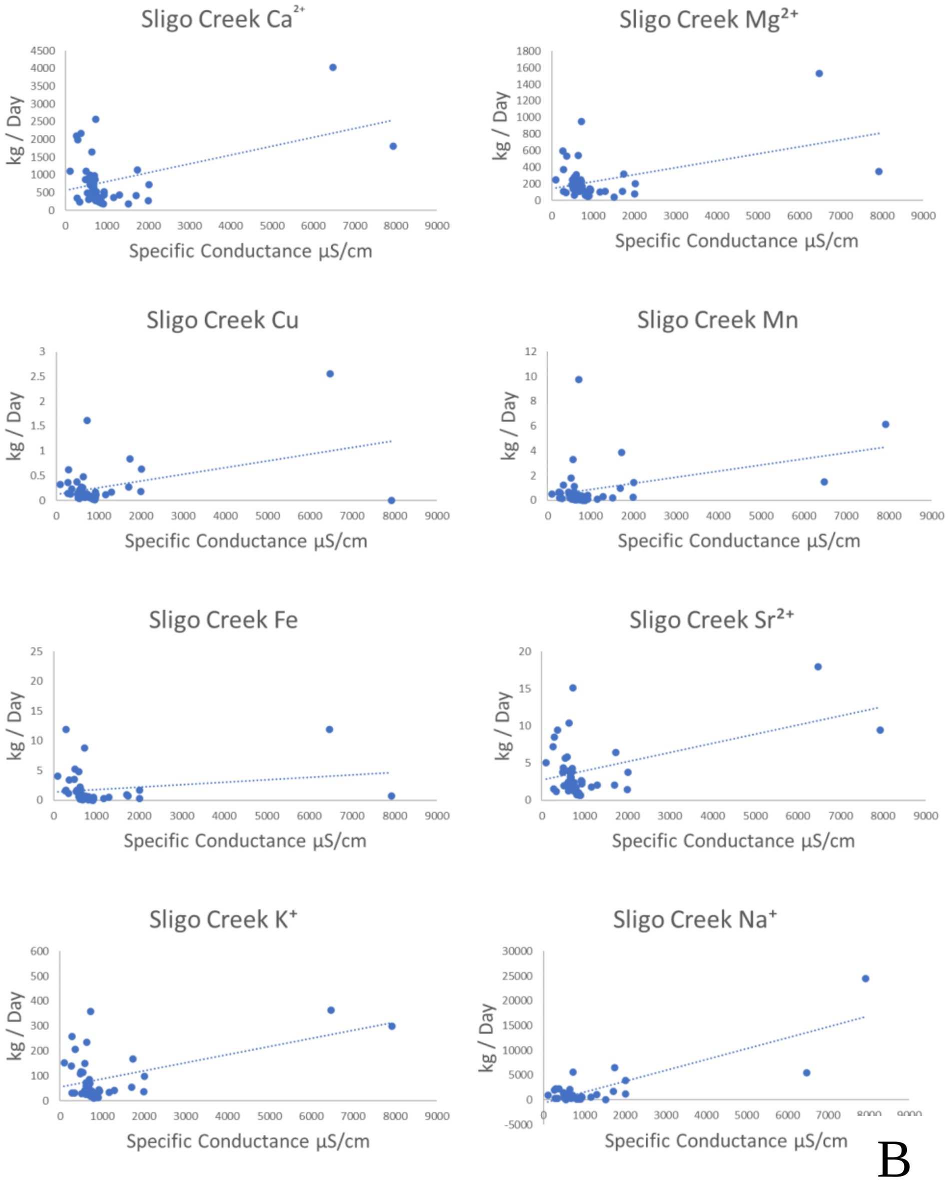
Sligo Creek Ca^{2+}
kg / Day
4500
4000
3500
3000
2500
2000
1500
1000
500
0
0
1000
2000
3000
4000
5000
6000
7000
8000
9000
Specific Conductance µS/cm
Sligo Creek Mg^{2+}
kg / Day
1800
1600
1400
1200
1000
800
600
400
200
0
Specific Conductance µS/cm
Sligo Creek Cu
kg / Day
3
2.5
2
1.5
1
0.5
0
Specific Conductance µS/cm
Sligo Creek Mn
kg / Day
12
10
8
6
4
2
0
Specific Conductance µS/cm
Sligo Creek Fe
kg / Day
25
20
15
10
5
0
Specific Conductance µS/cm
Sligo Creek Sr^{2+}
kg / Day
20
15
10
5
0
Specific Conductance µS/cm
Sligo Creek K^{+}
kg / Day
600
500
400
300
200
100
0
Specific Conductance µS/cm
Sligo Creek Na^{+}
kg / Day
30000
25000
20000
15000
10000
5000
0
-5000
Specific Conductance µS/cm

B

Supplemental Figure 2.5: Trend lines which best described relationships observed varied across analytes and sites. In the examples from Rock Creek, linear was most accurate for Na^+, power was most accurate for Ca^{2+}, and logarithmic was most accurate for Mn. These did not remain consistent across sites however with Mn also exhibiting alternating best fit lines across all regressions tested. Linear models were utilized for further analyses as they were the simplest and allowed for different analytes to be compared to one another with a uniform standard.

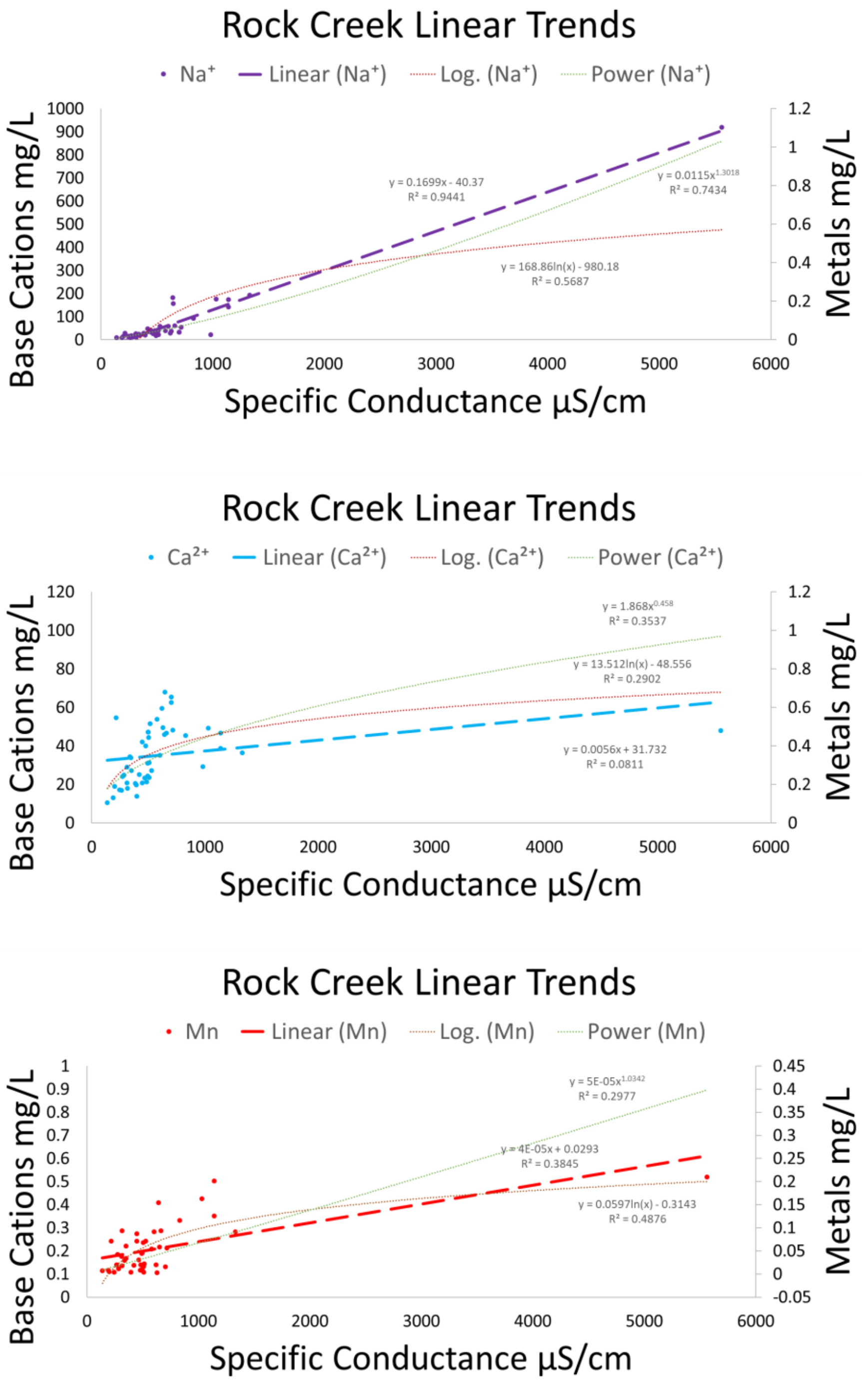

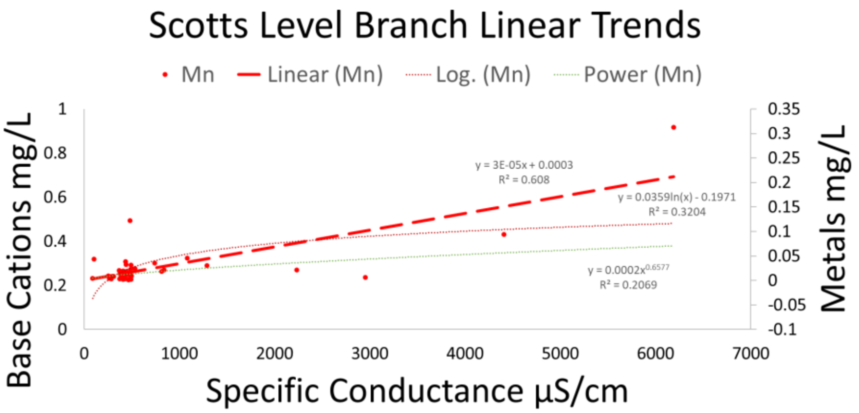
Scotts Level Branch Linear Trends
Mn
Linear (Mn)
Log. (Mn)
Power (Mn)
Base Cations mg/L
Metals mg/L
Specific Conductance µS/cm
y = 3E-05x + 0.0003
R² = 0.608
y = 0.0359ln(x) - 0.1971
R² = 0.3204
y = 0.0002x^0.6577
R² = 0.2069
1
0.8
0.6
0.4
0.2
0
0.35
0.3
0.25
0.2
0.15
0.1
0.05
0
-0.05
-0.1
0
1000
2000
3000
4000
5000
6000
7000

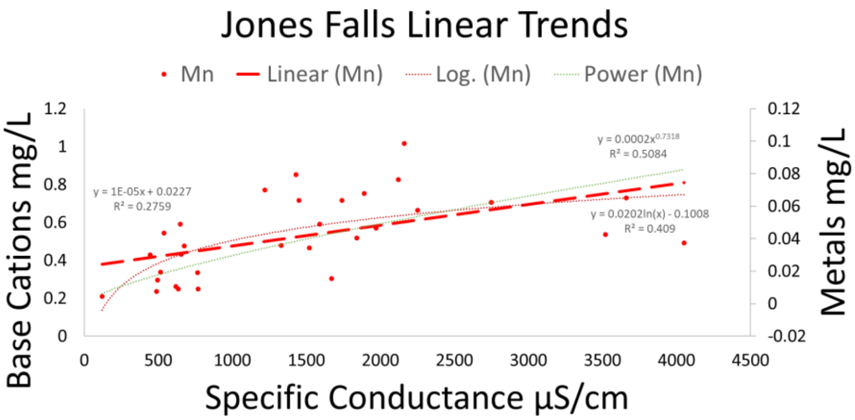
Jones Falls Linear Trends
Mn
Linear (Mn)
Log. (Mn)
Power (Mn)
Base Cations mg/L
Metals mg/L
Specific Conductance µS/cm
y = 1E-05x + 0.0227
R² = 0.2759
y = 0.0002x^0.7318
R² = 0.5084
y = 0.0202ln(x) - 0.1008
R² = 0.409
1.2
1
0.8
0.6
0.4
0.2
0
0.12
0.1
0.08
0.06
0.04
0.02
0
-0.02
0
500
1000
1500
2000
2500
3000
3500
4000
4500

Supplemental Figure 2.6: Time series of very high frequency (hourly) data collected one hour prior to the beginning of, and throughout the peak of a snowstorm between 1/29/2019 and 1/30/2019 ("USGS NWIS"). With specific conductance changing by > 1000 µS/cm per hour; capturing the quickly changing analyte concentrations was very difficult even with automated samplers.

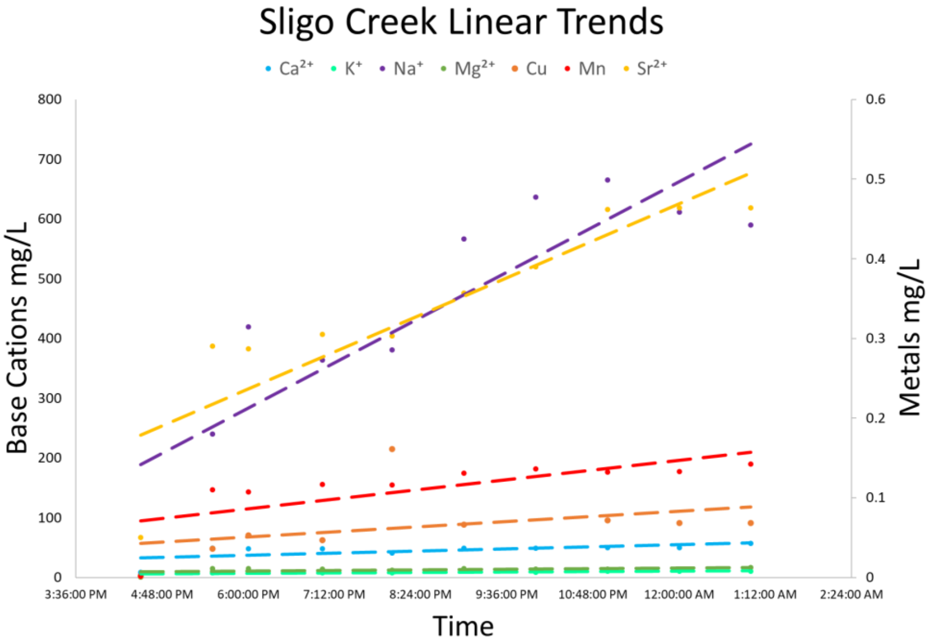

Supplemental Figure 2.7: A-B Discharge integrated daily loads of Mn and Cu compared to daily loads of Na^+ for Rock Creek and Sligo Creek (“USGS NWIS”). Linear (blue) and logarithmic (red) trendlines were applied in order to explore whether increasing metal loads were potentially caused by metal contamination in the salts being applied.

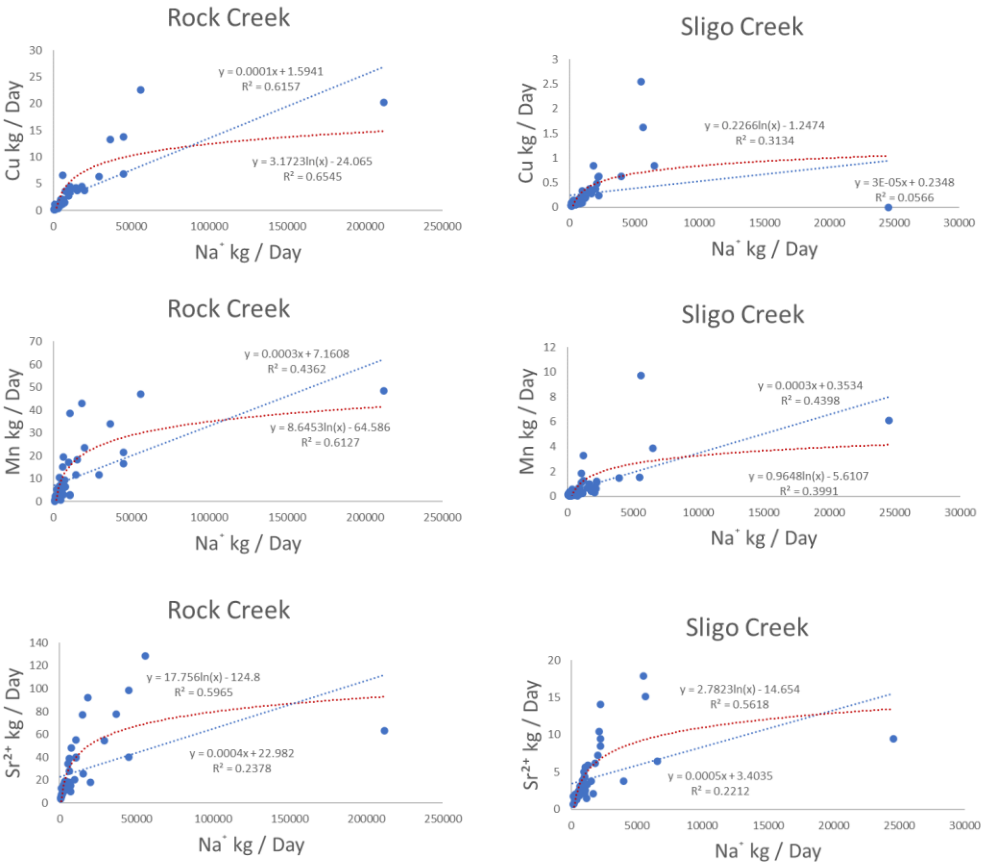

A

B

Chapter 3 Supplementary Materials

Supplemental Table 3.1: Tukey's Honestly-Significant-Difference test was used to compare mean cation retention in the three-way ANOVAs across different salts (NaCl, $CaCl_2$, $MgCl_2$). Mean retention rates for a given cation share a common letter in the post-hoc column when they are not statistically different from one another (p>0.05).

Salt	Cation	Mean Retention mg/L	SE	Post-hoc
NaCl	**Na^+**	1010.811	104.394	a
$CaCl_2$	**Ca^{2+}**	690.041	105.609	b
$MgCl_2$	**Mg^{2+}**	357.337	43.544	c

Supplemental Figure 3.1: Conceptual diagram of the experimental design used in this study. Eight stormwater BMPs are sampled, consisting of pairs of bioswales, bioretention sites, wetlands and constructed ponds. Sediment from each stormwater BMP is incubated with water collected from the same feature at six different levels of salinity. The same process is done with three different salts NaCl, CaCl2 and MgCl2. Four samples were lost to cross contamination so a total of 284 samples were analyzed via ICP-OES for major and trace elements.

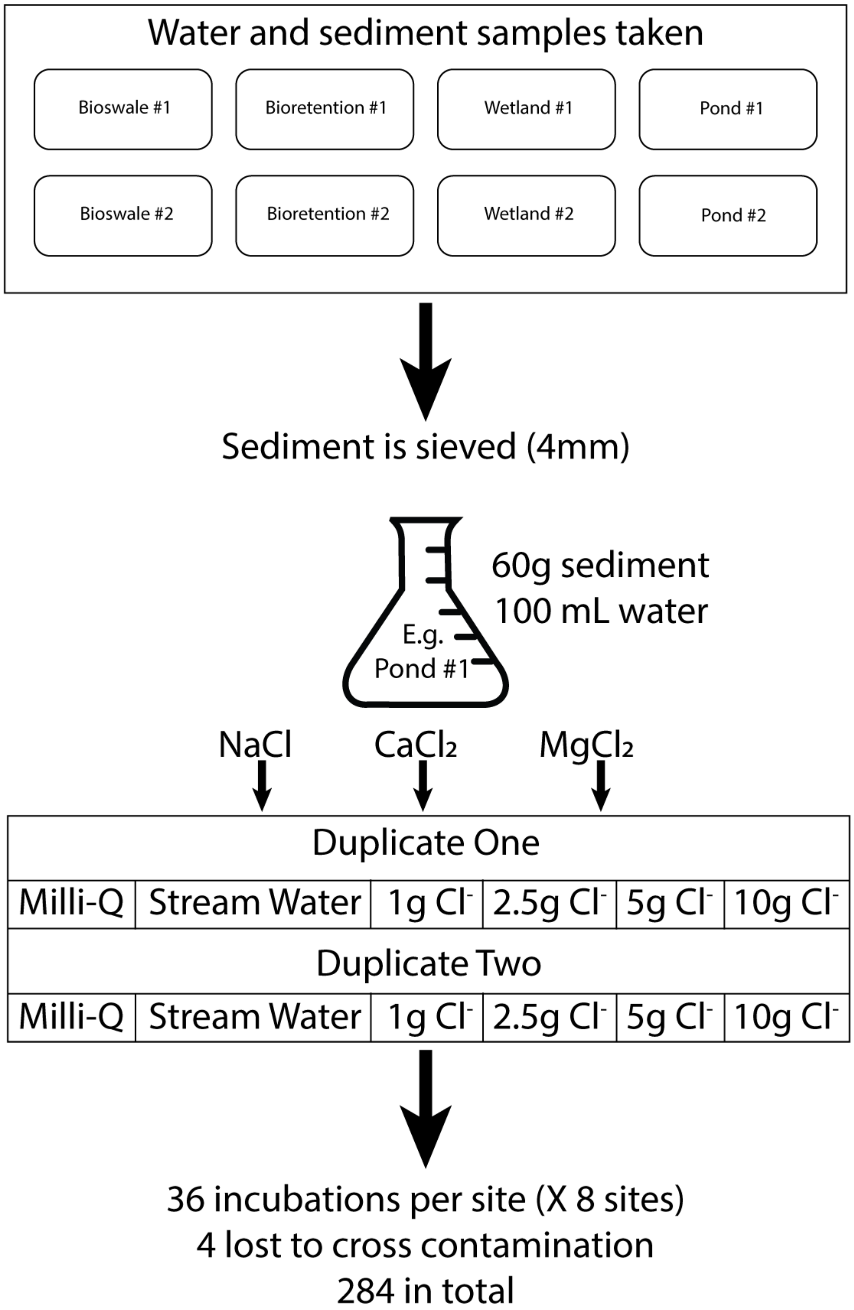

Supplemental Figure 3.2: A Quantile – Quantile plot of the entire dataset collected showing normality. Outliers are present but the majority of the dataset falls into the expected window of normality.

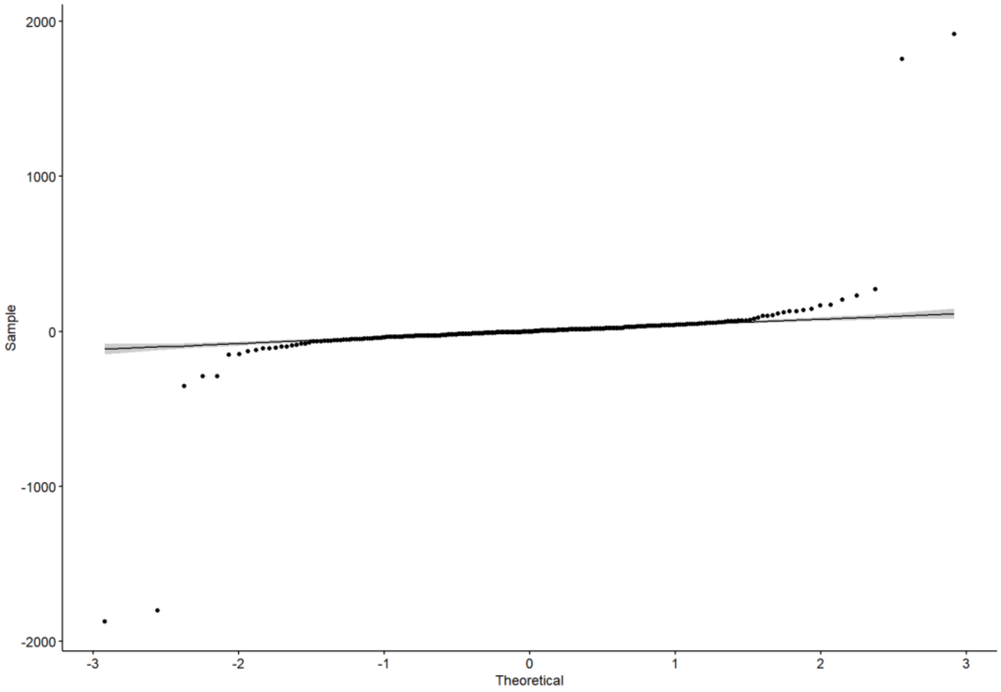

Supplemental Figure 3.3: Density plot of residuals from the entire dataset collected illustrates normality. While some outliers are present the bulk of the data is centered around zero and is not significantly heavy-tailed or light-tailed.

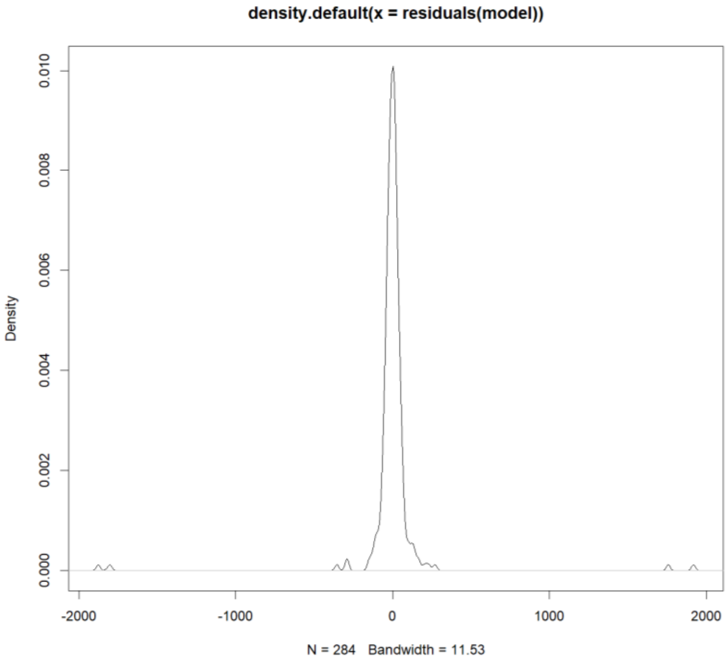

Supplemental Figure 3.4: NPOC, IC, and TN mobilized by salt type and concentration. Scales are matching between salt types to better illustrate changes in mobilization by salt type. For visual clarity, the X axis is plotted as a function of discrete salt treatment levels and not continuous concentrations producing what appear to be curvilinear trend lines, however, relationships are linear. Due to an instrument malfunction, data is not available at all sampling sites.

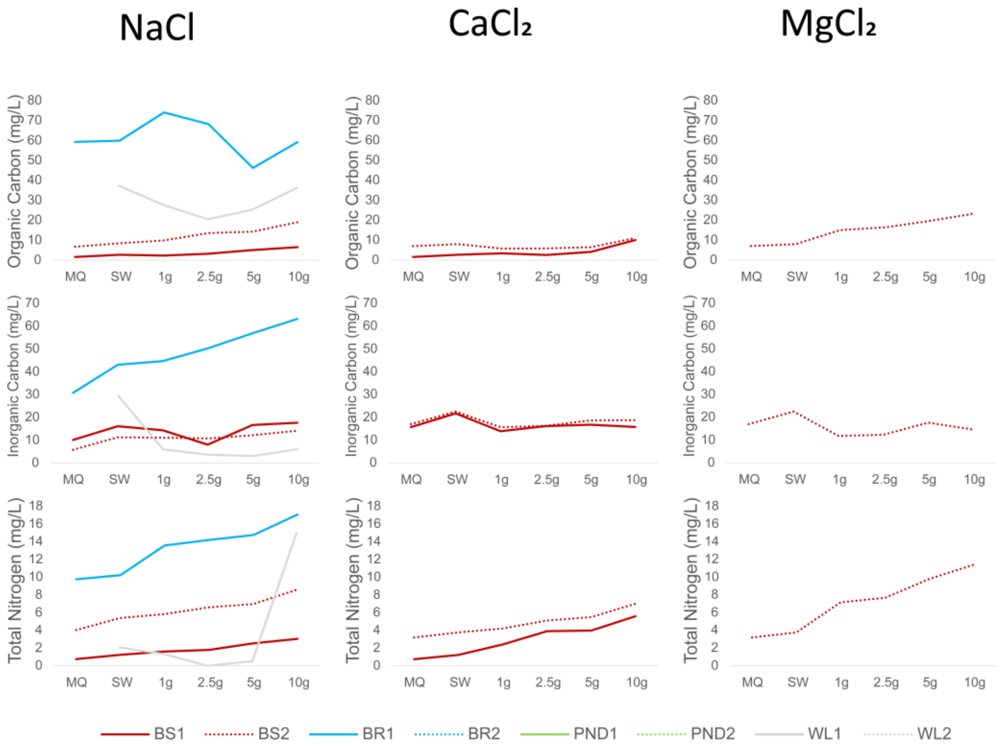

Supplemental Figure 4.1: Increasing trends in TDN concentration with increasing experimental salinization (Haq et al., 2018).

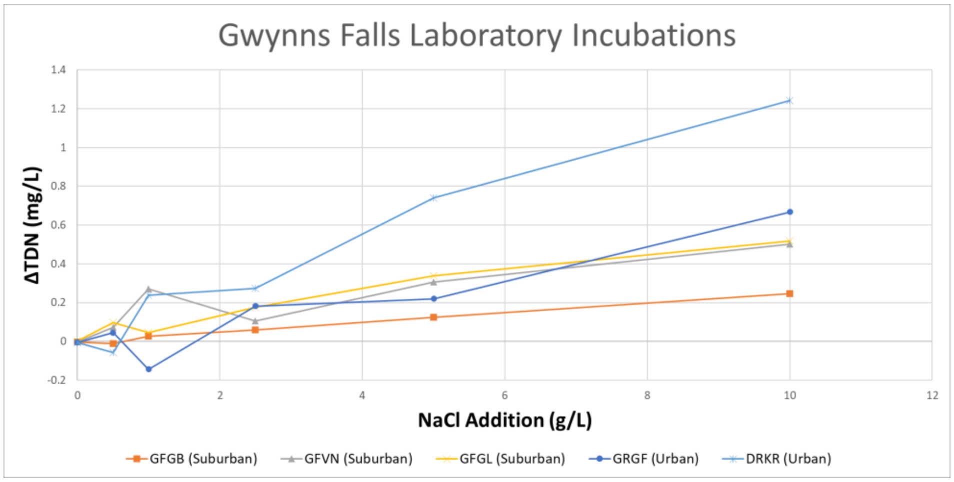

Bibliography

Abolfazli, E. and K. Strom, 2022. Deicing Road Salts May Contribute to Impairment of Streambeds through Alterations to Sedimentation Processes. ACS ES&T Water 2:148–155.

Adams, J.P., R. Kirst, L.E. Kearns, and M.P.S. Krekeler, 2009. Mn-Oxides and Sequestration of Heavy Metals in a Suburban Catchment Basin of the Chesapeake Bay Watershed. Environmental Geology 58:1269–1280.

Alberts, J.M., J.J. Beaulieu, and I. Buffam, 2017. Watershed Land Use and Seasonal Variation Constrain the Influence of Riparian Canopy Cover on Stream Ecosystem Metabolism. Ecosystems 20:553–567.

Amrhein, C., J.E. Strong, and P.A. Mosher, 1992. Effect of Deicing Salts on Metal and Organic Matter Mobilization in Roadside Soils. Environmental Science & Technology 26:703–709.

Anning, D.W. and M.E. Flynn, 2014. Dissolved-Solids Sources, Loads, Yields, and Concentrations in Streams of the Conterminous United States. USGS Numbered Series, U.S. Geological Survey, Reston, VA.

Ardón, M., J.L. Morse, B.P. Colman, and E.S. Bernhardt, 2013. Drought-Induced Saltwater Incursion Leads to Increased Wetland Nitrogen Export. Global Change Biology 19:2976–2985.

ASLA, 2022. Improving Water Efficiency: Residential Bioswales and Bioretention Ponds | Asla.Org. https://www.asla.org/bioswales.aspx. Accessed 6 Jun 2022.

Baker, A., S. Cumberland, and N. Hudson, 2008. Dissolved and Total Organic and Inorganic Carbon in Some British Rivers. Area 40:117–127.

Barbier, L., R. Suaire, I. Durickovic, J. Laurent, and M.-O. Simonnot, 2018. Is a Road Stormwater Retention Pond Able to Intercept Deicing Salt? Water, Air, & Soil Pollution 229:251.

Barnes, R.T. and P.A. Raymond, 2009. The Contribution of Agricultural and Urban Activities to Inorganic Carbon Fluxes within Temperate Watersheds. Chemical Geology 266:318–327.

Behbahani, A., R.J. Ryan, and E.R. McKenzie, 2021. Impacts of Salinity on the Dynamics of Fine Particles and Their Associated Metals during Stormwater Management. Science of The Total Environment 777:146135.

Berntssen, M.H.G., K. Hylland, S.E. Wendelaar Bonga, and A. Maage, 1999. Toxic Levels of Dietary Copper in Atlantic Salmon (Salmo Salar L.) Parr. Aquatic Toxicology 46:87–99.

Bonneau, J., T.D. Fletcher, J.F. Costelloe, and M.J. Burns, 2017. Stormwater Infiltration and the 'Urban Karst' – A Review. Journal of Hydrology 552:141–150.

Brooks, P.D., S.K. Schmidt, and M.W. Williams, 1997. Winter Production of CO2 and N2O from Alpine Tundra: Environmental Controls and Relationship to Inter-System C and N Fluxes. Oecologia 110:403–413.

Brooks, P.D., M.W. Williams, and S.K. Schmidt, 1998. Inorganic Nitrogen and Microbial Biomass Dynamics before and during Spring Snowmelt. Biogeochemistry 43:1–15.

Brookshire, J.E.N., S. Gerber, J.R. Webster, J.M. Vose, and W.T. Swank, 2011. Direct Effects of Temperature on Forest Nitrogen Cycling Revealed through Analysis of Long-Term Watershed Records. Global Change Biology 17:297–308.

Burgess, C., 2000. Valid Analytical Methods and Procedures. Royal Society of Chemistry.

Burgis, C.R., G.M. Hayes, D.A. Henderson, W. Zhang, and J.A. Smith, 2020. Green Stormwater Infrastructure Redirects Deicing Salt from Surface Water to Groundwater. Science of The Total Environment 729:138736.

Cañedo-Argüelles, M., C.P. Hawkins, B.J. Kefford, R.B. Schäfer, B.J. Dyack, S. Brucet, D. Buchwalter, J. Dunlop, O. Frör, J. Lazorchak, E. Coring, H.R. Fernandez, W. Goodfellow, A.L.G. Achem, S. Hatfield-Dodds, B.K. Karimov, P. Mensah, J.R. Olson, C. Piscart, N. Prat, S. Ponsá, C.-J. Schulz, and A.J. Timpano, 2016. Saving Freshwater from Salts. Science 351:914–916.

Cañedo-Argüelles, M., B.J. Kefford, C. Piscart, N. Prat, R.B. Schäfer, and C.-J. Schulz, 2013. Salinisation of Rivers: An Urgent Ecological Issue. Environmental Pollution 173:157–167.

Clements, W.H. and C. Kotalik, 2016. Effects of Major Ions on Natural Benthic Communities: An Experimental Assessment of the US Environmental Protection Agency Aquatic Life Benchmark for Conductivity. Freshwater Science 35:126–138.

Collins, K.A., T.J. Lawrence, E.K. Stander, R.J. Jontos, S.S. Kaushal, T.A. Newcomer, N.B. Grimm, and M.L. Cole Ekberg, 2010. Opportunities and Challenges for Managing Nitrogen in Urban Stormwater: A Review and Synthesis. Ecological Engineering 36:1507–1519.

Compton, J.E. and M.R. Church, 2011. Salt Additions Alter Short-Term Nitrogen and Carbon Mobilization in a Coastal Oregon Andisol. Journal of Environmental Quality 40:1601–1606.

Cooper, C.A., P.M. Mayer, and B.R. Faulkner, 2014. Effects of Road Salts on Groundwater and Surface Water Dynamics of Sodium and Chloride in an Urban Restored Stream. Biogeochemistry 121:149–166.

Corsi, S.R., D.J. Graczyk, S.W. Geis, N.L. Booth, and K.D. Richards, 2010. A Fresh Look at Road Salt: Aquatic Toxicity and Water-Quality Impacts on Local, Regional, and National Scales. Environmental Science & Technology 44:7376–7382.

Daley, M.L., J.D. Potter, and W.H. McDowell, 2009. Salinization of Urbanizing New Hampshire Streams and Groundwater: Effects of Road Salt and Hydrologic Variability. Journal of the North American Benthological Society 28:929–940.

Davies, P., I. Wright, S. Findlay, and O.J. Jonasson, 2010. The Effect of the In-Transport Process on Urban Water Chemistry – an Examination of the Contribution of Concrete Pipes and Gutters on Urban Water Quality. :10.

Davis, L., 1995. A Handbook of Constructed Wetlands. EPA. https://www.epa.gov/wetlands/handbook-constructed-wetlands.

Davis, A.P., 2008. Field Performance of Bioretention: Hydrology Impacts. Journal of Hydrologic Engineering 13:90–95.

Davis, A.P., W.F. Hunt, R.G. Traver, and M. Clar, 2009. Bioretention Technology: Overview of Current Practice and Future Needs. Journal of Environmental Engineering 135:109–117.

Davis, A.P., M. Shokouhian, H. Sharma, and C. Minami, 2001. Laboratory Study of Biological Retention for Urban Stormwater Management. Water Environment Research 73:5–14.

Davis, A.P., R. Stack, P. Kangas, and J.S. Angle, 2011. Water Quality Improvement Using Rain Gardens: University of Maryland Studies. :13.

Deeb, M., P.M. Groffman, J.L. Joyner, G. Lozefski, A. Paltseva, B. Lin, K. Mania, D.L. Cao, J. McLaughlin, T. Muth, B. Prithiviraj, J. Kerwin, and Z. Cheng, 2018. Soil and Microbial Properties of Green Infrastructure Stormwater Management Systems. Ecological Engineering 125:68–75.

Demars, S. and G. Benoit, 2019. Leaching of ANC and Chromium from Concrete: Effect of Aging Simulated by Sample Carbonation. Water, Air, & Soil Pollution 230:159.

Diamond Crystal, 2017. At What Temperature Does Salt Melt Ice? | Diamond Crystal® Salt. https://www.diamondcrystalsalt.com/blog/at-what-temperature-does-salt-melt-ice. Accessed 16 Feb 2022.

Diaz, R.J. and R. Rosenberg, 2008. Spreading Dead Zones and Consequences for Marine Ecosystems. Science 321:926–929.

DiBlasi, C.J., H. Li, A.P. Davis, and U. Ghosh, 2009. Removal and Fate of Polycyclic Aromatic Hydrocarbon Pollutants in an Urban Stormwater Bioretention Facility. Environmental Science & Technology 43:494–502.

D’Itri, F.M., 1992. Chemical Deicers and the Environment. CRC Press.

Duan, S. and S.S. Kaushal, 2015. Salinization Alters Fluxes of Bioreactive Elements from Stream Ecosystems across Land Use. Biogeosciences 12:7331–7347.

Duckworth, C.M.S. and M.S. Cresser, 1991. Factors Influencing Nitrogen Retention in Forest Soils. Environmental Pollution 72:1–21.

Dugan, H.A., S.L. Bartlett, S.M. Burke, J.P. Doubek, F.E. Krivak-Tetley, N.K. Skaff, J.C. Summers, K.J. Farrell, I.M. McCullough, A.M. Morales-Williams, D.C. Roberts, Z. Ouyang, F. Scordo, P.C. Hanson, and K.C. Weathers, 2017. Salting Our Freshwater Lakes. Proceedings of the National Academy of Sciences 114:4453–4458.

Dugan, H.A., J.C. Summers, N.K. Skaff, F.E. Krivak-Tetley, J.P. Doubek, S.M. Burke, S.L. Bartlett, L. Arvola, H. Jarjanazi, J. Korponai, A. Kleeberg, G. Monet, D. Monteith, K. Moore, M. Rogora, P.C. Hanson, and K.C. Weathers, 2017. Long-Term Chloride Concentrations in North American and European Freshwater Lakes. Scientific Data 4:170101.

Ebrahimpour, M., H. Alipour, and S. Rakhshah, 2010. Influence of Water Hardness on Acute Toxicity of Copper and Zinc on Fish. Toxicology and Industrial Health 26:361–365.

Eimers, M.C., J.M. Buttle, and S.A. Watmough, 2007. The Contribution of Rain-on-Snow Events to Annual NO3-N Export from a Forested Catchment in South-Central Ontario, Canada. Applied Geochemistry 22:1105–1110.

Elmore, A.J. and S.S. Kaushal, 2008. Disappearing Headwaters: Patterns of Stream Burial Due to Urbanization. Frontiers in Ecology and the Environment 6:308–312.

Environmental Monitoring Systems Laboratory, 1996. DETERMINATION OF TRACE ELEMENTS IN WATERS AND WASTES BY INDUCTIVELY COUPLED PLASMA - MASS SPECTROMETRY. Methods for the Determination of Metals in Environmental Samples. Elsevier, pp. 88–145.

EPA, 2011. A Field-Based Aquatic Life Benchmark For Conductivity In Central Appalachian Streams (Final Report). EPA/600/R-10/023F. https://cfpub.epa.gov/ncea/risk/recordisplay.cfm?deid=233809. Accessed 12 Jan 2023.

Esri, HERE, Garmin, Open Street Map contributors, and The GIS user community, ArcMap Basemap.

Fay, L. and X. Shi, 2012. Environmental Impacts of Chemicals for Snow and Ice Control: State of the Knowledge. Water, Air, & Soil Pollution 223:2751–2770.

Fenston, J., 2022. Polluted Rock Creek. NPR.Org. https://www.npr.org/local/305/2022/02/18/1081698926/polluted-rock-creek-tributary-to-get-sewer-upgrade-but-neighbors-worry-about-impact. Accessed 2 Jan 2023.

Fernandez, I.J., L.E. Rustad, S.A. Norton, J.S. Kahl, and B.J. Cosby, 2003. Experimental Acidification Causes Soil Base-Cation Depletion at the Bear Brook Watershed in Maine. Soil Science Society of America Journal 67:1909–1919.

Gaillardet, J., J. Viers, and B. Dupré, 2003. Trace Elements in River Waters. Treatise on Geochemistry 5:605.

Galella, J.G., S.S. Kaushal, P.M. Mayer, C.M. Maas, R.R. Shatkay, and R.A. Stutzke, 2023. Stormwater Best Management Practices: Experimental Evaluation of Chemical Cocktails Mobilized by Freshwater Salinization Syndrome. Frontiers in Environmental Science.

Galella, J.G., S.S. Kaushal, K.L. Wood, J.E. Reimer, and P.M. Mayer, 2021. Sensors Track Mobilization of `chemical Cocktails’ in Streams Impacted by Road Salts in the Chesapeake Bay Watershed. Environmental Research Letters 16:035017.

Gibs, J., F.D. Wilde, and H.A. Heckathorn, 2012. Use of Multiparameter Instruments for Routine Field Measurements. doi:10.3133/twri09A6.8.

Gill, L.W., P. Ring, B. Casey, N.M.P. Higgins, and P.M. Johnston, 2017. Long Term Heavy Metal Removal by a Constructed Wetland Treating Rainfall Runoff from a Motorway. Science of The Total Environment 601–602:32–44.

Granato, G.E., P.E. Church, and V.J. Stone, 1995. Mobilization of Major and Trace Constituents of Highway Runoff in Groundwater Potentially Caused by Deicing Chemical Migration. TRANSPORTATION RESEARCH RECORD:14.

Green, S.M. and M.S. Cresser, 2008. Nitrogen Cycle Disruption through the Application of De-Icing Salts on Upland Highways. Water, Air, and Soil Pollution 188:139–153.

Green, S.M., R. Machin, and M.S. Cresser, 2008a. Effect of Long-Term Changes in Soil Chemistry Induced by Road Salt Applications on N-Transformations in Roadside Soils. Environmental Pollution 152:20–31.

Green, SophieM., R. Machin, and MalcolmS. Cresser, 2008b. Long-Term Road Salting Effects on Dispersion of Organic Matter from Roadside Soils into Drainage Water. Chemistry & Ecology 24:221–231.

Green, S.M., R. Machin, and M.S. Cresser, 2008c. Does Road Salting Induce or Ameliorate DOC Mobilisation from Roadside Soils to Surface Waters in the Long Term? Environmental Monitoring and Assessment 153:435.

Groffman, P.M., D.J. Bain, L.E. Band, K.T. Belt, G.S. Brush, J.M. Grove, R.V. Pouyat, I.C. Yesilonis, and W.C. Zipperer, 2003. Down by the Riverside: Urban Riparian Ecology. Frontiers in Ecology and the Environment 1:315–321.

Groffman, P.M., N.L. Law, K.T. Belt, L.E. Band, and G.T. Fisher, 2004. Nitrogen Fluxes and Retention in Urban Watershed Ecosystems. Ecosystems 7:393–403.

Hale, R.L. and P.M. Groffman, 2006. Chloride Effects on Nitrogen Dynamics in Forested and Suburban Stream Debris Dams. Journal of Environmental Quality 35:2425–2432.

Haq, S., S.S. Kaushal, and S. Duan, 2018. Episodic Salinization and Freshwater Salinization Syndrome Mobilize Base Cations, Carbon, and Nutrients to Streams across Urban Regions. Biogeochemistry 141:463–486.

Herbert, E.R., P. Boon, A.J. Burgin, S.C. Neubauer, R.B. Franklin, M. Ardón, K.N. Hopfensperger, L.P.M. Lamers, and P. Gell, 2015. A Global Perspective on Wetland Salinization: Ecological Consequences of a Growing Threat to Freshwater Wetlands. Ecosphere 6:art206.

Hintz, W.D., L. Fay, and R.A. Relyea, 2022. Road Salts, Human Safety, and the Rising Salinity of Our Fresh Waters. Frontiers in Ecology and the Environment 20:22–30.

Hintz, W.D., D.K. Jones, and R.A. Relyea, 2019. Evolved Tolerance to Freshwater Salinization in Zooplankton: Life-History Trade-Offs, Cross-Tolerance and Reducing Cascading Effects. Philosophical Transactions of the Royal Society B: Biological Sciences 374:20180012.

Hintz, W.D. and R.A. Relyea, 2017a. Impacts of Road Deicing Salts on the Early-Life Growth and Development of a Stream Salmonid: Salt Type Matters. Environmental Pollution 223:409–415.

Hintz, W.D. and R.A. Relyea, 2017b. A Salty Landscape of Fear: Responses of Fish and Zooplankton to Freshwater Salinization and Predatory Stress. Oecologia 185:147–156.

Hintz, W.D. and R.A. Relyea, 2019. A Review of the Species, Community, and Ecosystem Impacts of Road Salt Salinisation in Fresh Waters. Freshwater Biology 64:1081–1097.

Horwitz, W. and R. Albert, 2006. The Horwitz Ratio (HorRat): A Useful Index of Method Performance with Respect to Precision. Journal of AOAC INTERNATIONAL 89:1095–1109.

Horwitz, W., L.V.R. Kamps, and K.W. Boyer, 1980. Quality Assurance in the Analysis of Foods for Trace Constituents. Journal of AOAC INTERNATIONAL 63:1344–1354.

Howarth, R.W. and R. Marino, 2006. Nitrogen as the Limiting Nutrient for Eutrophication in Coastal Marine Ecosystems: Evolving Views over Three Decades. Limnology and Oceanography 51:364–376.

Howarth, R.W., D.P. Swaney, T.J. Butler, and R. Marino, 2000. Rapid Communication: Climatic Control on Eutrophication of the Hudson River Estuary. Ecosystems 3:210–215.

Inamdar, S.P., E.K. Peck, M. Peipoch, A.J. Gold, M. Sherman, J. Hripto, P.M. Groffman, T.L.E. Trammell, D.J. Merritts, K. Addy, E. Lewis, R.C. Walter, and J. Kan, 2022. Saturated, Suffocated, and Salty: Human Legacies Produce Hot Spots of Nitrogen in Riparian Zones. Journal of Geophysical Research: Biogeosciences 127:e2022JG007138.

Jackson, R. and E. Jobbágy, 2005. From Icy Roads to Salty Streams. Proceedings of the National Academy of Sciences of the United States of America 102:14487–8.

James, K.R., B. Cant, and T. Ryan, 2003. Responses of Freshwater Biota to Rising Salinity Levels and Implications for Saline Water Management: A Review. Australian Journal of Botany 51:703.

Jiang, Q., G. Jin, H. Tang, J. Xu, and Y. Chen, 2021. N2O Production and Consumption Processes in a Salinity-Impacted Hyporheic Zone. Journal of Geophysical Research: Biogeosciences 126:e2021JG006512.

John, D.A. and J.S. Levanthal, 1995. Bioavailability Of Metals. Open-File Report, U.S. Geological Survey.

Johnson, H.M. and E.G. Stets, 2020. Nitrate in Streams During Winter Low-Flow Conditions as an Indicator of Legacy Nitrate. Water Resources Research 56:e2019WR026996.

Jones, T., 1996. Workers Stop Sewage Flow into City's Chinquapin Run Herring Run Has Had Similar Problem, Caused by Recent Heavy Rains. Baltimoresun.Com. https://www.baltimoresun.com/news/bs-xpm-1996-06-30-1996182113-story.html. Accessed 3 Mar 2020.

Jones, P.S. and A.P. Davis, 2013. Spatial Accumulation and Strength of Affiliation of Heavy Metals in Bioretention Media. Journal of Environmental Engineering 139:479–487.

Kachurina, O., H. Zhang, W. Raun, and E. Krenzer, 2000. Simultaneous Determination of Soil Aluminum, Ammonium- and Nitrate-nitrogen Using 1 M Potassium Chloride Extraction. Communications in Soil Science and Plant Analysis - COMMUN SOIL SCI PLANT ANAL 31:893–903.

Kaushal, S.S., 2016. Increased Salinization Decreases Safe Drinking Water. Environmental Science & Technology 50:2765–2766.

Kaushal, S.S. and K.T. Belt, 2012. The Urban Watershed Continuum: Evolving Spatial and Temporal Dimensions. Urban Ecosystems 15:409–435.

Kaushal, S.S., K. Delaney-Newcomb, S.E.G. Findlay, T.A. Newcomer, S. Duan, M.J. Pennino, G.M. Sivirichi, A.M. Sides-Raley, M.R. Walbridge, and K.T. Belt, 2014. Longitudinal Patterns in Carbon and Nitrogen Fluxes and Stream Metabolism along an Urban Watershed Continuum. Biogeochemistry 121:23–44.

Kaushal, S.S., S. Duan, T.R. Doody, S. Haq, R.M. Smith, T.A. Newcomer Johnson, K.D. Newcomb, J. Gorman, N. Bowman, P.M. Mayer, K.L. Wood, K.T. Belt, and W.P. Stack, 2017. Human-Accelerated Weathering Increases Salinization, Major Ions, and Alkalinization in Fresh Water across Land Use. Applied Geochemistry 83:121–135.

Kaushal, S.S., A.J. Gold, S. Bernal, T.A.N. Johnson, K. Addy, A. Burgin, D.A. Burns, A.A. Coble, E. Hood, Y. Lu, P. Mayer, E.C. Minor, A.W. Schroth, P. Vidon, H. Wilson, M.A. Xenopoulos, T. Doody, J.G. Galella, P. Goodling, K. Haviland, S. Haq, B. Wessel, K.L. Wood, N. Jaworski, and K.T. Belt, 2018.

Watershed ‘Chemical Cocktails’: Forming Novel Elemental Combinations in Anthropocene Fresh Waters. Biogeochemistry 141:281–305.

Kaushal, S.S., P.M. Groffman, L.E. Band, E.M. Elliott, C.A. Shields, and C. Kendall, 2011. Tracking Nonpoint Source Nitrogen Pollution in Human-Impacted Watersheds. Environmental Science & Technology 45:8225–8232.

Kaushal, S.S., P.M. Groffman, L.E. Band, C.A. Shields, R.P. Morgan, M.A. Palmer, K.T. Belt, C.M. Swan, S.E.G. Findlay, and G.T. Fisher, 2008. Interaction between Urbanization and Climate Variability Amplifies Watershed Nitrate Export in Maryland. Environmental Science & Technology 42:5872–5878.

Kaushal, S., P. Groffman, G. Likens, K. Belt, W. Stack, V. Kelly, L. Band, and G. Fisher, 2005. Increased Salinization of Fresh Water in the Northeastern United States. Proceedings of the National Academy of Sciences of the United States of America 102:13517–20.

Kaushal, S.S. and W.M. Lewis, 2005. Fate and Transport of Organic Nitrogen in Minimally Disturbed Montane Streams of Colorado, USA. Biogeochemistry 74:303–321.

Kaushal, S.S., Likens Gene E., Pace Michael L., Haq Shahan, Wood Kelsey L., Galella Joseph G., Morel Carol, Doody Thomas R., Wessel Barret, Kortelainen Pirkko, Räike Antti, Skinner Valerie, Utz Ryan, and Jaworski Norbert, 2019. Novel ‘chemical Cocktails’ in Inland Waters Are a Consequence of the Freshwater Salinization Syndrome. Philosophical Transactions of the Royal Society B: Biological Sciences 374:20180017.

Kaushal, S.S., G.E. Likens, M.L. Pace, S. Haq, K.L. Wood, J.G. Galella, C. Morel, T.R. Doody, B. Wessel, P. Kortelainen, A. Räike, V. Skinner, R. Utz, and N. Jaworski, 2019. Novel ‘chemical Cocktails’ in Inland Waters Are a Consequence of the Freshwater Salinization Syndrome. Philosophical Transactions of the Royal Society B: Biological Sciences 374:20180017.

Kaushal, S.S., G.E. Likens, M.L. Pace, J.E. Reimer, C.M. Maas, J.G. Galella, R.M. Utz, S. Duan, J.R. Kryger, A.M. Yaculak, W.L. Boger, N.W. Bailey, S. Haq, K.L. Wood, B.M. Wessel, C.E. Park, D.C. Collison, B.Y. ’aaqob I. Aisin, T.M. Gedeon, S.K. Chaudhary, J. Widmer, C.R. Blackwood, C.M. Bolster, M.L. Devilbiss, D.L. Garrison, S. Halevi, G.Q. Kese, E.K. Quach, C.M.P. Rogelio, M.L. Tan, H.J.S. Wald, and S.A. Woglo, 2021. Freshwater Salinization Syndrome: From Emerging Global Problem to Managing Risks. Biogeochemistry 154:255–292.

Kaushal, S.S., G.E. Likens, M.L. Pace, R.M. Utz, S. Haq, J. Gorman, and M. Grese, 2018a. Freshwater Salinization Syndrome on a Continental Scale. Proceedings of the National Academy of Sciences 115:E574–E583.

Kaushal, S.S., G.E. Likens, M.L. Pace, R.M. Utz, S. Haq, J. Gorman, and M. Grese, 2018b. Freshwater Salinization Syndrome on a Continental Scale. Proceedings of the National Academy of Sciences 115:E574–E583.

Kaushal, S.S., G.E. Likens, R.M. Utz, M.L. Pace, M. Grese, and M. Yepsen, 2013. Increased River Alkalinization in the Eastern U.S. Environmental Science & Technology:130724203606002.

Kaushal, S., P. Mayer, G. Likens, J. Reimer, C. Maas, M. Rippy, S. Grant, I. Hart, R. Utz, R. Shatkay, B. Wessel, C. Maietta, M. Pace, S. Duan, W. Boger, A. Yaculak, J. Galella, K. Wood, C. Morel, W. Nguyen, S. Querubin, R. Sukert, A. Lowien, A. Houde, A. Roussel, A. Housten, A. Cacopardo, C. Ho, H. Talbot-Wendlandt, J. Widmer, J. Slagle, J. Bader, J.H. Chong, J. Wollney, J. Kim, and L. Shepherd, 2022. Five State Factors Control Progressive Stages of Freshwater Salinization Syndrome. Limnology and Oceanography Letters.

Kaushal, S.S., P.M. Mayer, P.G. Vidon, R.M. Smith, M.J. Pennino, T.A. Newcomer, S. Duan, C. Welty, and K.T. Belt, 2014. Land Use and Climate Variability Amplify Carbon, Nutrient, and Contaminant Pulses: A Review with Management Implications. JAWRA Journal of the American Water Resources Association 50:585–614.

Kaushal, S.S., W.H. McDowell, W.M. Wollheim, T.A.N. Johnson, P.M. Mayer, K.T. Belt, and M.J. Pennino, 2015. Urban Evolution: The Role of Water. Water 7:4063–4087.

Kaushal, S., J.E. Reimer, P.M. Mayer, R.R. Shatkay, C. Maas, W.D. Nguyen, W.L. Boger, A.M. Yaculak, T.R. Doody, M. Pennino, N.W. Bailey, J.G. Galella, A. Weingrad, D.C. Collison, K.L. Wood, S. Haq, T.N. Johnson, S. Duan, and K.T. Belt, 2022. Freshwater Salinization Syndrome Alters Retention and Release of ‘Chemical Cocktails’ along Flowpaths: From Stormwater Management to Urban Streams. Freshwater Science. doi:10.1086/721469.

Kaushal, S.S., J.E. Reimer, P.M. Mayer, R.R. Shatkay, C.M. Maas, W.D. Nguyen, W.L. Boger, A.M. Yaculak, T.R. Doody, M.J. Pennino, N.W. Bailey, J.G. Galella, A. Weingrad, D.C. Collison, K.L. Wood, S. Haq, T.A. Newcomer-Johnson, S. Duan, and K.T. Belt, 2022. Freshwater Salinization Syndrome Alters Retention and Release of Chemical Cocktails along Flowpaths: From Stormwater Management to Urban Streams. Freshwater Science 41:420–441.

Kaushal, S.S., K.L. Wood, J.G. Galella, A.M. Gion, S. Haq, P.J. Goodling, K.A. Haviland, J.E. Reimer, C.J. Morel, B. Wessel, W. Nguyen, J.W. Hollingsworth, K. Mei, J. Leal, J. Widmer, R. Sharif, P.M. Mayer, T.A. Newcomer Johnson, K.D. Newcomb, E. Smith, and K.T. Belt, 2020. Making ‘Chemical Cocktails’ – Evolution of Urban Geochemical Processes across the Periodic Table of Elements. Applied Geochemistry 119:104632.

Kelly, P.T., W.H. Renwick, L. Knoll, and M.J. Vanni, 2019. Stream Nitrogen and Phosphorus Loads Are Differentially Affected by Storm Events and the Difference May Be Exacerbated by Conservation Tillage. Environmental Science & Technology 53:5613–5621.

Kim, S. and C. Koretsky, 2011. Influence of NaCl and CaCl2 on Lake Sediment Biogeochemistry. Applied Geochemistry 26:S198–S201.

Kim, S. and C. Koretsky, 2013. Effects of Road Salt Deicers on Sediment Biogeochemistry. Biogeochemistry 112:343–358.

Kinsman-Costello, L., E. Bean, A. Goeckner, J.W. Matthews, M. O'Driscoll, M.M. Palta, A.L. Peralta, A.J. Reisinger, G.J. Reyes, A.R. Smyth, and M. Stofan, 2022. Mud in the City: Effects of Freshwater Salinization on Inland Urban Wetland Nitrogen and Phosphorus Availability and Export. Limnology and Oceanography Letters. doi:10.1002/lol2.10273.

Kissner, 2012a. Calcium Chloride Ice Melt. Ice Melter Distributor | Salt Supplier | KISSNER. https://www.kissner.com/calcium-chloride-ice-melt/. Accessed 16 Feb 2022.

Kissner, 2012b. Magnesium Chloride Ice Melt. Ice Melter Distributor | Salt Supplier | KISSNER. https://www.kissner.com/magnesium-chloride-ice-melt/. Accessed 16 Feb 2022.

Knox, A.S., M.H. Paller, J.C. Seaman, J. Mayer, and C. Nicholson, 2021. Removal, Distribution and Retention of Metals in a Constructed Wetland over 20 Years. Science of The Total Environment 796:149062.

Koch, B.J., C.M. Febria, M. Gevrey, L.A. Wainger, and M.A. Palmer, 2014. Nitrogen Removal by Stormwater Management Structures: A Data Synthesis. JAWRA Journal of the American Water Resources Association 50:1594–1607.

Kołodziejczyk, U. and M. Ćwiąkała, 2009. Evaluation of the Efficiency of Use of Aggregates and Chemical Compounds for Winter Road Maintenance. Civil and Environmental Engineering Reports:67–76.

Kondakis, X.G., N. Makris, M. Leotsinidis, M. Prinou, and T. Papapetropoulos, 1989. Possible Health Effects of High Manganese Concentration in Drinking Water. Archives of Environmental Health: An International Journal 44:175–178.

Kunz, J.L., J.M. Conley, D.B. Buchwalter, T.J. Norberg-King, N.E. Kemble, N. Wang, and C.G. Ingersoll, 2013. Use of Reconstituted Waters to Evaluate Effects of Elevated Major Ions Associated with Mountaintop Coal Mining on Freshwater Invertebrates. Environmental Toxicology and Chemistry 32:2826–2835.

Lancaster, N.A., J.T. Bushey, C.R. Tobias, B. Song, and T.M. Vadas, 2016. Impact of Chloride on Denitrification Potential in Roadside Wetlands. Environmental Pollution 212:216–223.

Lazur, A., T. VanDerwerker, and K. Koepenick, 2020. Review of Implications of Road Salt Use on Groundwater Quality—Corrosivity and Mobilization of Heavy Metals and Radionuclides. Water, Air, & Soil Pollution 231:474.

Löfgren, S., 2001. The Chemical Effects of Deicing Salt on Soil and Stream Water of Five Catchments in Southeast Sweden. Water, Air, and Soil Pollution 130:863–868.

Loperfido, J.V., G.B. Noe, S.T. Jarnagin, and D.M. Hogan, 2014. Effects of Distributed and Centralized Stormwater Best Management Practices and Land Cover on Urban Stream Hydrology at the Catchment Scale. Journal of Hydrology 519:2584–2595.

Maas, C.M., W.P. Anderson, and K. Cockerill, 2021. Managing Stormwater by Accident: A Conceptual Study. Water 13:1492.

Mahrosh, U., M. Kleiven, S. Meland, B.O. Rosseland, B. Salbu, and H.-C. Teien, 2014. Toxicity of Road Deicing Salt (NaCl) and Copper (Cu) to Fertilization and Early Developmental Stages of Atlantic Salmon (Salmo Salar). Journal of Hazardous Materials 280:331–339.

Mayer, P.M., P.M. Groffman, E.A. Striz, and S.S. Kaushal, 2010. Nitrogen Dynamics at the Groundwater–Surface Water Interface of a Degraded Urban Stream. Journal of Environmental Quality 39:810–823.

McBride, M.B., 1994. Environmental Chemistry of Soils. Oxford University Press.

McGuire, K.M. and K.E. Judd, 2020. Road Salt Chloride Retention in Wetland Soils and Effects on Dissolved Organic Carbon Export. Chemistry and Ecology 36:342–359.

Mihiranga, H.K.M., Y. Jiang, X. Li, W. Wang, K. De Silva, M.N. Kumwimba, X. Bao, and S.P. Nissanka, 2021. Nitrogen/Phosphorus Behavior Traits and Implications during Storm Events in a Semi-Arid Mountainous Watershed. Science of The Total Environment 791:148382.

Miller, C.V., J.G. Chanat, and J.M. Bell, 2008. Effect of Long-Term Changes in Soil Chemistry Induced by Road Salt Applications on N-Transformations in Roadside Soils. Environmental Pollution 152:20–31.

Minaudo, C., R. Dupas, C. Gascuel-Odoux, O. Fovet, P.-E. Mellander, P. Jordan, M. Shore, and F. Moatar, 2017. Nonlinear Empirical Modeling to Estimate

Phosphorus Exports Using Continuous Records of Turbidity and Discharge. Water Resources Research 53:7590–7606.

Minaudo, C., R. Dupas, C. Gascuel-Odoux, V. Roubeix, P.-A. Danis, and F. Moatar, 2019. Seasonal and Event-Based Concentration-Discharge Relationships to Identify Catchment Controls on Nutrient Export Regimes. Advances in Water Resources 131:103379.

Moore, J., D.L. Bird, S.K. Dobbis, and G. Woodward, 2017. Nonpoint Source Contributions Drive Elevated Major Ion and Dissolved Inorganic Carbon Concentrations in Urban Watersheds. Environmental Science & Technology Letters 4:198–204.

Moore, J., R.M. Fanelli, and A.J. Sekellick, 2020. High-Frequency Data Reveal Deicing Salts Drive Elevated Specific Conductance and Chloride along with Pervasive and Frequent Exceedances of the U.S. Environmental Protection Agency Aquatic Life Criteria for Chloride in Urban Streams. Environmental Science & Technology 54:778–789.

Morel, C.J., S.S. Kaushal, M.L. Tan, and K.T. Belt, 2020. Developing Sensor Proxies for “Chemical Cocktails” of Trace Metals in Urban Streams. Water 12:2864.

Moriasi, D.N., J. G. Arnold, M. W. Van Liew, R. L. Bingner, R. D. Harmel, and T. L. Veith, 2007. Model Evaluation Guidelines for Systematic Quantification of Accuracy in Watershed Simulations. Transactions of the ASABE 50:885–900.

MRLC, 2020. MRLC. Data | Multi-Resolution Land Characteristics (MRLC) Consortium. https://www.mrlc.gov/data. Accessed 3 Mar 2020.

(MRLC), 2022. https://www.mrlc.gov/. Accessed 13 Oct 2022.

Nash, J.E. and J.V. Sutcliffe, 1970. River Flow Forecasting through Conceptual Models Part I — A Discussion of Principles. Journal of Hydrology 10:282–290.

Nelson, S.S., D.R. Yonge, and M.E. Barber, 2009. Effects of Road Salts on Heavy Metal Mobility in Two Eastern Washington Soils. Journal of Environmental Engineering 135:505–510.

Nieder, R., D.K. Benbi, and H.W. Scherer, 2011. Fixation and Defixation of Ammonium in Soils: A Review. Biology and Fertility of Soils 47:1–14.

Norrström, A.-C. and E. Bergstedt, 2001. The Impact of Road De-Icing Salts (NaCl) on Colloid Dispersion and Base Cation Pools in Roadside Soils. Water, Air, and Soil Pollution 127:281–299.

Norrstrom, A.-C. and E. Bergstedt, The Impact of Road De-Icing Salts (NaCl) on Colloid Dispersion and Base Cation Pools in Roadside Soils.

Norrström, A.C. and G. Jacks, 1998. Concentration and Fractionation of Heavy Metals in Roadside Soils Receiving De-Icing Salts. Science of The Total Environment 218:161–174.

Oswald, C.J., G. Giberson, E. Nicholls, C. Wellen, and S. Oni, 2019. Spatial Distribution and Extent of Urban Land Cover Control Watershed-Scale Chloride Retention. Science of The Total Environment 652:278–288.

Palta, M.M., N.B. Grimm, and P.M. Groffman, 2017. "Accidental" Urban Wetlands: Ecosystem Functions in Unexpected Places. Frontiers in Ecology and the Environment 15:248–256.

Parks, R., 2016. Montebello Waste Lakes. Water and Me. https://rep5355.com/2016/07/05/montebello-waste-lakes/. Accessed 3 Mar 2020.

Passeport, E., P. Vidon, K.J. Forshay, L. Harris, S.S. Kaushal, D.Q. Kellogg, J. Lazar, P. Mayer, and E.K. Stander, 2013. Ecological Engineering Practices for the Reduction of Excess Nitrogen in Human-Influenced Landscapes: A Guide for Watershed Managers. Environmental Management 51:392–413.

Pecher, W.T., M.E.A. Madadha, P. DasSarma, F. Ekulona, E.J. Schott, K. Crowe, B.S. Gut, and S. DasSarma, 2019. Effects of Road Salt on Microbial Communities: Halophiles as Biomarkers of Road Salt Pollution. PLOS ONE 14:e0221355.

Peinemann, N., G. Guggenberger, and W. Zech, 2005. Soil Organic Matter and Its Lignin Component in Surface Horizons of Salt-Affected Soils of the Argentinian Pampa. CATENA 60:113–128.

Pennino, M.J., S.S. Kaushal, J.J. Beaulieu, P.M. Mayer, and C.P. Arango, 2014. Effects of Urban Stream Burial on Nitrogen Uptake and Ecosystem Metabolism: Implications for Watershed Nitrogen and Carbon Fluxes. Biogeochemistry 121:247–269.

Pennino, M.J., S.S. Kaushal, S.N. Murthy, J.D. Blomquist, J.C. Cornwell, and L.A. Harris, 2016. Sources and Transformations of Anthropogenic Nitrogen along an Urban River–Estuarine Continuum. Biogeosciences 13:6211–6228.

Perera, N., B. Gharabaghi, and K. Howard, 2013. Groundwater Chloride Response in the Highland Creek Watershed Due to Road Salt Application: A Re-Assessment after 20years. Journal of Hydrology 479:159–168.

Rieuwerts, J.S., I. Thornton, M.E. Farago, and M.R. Ashmore, 1998. Factors Influencing Metal Bioavailability in Soils: Preliminary Investigations for the Development of a Critical Loads Approach for Metals. Chemical Speciation & Bioavailability 10:61–75.

Robinson, H.K. and E.A. Hasenmueller, 2017. Transport of Road Salt Contamination in Karst Aquifers and Soils over Multiple Timescales. Science of The Total Environment 603–604:94–108.

Rysgaard, S., P. Thastum, T. Dalsgaard, P.B. Christensen, and N.P. Sloth, 1999. Effects of Salinity on NH4+ Adsorption Capacity, Nitrification, and Denitrification in Danish Estuarine Sediments. Estuaries 22:21–30.

Schueler, T. and R. Claytor, 2009. Maryland Stormwater Design Manual. Maryland Department of the Environment. https://mde.maryland.gov/programs/water/StormwaterManagementProgram/Pages/default.aspx. Accessed 19 Jun 2022.

Schulz, C.-J. and M. Cañedo-Argüelles, 2019. Lost in Translation: The German Literature on Freshwater Salinization. Philosophical Transactions of the Royal Society B: Biological Sciences 374:20180007.

Seitzinger, S.P., W.S. Gardner, and A.K. Spratt, 1991. The Effect of Salinity on Ammonium Sorption in Aquatic Sediments: Implications for Benthic Nutrient Recycling. Estuaries 14:167–174.

Semadeni-Davies, A., 2006. Winter performance of an urban stormwater pond in southern Sweden. Hydrological Processes 20:165–182.

Shanley, J.B., 1994. Effects of Ion Exchange on Stream Solute Fluxes in a Basin Receiving Highway Deicing Salts. Journal of Environmental Quality 23:977–986.

Shaver, K., 2015. The Snow Brought out the Salt, Which Caused Montgomery’s Brown Water. Washington Post. https://www.washingtonpost.com/local/montgomery-residents-complain-about-brown-tap-water/2015/06/17/d7910098-146c-11e5-9518-f9e0a8959f32_story.html. Accessed 3 Jan 2020.

Shaw, S.B., Marjerison Rebecca D., Bouldin David R., Parlange Jean-Yves, and Walter M. Todd, 2012. Simple Model of Changes in Stream Chloride Levels Attributable to Road Salt Applications. Journal of Environmental Engineering 138:112–118.

Shuman, L.M. and R.R. Duncan, 1990. Soil Exchangeable Cations and Aluminum Measured by Ammonium Chloride, Potassium Chloride, and Ammonium Acetate. Communications in Soil Science and Plant Analysis 21:1217–1228.

Snodgrass, J.W., R.E. Casey, D. Joseph, and J.A. Simon, 2008. Microcosm Investigations of Stormwater Pond Sediment Toxicity to Embryonic and Larval Amphibians: Variation in Sensitivity among Species. Environmental Pollution 154:291–297.

Snodgrass, J.W., J. Moore, S.M. Lev, R.E. Casey, D.R. Ownby, R.F. Flora, and G. Izzo, 2017. Influence of Modern Stormwater Management Practices on Transport of Road Salt to Surface Waters. Environmental Science & Technology 51:4165–4172.

Steele, M.K. and J.A. Aitkenhead-Peterson, 2013. Salt Impacts on Organic Carbon and Nitrogen Leaching from Senesced Vegetation. Biogeochemistry 112:245–259.

Stets, E.G., L.A. Sprague, G.P. Oelsner, H.M. Johnson, J.C. Murphy, K. Ryberg, A.V. Vecchia, R.E. Zuellig, J.A. Falcone, and M.L. Riskin, 2020. Landscape Drivers of Dynamic Change in Water Quality of U.S. Rivers. Environmental Science & Technology 54:4336–4343.

StreamStats, 2020. StreamStats. https://streamstats.usgs.gov/ss/. Accessed 3 Mar 2020.

StreamStats, 2022. https://streamstats.usgs.gov/ss/. Accessed 13 Oct 2022.

Stutter, M., J.J.C. Dawson, M. Glendell, F. Napier, J.M. Potts, J. Sample, A. Vinten, and H. Watson, 2017. Evaluating the Use of In-Situ Turbidity Measurements to Quantify Fluvial Sediment and Phosphorus Concentrations and Fluxes in Agricultural Streams. Science of The Total Environment 607–608:391–402.

Sun, H., J. Alexander, B. Gove, and M. Koch, 2015. Mobilization of Arsenic, Lead, and Mercury under Conditions of Sea Water Intrusion and Road Deicing Salt Application. Journal of Contaminant Hydrology 180:12–24.

Swank, W.T. and J.M. Vose, 1997. Long-Term Nitrogen Dynamics of Coweeta Forested Watersheds in the Southeastern United States of America. Global Biogeochemical Cycles 11:657–671.

Teledyne, 2022. 3700 Full-Size Sampler. https://www.teledyneisco.com/en-us/water-and-wastewater/3700-sampler. Accessed 21 Jun 2022.

Testa, J.M., W.M. Kemp, and W.R. Boynton, 2018. Season-Specific Trends and Linkages of Nitrogen and Oxygen Cycles in Chesapeake Bay. Limnology and Oceanography 63:2045–2064.

Thorslund, J., M.F.P. Bierkens, G.H.P. Oude Essink, E.H. Sutanudjaja, and M.T.H. van Vliet, 2021. Common Irrigation Drivers of Freshwater Salinisation in River Basins Worldwide. Nature Communications 12:4232.

Throwe, J., B. Anderson, L. Beary, J. Beecher, T. Chapman, R. Chow, E. Crooks, L. Daniel, and E.H. Chu, 2020. ENVIRONMENTAL FINANCIAL ADVISORY BOARD. :123.

Tiwari, A. and J.W. Rachlin, 2018. A Review of Road Salt Ecological Impacts. Northeastern Naturalist 25:123–142.

Trowbridge, P.R., J.S. Kahl, D.A. Sassan, D.L. Heath, and E.M. Walsh, 2010. Relating Road Salt to Exceedances of the Water Quality Standard for Chloride in New Hampshire Streams. Environmental Science & Technology 44:4903–4909.

US EPA, O., 2015a. Secondary Drinking Water Standards: Guidance for Nuisance Chemicals. US EPA. https://www.epa.gov/sdwa/secondary-drinking-water-standards-guidance-nuisance-chemicals. Accessed 23 Jul 2020.

US EPA, 2015b. Secondary Drinking Water Standards: Guidance for Nuisance Chemicals. https://www.epa.gov/sdwa/secondary-drinking-water-standards-guidance-nuisance-chemicals. Accessed 9 Jan 2023.

US EPA, 2015c. Lead and Copper Rule. https://www.epa.gov/dwreginfo/lead-and-copper-rule. Accessed 14 Jan 2023.

US EPA, 2015d. National Primary Drinking Water Regulations. https://www.epa.gov/ground-water-and-drinking-water/national-primary-drinking-water-regulations. Accessed 14 Jan 2023.

USGS, 2018. https://www.usgs.gov/special-topics/water-science-school/science/how-streamflow-measured?qt-science_center_objects=0#qt-science_center_objects. Accessed 27 Nov 2022.

USGS, S., 2020. How Streamflow Is Measured. How Streamflow Is Measured. https://www.usgs.gov/special-topic/water-science-school/science/how-streamflow-measured?qt-science_center_objects=0#qt-science_center_objects. Accessed 21 Dec 2020.

USGS NWIS, 2020. USGS NWIS. USGS National Water Information System: Web Interface. https://waterdata.usgs.gov/nwis. Accessed 3 Mar 2020.

Van Meter, R.J., C.M. Swan, and J.W. Snodgrass, 2011. Salinization Alters Ecosystem Structure in Urban Stormwater Detention Ponds. Urban Ecosystems 14:723–736.

Vaughan, M.C.H., W.B. Bowden, J.B. Shanley, A. Vermilyea, R. Sleeper, A.J. Gold, S.M. Pradhanang, S.P. Inamdar, D.F. Levia, A.S. Andres, F. Birgand, and A.W. Schroth, 2017. High-Frequency Dissolved Organic Carbon and Nitrate Measurements Reveal Differences in Storm Hysteresis and Loading in Relation to Land Cover and Seasonality. Water Resources Research 53:5345–5363.

Villa, A., J. Fölster, and K. Kyllmar, 2019. Determining Suspended Solids and Total Phosphorus from Turbidity: Comparison of High-Frequency Sampling with Conventional Monitoring Methods. Environmental Monitoring and Assessment 191:605.

Vogler, J.B. and J. Vukomanovic, 2021. Trends in United States Human Footprint Revealed by New Spatial Metrics of Urbanization and Per Capita Land Change. Sustainability 13:12852.

Wagner, R.J., R.W. Boulger, C.J. Oblinger, and B.A. Smith, 2006. Guidelines and Standard Procedures for Continuous Water-Quality Monitors: Station Operation, Record Computation, and Data Reporting. Techniques and Methods. https://pubs.usgs.gov/tm/2006/tm1D3/pdf/TM1D3.pdf.

Wen, Y., 2012a. Impacts of Road De-Icing Salts on Manganese Transport to Groundwater in Roadside Soils. http://urn.kb.se/resolve?urn=urn:nbn:se:kth:diva-109261. Accessed 7 Apr 2020.

Wen, Y., 2012b. IMPACTS OF ROAD DE-ICING SALTS ON MANGANESE TRANSPORT TO GROUNDWATER IN ROADSIDE SOILS. Royal Institute of Technology (KTH), TOCKHOLM, Sweden.

Williams, M.R., B.M. Wessel, and S. Filoso, 2016. Sources of Iron (Fe) and Factors Regulating the Development of Flocculate from Fe-Oxidizing Bacteria in Regenerative Streamwater Conveyance Structures. Ecological Engineering 95:723–737.

Wollheim, W.M., S. Bernal, D.A. Burns, J.A. Czuba, C.T. Driscoll, A.T. Hansen, R.T. Hensley, J.D. Hosen, S. Inamdar, S.S. Kaushal, L.E. Koenig, Y.H. Lu, A. Marzadri, P.A. Raymond, D. Scott, R.J. Stewart, P.G. Vidon, and E. Wohl, 2018. River Network Saturation Concept: Factors Influencing the Balance of Biogeochemical Supply and Demand of River Networks. Biogeochemistry 141:503–521.

Wood, K.L., S.S. Kaushal, P.G. Vidon, P.M. Mayer, and J.G. Galella, 2022. Tree Trade-Offs in Stream Restoration: Impacts on Riparian Groundwater Quality. Urban Ecosystems 25:773–795.

Yu, J., H. Yu, and L. Xu, 2013. Performance Evaluation of Various Stormwater Best Management Practices. Environmental Science and Pollution Research 20:6160–6171.